TO MY PARENTS

Thesis submitted for the Degree of

Doctor of Philosophy

in the University of Oxford

SOME PROBLEMS IN EXTRAGALACTIC ASTROPHYSICS

T.B. Austin,

New College.

Summer 1974

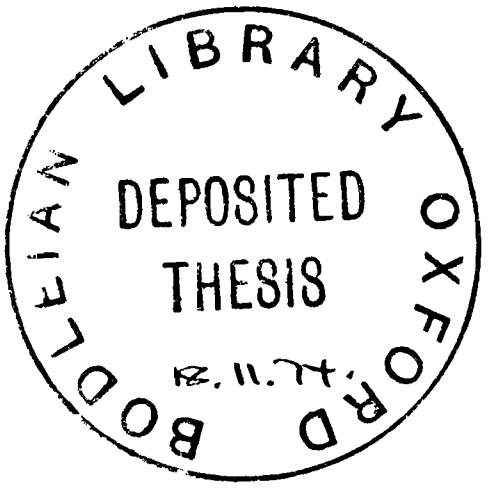

CONTENTS

ABSTRACT

In this thesis the use of clusters in the angular diameter-redshift (θ-z) test in discriminating between the Friedmann models of relativistic cosmology is examined. The apparent magnitude-redshift (m-z) test as applied to brightest cluster galaxies by Peach (1970) and Sandage (1972) has not yet given a significant decision between the closed and open world models, partly due to the intrinsic dispersion of the absolute magnitudes, but, more importantly, to an ignorance of the evolution of these magnitudes during the light travel time. An extension of these observations to clusters of large redshift will improve matters but the evolutionary problem remains to be solved. It was therefore considered of interest to look into the rival merits of the θ-z test using clusters as objects of standard size (Peach and Beard (1969)).

Counts of galaxies in the fields of nine rich clusters with z ranging from 0.13 to 0.20 have been made on V plates taken with the Palomar 48-in. Schmidt telescope. The surface density of galaxies as a function of distance from the cluster centre is discussed in the context of three previously suggested approaches to a definition of angular size. Least squares fits of the data to the projected isothermal gas sphere lead to a parameter β characterising the radius of the cluster core. The mean distance of galaxies from the line of sight through the cluster centre, $\bar{r}$, is a measure characterising the size of the cluster as a whole. The use of secondary maxima in the density distribution is considered and dismissed.

$R_{\bar{r}}$ and $R_{3\beta}$, the intrinsic cluster and core radii in Mpc, are found to be related through the empirical equation

$$R_{\bar{r}} = (0.31\pm0.02)\ R_{3\beta}^{-1} + (4.36\pm0.49 \times 10^{-3})N_{SH} - (0.14\pm0.09)$$

where N_{SH} is the cluster population. This equation is used to define a new measure of angular radius $\bar{r}_c$ by reducing the observed value of $\bar{r}$ to that which would be observed for a cluster of standard radius on the assumption that $R_{3\beta}$ and N_{SH} uniquely determine $R_{\bar{r}}$. A plot of $\bar{r}_c$ against z is given which shows a standard deviation of the residuals of $\bar{r}_c$ from a mean line with $q_o = +1$ of only 18%. It is suggested that the use of this parameter as a measure of angular size makes the angular diameter-redshift test using clusters of galaxies competitive with the apparent magnitude-redshift test using brightest cluster galaxies.

Magnitudes have been measured by photographic photometry for galaxies within 5 arcmin of the centre of the very rich cluster A1413. The differential luminosity function shows a maximum at an absolute total V magnitude of -21.30. The absolute magnitude difference between this and the brightest cluster member is 3.59, which is closely consistent with the correlation of Bautz and Abell (1973) between this parameter and cluster richness and form type. It is confirmed that the absolute magnitude of the maximum has a dispersion of only 14% for the eleven clusters for which it has been observed.

There is a significant difference between the distribution of the bright and faint galaxies; the former have a distribution consistent with spherical symmetry while the fainter galaxies show a prolate distribution aligned with the major axis of the brightest cluster member. Counts in the field of the cluster show that this effect extends over most of the cluster volume.

These results raise at least three general problems for which there is at present no solution. Firstly, there is a need for a physical explanation of the correlation between R_r, C and N_{SH}, and secondly, but not independently, answers are needed to a number of questions, such as the effects of evolution and segregation on size, relevant to the use of the correlation in the (θ-z) plot. Thirdly an explanation is needed of the observation of a peak in the differential luminosity function of clusters of galaxies and the observation in A1413 of a magnitude-dependent radial density distribution. A brief comparison of these results is made with theory, in particular with the N-body calculations of Aarseth (1971) on clusters of galaxies and with Icke's (1973) model for the formation of cluster galaxies.

CHAPTER 1

GALAXIES AND CLUSTERS OF GALAXIES

1.1 Introduction

What are galaxies? In the Hubble Atlas of Galaxies Sandage (1961b) writes: "No one knew before 1900. Very few people knew in 1920. All astronomers knew after 1924. Galaxies are the largest single aggregates of stars ... (they) are the units of matter which define the granular structure of the universe". Still, however, astronomers ask the same question, and this half a century after Hubble (1925) showed conclusively that the Andromeda Nebula lay outside the Milky Way, and after a time in which the waveband of astronomical observation has expanded from the optical band alone, comprising a mere half decade in energy (4×10^{14} Hz to 10^{15} Hz), to a bandwidth of 17 decades from long radio wavelengths (10^{6} Hz) to hard γ-rays (10^{23} Hz). Our present ideas and theories are apparently incapable of explaining many well observed features of galaxies; the wide variety of phenomena in Arp's Atlas of Peculiar Galaxies (Arp, 1966), the violent events observed in the nuclei of galaxies (Burbidge, 1970), the energetic extragalactic radio sources, the nature of quasars and the tendency of galaxies to occur in groups and clusters. We do not understand fully the relatively simple things about galaxies, such as the morphological difference between spirals and ellipticals and the reasons why disk-shaped stellar systems with gas have spiral structure. It is the hope of all astronomers that by careful studies of galaxies and systems of galaxies they will be able to probe the large scale structure of the universe in terms of cosmological models, and to understand

the early state of the universe that led to the formation and evolution of galaxies.

1.2 Historical Background

Faint, nebulous objects with a discernible surface area have been known in the sky since the invention of the telescope. Speculation as to their nature was not confined to astronomers, and such men as the philosopher Immanuel Kant (1742-1804) and Thomas Wright (1711-1786) entered the field. Kant, in his "Allgemeine Naturgeschichte" of 1755, and Wright, in his book "An Original Theory or New Hypothesis of the Universe", introduced and discussed on purely philosophical grounds the island-universe hypothesis, which held that the small white nebulae scattered over the sky were systems of stars at such great distances that the individual stellar contents could not be distinguished. Owing to the lack of observational data the idea did not flourish.

Although the nature of the nebulae was not understood until much later, catalogues of the objects were made by many of the prominent observers of the eighteenth and nineteenth centuries. The original catalogues contained nebulae that we now know to be no more than luminous gas as well as those we know to be external galaxies. For instance, of the 107 bright objects included in the famous list by Messier (1730-1817) only 35 are galaxies. Later on Sir William Herschel, from 1786 until 1802, published several catalogues in which he listed the positions and the structural features of several thousand nebulae. His son, Sir John Herschel, published his general catalogue (GC) in 1864. It represents the first systematic survey of the entire sky to a fairly uniform limit of apparent brightness and contains about 4630 nebulae and clusters of stars observed by his father

and himself, together with 450 discovered by others. This catalogue was replaced by Dreyer's New General Catalogue in 1890 (the NGC catalogue). The two Index Catalogues (IC) supplemented it in 1907. The great majority of the 7840 NGC objects and the 5386 IC objects are extragalactic nebulae.

Long before the era of extragalactic astronomy it was recognised that the small scale distribution of nebulae in space was not random. Even in the small sample of 35 extra-galactic nebulae in Messier's catalogue, nearly half, 16, are probably members of the Virgo Cluster of Galaxies. Plots of the distributions on the sky of the nebulae in the GC, NGC and IC lists reveal several pronounced concentrations now recognised as clusters of galaxies. The irregularity in the apparent distribution of galaxies, their avoidance of the plane of the Milky Way and the existence of some of the nearest clusters were known to the Herschels. Alexander von Humboldt (1866) studied their work, and wrote in his book "Cosmos": "This zone which has been termed the nebulous region of Virgo contains one third of all the nebulous bodies in a space embracing the eighth part of the surface of all the celestial hemisphere".

1.3 The Distribution of Galaxies

After Hubble's (1925) conclusive demonstration of the extragalactic nature of the great majority of the catalogued nebulae, several systematic surveys of the distribution of galaxies were made. Among these are the extensive surveys by Shapley and coworkers at Harvard in the two decades following 1930. At least four distinct clusters - the Virgo cluster, the Ursa Major cloud, and two clusters in Fornax - are apparent in the distribution of bright galaxies in the Shapley-Ames catalogue

(1932). This catalogue was a survey of galaxies brighter than thirteenth magnitude (old scale), and contains 1249 objects (1188 NGC nebulae, 48 IC nebulae and 13 others). Shapley himself (1933) catalogued and described 25 clusters. The Harvard Surveys to faint limiting magnitudes (m~18) in the Southern Hemisphere revealed still greater clustering, and Shapley (1957) called attention to a major unevenness in the distribution on the sky that apparently cannot be described by local clustering, but which suggests "metagalactic structure" or superclustering.

Hubble's (1934) fundamental investigation of the distribution of galaxies provided further information on the clustering tendency. Primarily interested in the possible change in space density with depth as a measure of the expansion of the universe, Hubble counted galaxies in small areas widely distributed over the sky using several limiting magnitudes to about 20.0. These 1283 small selected regions were intentionally chosen to avoid most of the well known clusters. From this scanty evidence Hubble estimated there to be one great cluster, with hundreds of member galaxies, for every 50 square degrees of the sky. He estimated that if the great clusters averaged 500 members each, they would account for about one per cent of the total number of observed galaxies. Even after omitting the great clusters from the analysis, Hubble found the galaxian distribution to be non-random, there being a tendency for small scale clustering (Hubble, 1936a). From his preliminary survey of the extragalactic universe, which he had first opened a decade earlier, Hubble (1936b) concluded: "The nebulae are distributed singly, in groups, and occasionally in great clusters, but when large volumes of space are compared, the tendency to cluster averages out. To the very limits of the telescope the large scale distribution of nebulae

is approximately uniform". We now know that the reason for the widely different conclusions arrived at by Shapley and Hubble was the notorious difficulty in recognising and defining clusters of galaxies on large reflecting telescopes, as opposed to small wide-angle telescopes.

Meanwhile additional clusters were being discovered. Zwicky (1957) found several new clusters with the 18-in. Schmidt telescope at Palomar, built almost exclusively for this purpose, and later many more with the 48-in. Schmidt and 200-in. telescopes. The general prevalence of clustering led him to propose that all galaxies belong to clusters, and that the universe can be regarded as divided into cluster "cells" with a mean diameter, on a distance scale with Hubble parameter H_o = 100h km s^{-1} Mpc^{-1}, of $40h^{-1}$ Mpc.

1.3a) Recent Surveys of the Sky; Clusters of Galaxies

In the two decades after 1945, two photographic surveys showed that clusters of galaxies were extremely numerous, and that galaxies in clusters were the rule rather than the exception. These were the Lick 20-in. Astrographic Survey and the National Geographic Society - Palomar Observatory Sky Survey using the Palomar 48-in. Schmidt telescope. From counts of galaxy images on the Lick photographs, Shane and his coworkers (Shane and Wirtanen, 1954, 1967) have prepared catalogues and charts of the surface density of galaxies. They have called attention to many striking clusters and clouds of galaxies, and even to apparent superclusters. The Lick counts have been analysed statistically by Neyman and Scott (1952, 1959) (see also: Neyman, Scott and Shane (1953, 1954); Scott, Shane and Swanson (1954)). They found that the serial correlation between counts in 1^o x 1^o squares

persists to square separations of about 4^{o}. From the shape of the correlation function they derived parameters that described the scale and amplitude of the clustering, on the assumption that all galaxies are in clusters. They found typical clusters to have populations of the order of 100 and diameters of the order of a few Mpc. The furthest extent of the clustering of about 4^{o}, for a 90^{o} x 45^{o} field in the Northern Galactic Hemisphere, has a corresponding linear scale of $10h^{-1}$ Mpc at the estimated average distance, $220h^{-1}$ Mpc, of the survey, with $H_{o} = 100h$ km s^{-1} Mpc^{-1}. The Lick counts have also been analysed by Limber (1953, 1954) and by Layzer (1956).

Tens of thousands of discrete groups and clusters of galaxies can be identified on the Palomar Sky Survey photographs. Zwicky et al. (1961-1968) have catalogued some 9700 clusters north of declination -3^{o}; only rich clusters containing at least 50 galaxies in the first three magnitudes fainter than the brightest were included. Abell (1958) has catalogued the richest of the clusters visible on the Sky Survey and finds 2712 clusters north of declination -27^{o}. A rich cluster was defined as one containing "at least 50 members that are not more than 2 mag. fainter than the third brightest member". The survey covers 30,206 square degrees or about three quarters of the sphere. However, areas near the Milky Way were rejected and a homogeneous statistical sample of 1682 clusters was selected in a region of complete identification (generally $|b^{II}| > 25^{o}$ to 40^{o}).

1.3b) Higher Order Clustering

There is no question now that galaxies are clustered, and it may be that the clustering tendency is fundamental. However the nature of the higher order of clustering is still a matter of controversy. De Vaucouleurs (1970, 1971) has reviewed

the evidence, and concludes that observationally the universe is found to be clumpy on almost all scale lengths with some preference apparently for clusters of galaxies of characteristic size 100kpc (pairs and multiplets), 1 Mpc (groups and clusters), 10 Mpc (superclusters) and 100 Mpc (third-order clusters), and so on. From the observations it is deduced that the large scale distribution of galaxies and clusters of galaxies is arranged in a hierarchial fashion. However, whether these associations form distinct systems of increasing order or are part of a continuous spectrum of associations (Kiang and Saslaw, 1969) is not clear. These views differ from those of Yu and Peebles (1969) and Zwicky (1962) who found little evidence for clustering beyond the first order.

In recent years there has been a renewed attack on the nature of the higher order clustering of galaxies using new and improved statistical techniques. Bogart and Wagoner (1973) have analysed the distribution of the clusters in Abell's (1958) catalogue. Their technique consisted of a nearest neighbour statistical test for angular correlations between clusters in Abell's various distance groups. Hauser and Peebles (1973) have also studied the distribution of Abell clusters using a method based on the analysis of power spectra and covariance functions. Both studies showed that the Abell clusters were significantly clustered on a scale of $20h^{-1}$ Mpc (H_o = 100h km s^{-1} Mpc^{-1}), with an average of 2 to 3 clusters per supercluster. Peebles (1974) has applied the technique of power spectra analysis to the analysis of the galaxy counts in the Zwicky catalogue and the Shane-Wirtanen catalogue. He finds that these catalogues show that galaxies are clustered out to a scale of $30h^{-1}$ Mpc, with no evidence of a natural division between groups and clusters of galaxies, or

between clusters and superclusters. He has argued that the rich compact clusters of galaxies, although prominent objects, may only be extremes drawn from an essentially continuous distribution.

Clustering on scales as large as, or larger than, those proposed by de Vaucouleurs and Peebles might be investigated by studying the distribution of quasars with redshift and direction. A large sample of quasars could be used as probes for density inhomogeneities on scales 100-1000 Mpc (Rees, 1971). Such inhomogeneities may be detectable in the future by searching for angular variations in the cosmic microwave background attributable to gravitational effects (Sachs and Wolfe, 1967; Rees and Sciama, 1968).

1.4 Morphology of Clusters

Clusters of galaxies have a wide variety of forms, from rich aggregates of thousands of members, to the relatively poor groups, like the Local Group containing 27 members. The smaller groups appear to be the most numerous, but exact statistics on the frequency distribution of cluster types are not known. Zwicky et al. (1961-1968) classify clusters as compact, medium compact and open. A compact cluster is one with a single pronounced concentration of galaxies, in which 10 or more galaxies appear (in projection) to be in contact; a medium compact cluster is one with a single concentration within which galaxies appear to be separated by several galaxy diameters or one in which there are several pronounced concentrations of galaxies; an open cluster is one without any pronounced peak of population, but which appears as a loose cloud of galaxies superimposed on the general field.

Morgan (1961) suggested a classification of clusters on the basis of a study of the 20 nearest clusters in the Abell catalogue.

He found that these clusters could be divided into two categories, according to the types of galaxies encountered among their brightest members: (i) those containing appreciable numbers of galaxies of minor central concentration of light (late spirals and irregulars) and (ii) those containing few of the latter.

These two classification schemes are strongly correlated, and Abell (1965, 1974) proposed that the main features of both systems were preserved by simply classifying clusters as regular or irregular. The irregular clusters correlate with Zwicky's medium compact and open clusters, and with Morgan's type (i) clusters. Bautz and Morgan (1970) have introduced another scheme which they have applied mainly to the rich clusters. This classification describes the degree to which the brightest members stand out against the general cluster background. A BM Type I cluster usually contains a centrally located, dominant cD galaxy, A2199 in Abell's catalogue being a type cluster. A BM Type III cluster usually contains no dominant galaxies, cluster types being the Virgo cluster and the Corona Borealis cluster A2065. Oemler (1974a), from a study of 15 rich clusters, finds that cluster properties are such that they may be divided into three groups. Spiral rich clusters have compositions similar to that of the field, irregular mass distributions of low density and no central concentration, and show no signs of segregation of members according to mass or morphological type. Clusters with cD galaxies are rich in ellipticals, have smooth, spherical mass distributions of high density and central concentration, have a strong deficiency of spirals in the core and show a considerable tendency towards energy equipartition. Spiral poor clusters, which are dominated by SO galaxies, also show segregation by mass and morphological type, but are not as smooth, dense or centrally condensed as the cD clusters.

The physical significance and importance of these classification schemes is by no means clear, but much discussion has been made over the years of the problem of selecting only the richest and most outstanding clusters for observational use in the classical redshift - magnitude and angular diameter - redshift cosmological tests (Scott, 1957). There is no doubt that clusters are selected for study in this way, because it is only for such that there is a negligible probability of their not being accidental coincidences of smaller groups or individual galaxies in the line of sight. In this regard Sandage and Hardy (1973) have found a correlation of the luminosity of the brightest cluster galaxy with Bautz-Morgan type, the intrinsic luminosity being larger in Type I clusters than in Type III clusters.

1.5 Thesis Investigation

The position and importance of rich clusters of galaxies in extragalactic astrophysics has now been seen. This thesis is devoted to a study of rich clusters based on plates taken with the Palomar 48-in. Schmidt telescope. The aim of a general study of clusters is two-fold; first to investigate those properties of clusters which are of importance in their use as cosmological test objects, and second, to investigate their structure and photometric properties with a view to obtaining information which may be relevant to their formation and to the formation of their member galaxies. Studies of the former type include discussions of cluster sizes and of the photometry of the brighter cluster galaxies. Those of the latter type include measurements of colour changes across individual galaxies and across clusters, investigations of the possibility of intracluster absorption, and the construction of luminosity functions and models of the mass

distribution in clusters. The two types of study often overlap but their motivation can be quite distinct.

In the present thesis the use of rich clusters in the angular diameter - redshift (θ-z) test in discriminating between the Friedmann models of relativistic cosmology is discussed. This is covered in Chapter 2. In Chapter 3 one cluster, A1413, from the sample studied in Chapter 2 is investigated in detail, and its structure and luminosity function are determined. A summary and brief discussion of the results of this work in regard to various theories of galaxy formation and evolution is given in Chapter 4.

CHAPTER 2

GALAXY COUNTS FOR NINE CLUSTERS OF INTERMEDIATE REDSHIFT AND THE ANGULAR DIAMETER-REDSHIFT RELATION

2.1 INTRODUCTION

In the context of traditional cosmological models of the universe, as first discussed by Friedmann (1922) and later specialised by Robertson (1935, 1936) and Walker (1936) for the special case of an isotropic and homogeneous universe, it is the aim of the classical cosmological tests, relating apparent intensities, apparent sizes and counts of galaxies to their redshift, to choose between the various models and find the one that best fits the real world. In classical optical cosmology the main work has been directed towards the calibration of the local velocity-distance relation and the determination of the Hubble parameter H_o, together with the search for second order effects in this relation leading to estimates of the deceleration parameter q_o.

In the middle fifties there was renewed interest in using these tests and many papers were published that treated the fitting of observational data to theoretical predictions (Robertson (1955); McVittie (1956); Mattig (1958)). The observational quantities which are available for use are (1) the apparent magnitude of galaxies, (2) the angular diameters of galaxies and clusters of galaxies and (3) galaxy counts. The search for second-order effects through the extension of galaxy counts to successively fainter magnitude limits has not been actively pursued since the pioneering work of Hubble (1936a) who showed that the Euclidean approximation to the counts expressed in magnitudes,

$$\log_{10} N = 0.6\ m + \text{constant}$$

was in good agreement with the distribution of faint galaxies to apparent magnitude M_{pg} about 19. The enormity of the task, the many awkward selection effects, and the inability to count accurately to a definite limiting magnitude has discouraged any attempts to extend the counts to fainter magnitudes. Furthermore there are the problems of obscuration by dust in our galaxy and of the clustering and possible superclustering of galaxies which can cause significant fluctuations in the counts. Also, Sandage (1961a) showed that the differences between the predicted counts for different world models are very small to a limiting magnitude of about 21.

The counting of radio sources was recognised as a practicable test as soon as it was discovered that radio sources in the galactic polar direction were distant extragalactic objects. They were also found to be distributed isotropically on the celestial sphere. The counts of radio sources give a positive result in the sense that they disagree with the prediction of all uniform models. Many more faint sources are observed than would be predicted by all simple cosmological models. Detailed reviews of the radio source counts have been given by Ryle (1958) and Scheuer (1974). The basic results of the source counts argue for an evolution of the properties of radio sources over cosmological time scales. Similar evolution needs to be invoked for an explanation of the results of the luminosity volume test as applied to samples of QSO's (Schmidt 1968). No more discussion of these tests will be given here but the reader is referred to a more complete list of references given by Longair and Rees (1974).

The apparent magnitude-redshift (m-z) test as applied to

brightest cluster galaxies by Peach (1970), Sandage (1972) and Sandage and Hardy (1973) has not yet given a significant decision between the closed and open world models, partly due to the intrinsic dispersion of the absolute magnitudes, but, more importantly, to an ignorance of the evolution of the absolute magnitudes during the light travel time, 5×10^9 yrs to $z = 0.2$. An extension of these observations to clusters of large redshift will improve matters but the evolutionary problem remains to be solved. A critical review of the problems associated with the application of the (m-z) test to brightest cluster galaxies has been given by Peach (1972). Therefore it is of interest to look into the rival merits of the angular diameter-redshift (θ-z) test using clusters of galaxies as objects of standard size (Peach and Beard, 1969).

If this method is to be worth serious consideration it is necessary to be convinced that rich clusters are either of a closely similar size, or, if their sizes differ, that there is a correlation of size with some observable parameter, which will permit the observed angular diameter to be reduced to a system in which the dispersion of corrected intrinsic sizes is small. Galaxy counts in the fields of nine rich clusters were undertaken to look for such a parameter and the method and results of the counts will be described in this Chapter. Number counts have already been published by other authors for a further 12 clusters. These present some difficulties of interpretation as they are made with differing telescope-plate combinations and with differing criteria for the identification of galaxies. Some of this material is incorporated in the analysis in part 2.5 of this Chapter, where it is suggested that the radius of the core of a cluster correlates with the radius

of the halo and the cluster population and in which an operational definition of angular diameter showing very small dispersion is given (Austin and Peach, 1974a).

2.1a Basic Formulae and Their Application

For the zero pressure Friedmann models with zero cosmological constant the relation between the angular diameter of a test object Θ_o, its linear diameter D, and its redshift Z is (Mattig, 1958)

$$\Theta_o = D(1+Z)^2 \, H_o \, q_o^2 \times \{c(q_o Z + (q_o-1)[\sqrt{(1+2q_o Z)} - 1])\}^{-1} \qquad (2.1)$$

The Hubble parameter H_o and the deceleration parameter q_o are defined as

$$H_o = \dot{R}_o/R_o \quad \text{and} \quad q_o = - \ddot{R}_o R_o/\dot{R}_o^2$$

where R is the time-dependent scale factor in the Robertson-Walker line element and subscript zero indicates that the quantities are evaluated at the present cosmic time. The deceleration parameter is related to the mean density ρ_o by

$$q_o = \frac{4\pi G}{3H_o^2} \rho_o$$

where G is the gravitational constant, and with the spatial curvature by

$$kc^2/R_o^2 = \dot{H}_o^2 (2q_o-1)$$

With a sample of test objects with a small dispersion in D and provided that D is time independent one could measure Θ_o and Z and use relation (2.1) to determine q_o with an accuracy dependent on the dispersion in D and the redshift interval sampled. For particular values of q_o relation (2.1) can be expanded in powers of Z and reduced to:

for $q_o = +1$, $\Theta_o = D(1+Z)^2 H_o/CZ$

for $q_o = 0$, $\Theta_o = D(1+Z)^2 H_o/CZ(1+Z/2)$

for $q_o = -1$, $\Theta_o = D(1+Z)^2 H_o/CZ(1+Z)$

In general,

$$D_{q_o = +1} = D_{q_o} (1 + (\frac{q_o - 1}{2}) Z.....) ,$$

for low Z,

where $D_{q_o = +1}$ is the intrinsic diameter of a source with a particular observed angular diameter in a world model with $q_o = +1$.

2.2 Techniques

The plates used in these counts are 25 min limiting exposures on 103aD + Wr12 made in March 1972 using the Palomar 48-in. Schmidt telescope during an observing period of above average sky conditions with a seeing disc of less than 1 arcsec. Photometry of the plates shows an average V-band sky brightness of 21.7 mag $arcsec^{-2}$ at a plate density of between 0.4 and 0.5; the photometric calibration is based on tube sensitometer spots with a photoelectric zero point. The observations and the calibration of the plates will be described in more detail in Chapter 3. (The clusters analysed here are the high redshift subset of 15 clusters observed in this run, a sample chosen from a list of clusters with photoelectric observations by Sandage (1972), listed by Peach (1969)).

The fields of the clusters were viewed at a magnification of x 12 and images attributed to galaxies were marked on positive enlargements of the plates. The enlargements were arranged to have the same linear scale in mm Mpc^{-1} for each cluster on the

assumption that the cluster's distance is given by its redshift in a world model with $q_o = +1$ and $H_o = 50$ km s^{-1} Mpc^{-1}. This was done in an attempt to count with the same linear resolution in each cluster. Galaxy images were counted to an average distance of $4z^{-1}$ arcmin from the cluster centre; this is more than twice the radius within which the clusters in Abell's (1958) catalogue were considered to be contained. The limiting radius to which counts were made corresponds to a linear distance at the cluster of about 5 Mpc, and in each case considered is well beyond any measurable contribution of the cluster to the surface density of galaxy images.

The criterion in marking images on the plates as the images of galaxies is that any image not unambiguously that of a star is marked as a galaxy. The only other criterion that could be used consistently in this type of work is that only images that are definitely galaxies are marked as such. However, for high redshift clusters on 48-in. Schmidt plates so few images would then be counted that no useful information on the structure of the clusters could be obtained. It should be emphasised that no counts can be said to have an exact limiting magnitude because of the dispersion of average surface brightness of galaxies in a particular magnitude interval and the dependence of surface brightness on morphological type. From photometry of the plates it is clear that counts are usually made to a limiting surface brightness below which even bright galaxies may be missed. These points are well illustrated in a discussion by Zwicky (1957). There is no doubt that the procedure used here leads to the inclusion in the counts of a number of faint stars which are indistinguishable from galaxies near the limit of detection, and to the counting of some plate flaws. The latter

may be neglected in comparison with the stellar contribution which can be roughly estimated as follows.

The mean background (and foreground) count in the nine fields of this study is 1480 $\pm$ 220 images deg^{-2}. From photometry of the plates, to be described in Chapter 3, it is estimated that faint stars contribute to the counts below a V magnitude of about $18^{m}.2$, although this value will be partially dependent on the observing conditions during the plate exposure. Using an analysis by Sternberg (1972) of stellar photometry by Becker (1965) and Fenkart (1967) made in the RGU bands in SA57, it is estimated that there is a stellar background count in the magnitude interval between the above value and the plate limit of about $20^{m}.0$ of around 500 stars deg^{-2} at the galactic pole. This gives a proportion of stars in the counts at high galactic latitude of 35% possibly rising to much higher percentages at low galactic latitudes. A plot of the background counts against galactic latitude shows a marginal increase in the background with decreasing latitude. Assuming that the stellar component is distributed at random across the field of the clusters it will have little effect on the subsequent discussion.

The print with the marked images was divided into an array of squares and the number in each square counted. These counts were then summed in rows and columns; plots of these sums against distance across the field were used to locate the cluster centre as the centre of the symmetrical maximum given by the counts. This was possible to the precision of the width of the squares, or about 1 arcmin. Centres found in this way are given in Table I together with the other cluster parameters. The images were then recounted in rings drawn round these centres; a fixed

TABLE I

Parameters of the nine observed clusters

Cluster	Centre (1950) α	δ	Galactic coordinates l^{II}	b^{II}	Red-shift	Bautz–Morgan type	Rich-ness	N_{SH}	$N(R)$	β (arcmin)	$R_{3\beta}$ (Mpc)	$\bar{r}$ (arcmin)	$R_{\bar{r}}$ (Mpc)	C	$\bar{r}_c$ (arc-min)
A1930	$14^h\,30^m.3$	$+31°\,51'.0$	51°	+67°	0·1312	III	1	61	73	0·99±0·16	0·548	4·6±1·0	0·850	0·645±0·175	9·00
A1132	$10^h\,55^m.4$	$+57°\,04'.0$	149°	+54°	0·1345	II–III	1	35	109	0·62±0·10	0·350	4·2±0·9	0·790	0·444±0·119	6·32
Ursa Major II															
A1413	$11^h\,52^m.7$	$+23°\,40'.6$	225°	+77°	0·1426	I	3	155	147	0·85±0·18	0·501	5·1±0·5	1·003	0·498±0·116	5·96
A2100	$15^h\,34^m.4$	$+37°\,47'.6$	61°	+54°	0·1532	III	3	159	85	0·56±0·16	0·348	6·5±0·4	1·347	0·258±0·075	6·07
A1553	$12^h\,28^m.3$	$+10°\,50'.2$	285°	+73°	0·1651	II–III	2	119	180	0·60±0·08	0·394	5·1±0·5	1·117	0·354±0·059	5·91
A1677	$13^h\,3^m.5$	$+31°\,10'.1$	82°	+85°	0·1831	III	2	111	155	0·33±0·16	0·233	8·2±0·9	1·930	0·120±0·060	6·61
Coma B															
A801	$9^h\,25^m.3$	$+20°\,43'.7$	209°	+43°	0·1917	I–II	2	95	115	0·61±0·12	0·445	4·3±0·7	1·043	0·426±0·109	5·97
A1643	$12^h\,53^m.5$	$+44°\,21'.3$	121°	+73°	0·1979	III	1	136	79	0·47±0·08	0·350	5·0±0·7	1·240	0·282±0·067	5·05
A732	$8^h\,55^m.3$	$+3°\,22'.1$	226°	+29°	0·2018	II–III	1	71	133	0·28±0·10	0·211	8·3±0·8	2·087	0·102±0·038	6·14
Hydra II															

ring size was used to give the same linear resolution at each cluster. The counts were tabulated in NSEW quadrants and then summed.

2.3 Galaxy counts for nine clusters

The counts for the nine clusters are listed in Tables III to XI. In these tables the number of images in each quadrant is given for every ring counted, together with the mean surface density of galaxies in that ring. Also listed are the cumulative number counts $N_o(r)$ for the actual observations and $N_c(r)$ for the cluster alone after correction for the field, as described later in part 2.4b of this section. The counts for all the clusters in Table I are also presented in Figs 1-9 as plots of the surface density of galaxies as a function of distance from the assumed cluster centre. The error bar for each point is the square root of the number of galaxies counted in that ring. This error bar has an average value of 22% for the first ring falling to around 11% for the outer rings.

While the figures give surface density as a function of radius alone, the clusters do not in general show a high degree of circular symmetry. Four seem definitely non-circular. A simple application of the χ^2 test for the equality of the counts in the four quadrants in the inner parts of the clusters suggests that the clusters A801, A1413, A1553 and A2100 are non-circular at the 5% significance level, i.e. that in more than 95% of cases one would expect better agreement with the hypothesis of circular symmetry, were these clusters indeed circular. This result is not as damaging as it may seem to an assumption that the clusters are intrinsically roughly spherically symmetric. Two of the anomalous clusters A1553 and A2100 are probably contaminated by

TABLE III

Counts for cluster A1930

Ring No.	Quadrant				Mean density	Mean radius	$N_o(r)$	$N_c(r)$
	NW	SW	SE	NE	(gal mm^{-2})	(mm)		
1	3	7	4	3	2.02	1.09	17	13
2	13	5	13	5	1.40	2.55	53	37
3	8	3	10	11	0.76	4.15	85	49
4	10	14	6	8	0.64	5.77	123	59
5	8	11	16	9	0.57	7.41	167	67
6	11	14	10	9	0.47	9.04	211	67
7	12	15	20	11	0.53	10.67	269	73
8	19	8	14	14	0.44	12.31	324	69
9	14	19	17	18	0.47	13.95	392	69
10	21	13	13	20	0.42	15.58	459	60
11	17	20	31	21	0.50	17.22	548	66
12	22	32	18	19	0.47	18.86	639	65
13	25	30	19	21	0.45	20.50	734	61
14	24	36	32	30	0.53	22.13	856	76

Mean background count = 0.47 gal mm^{-2}

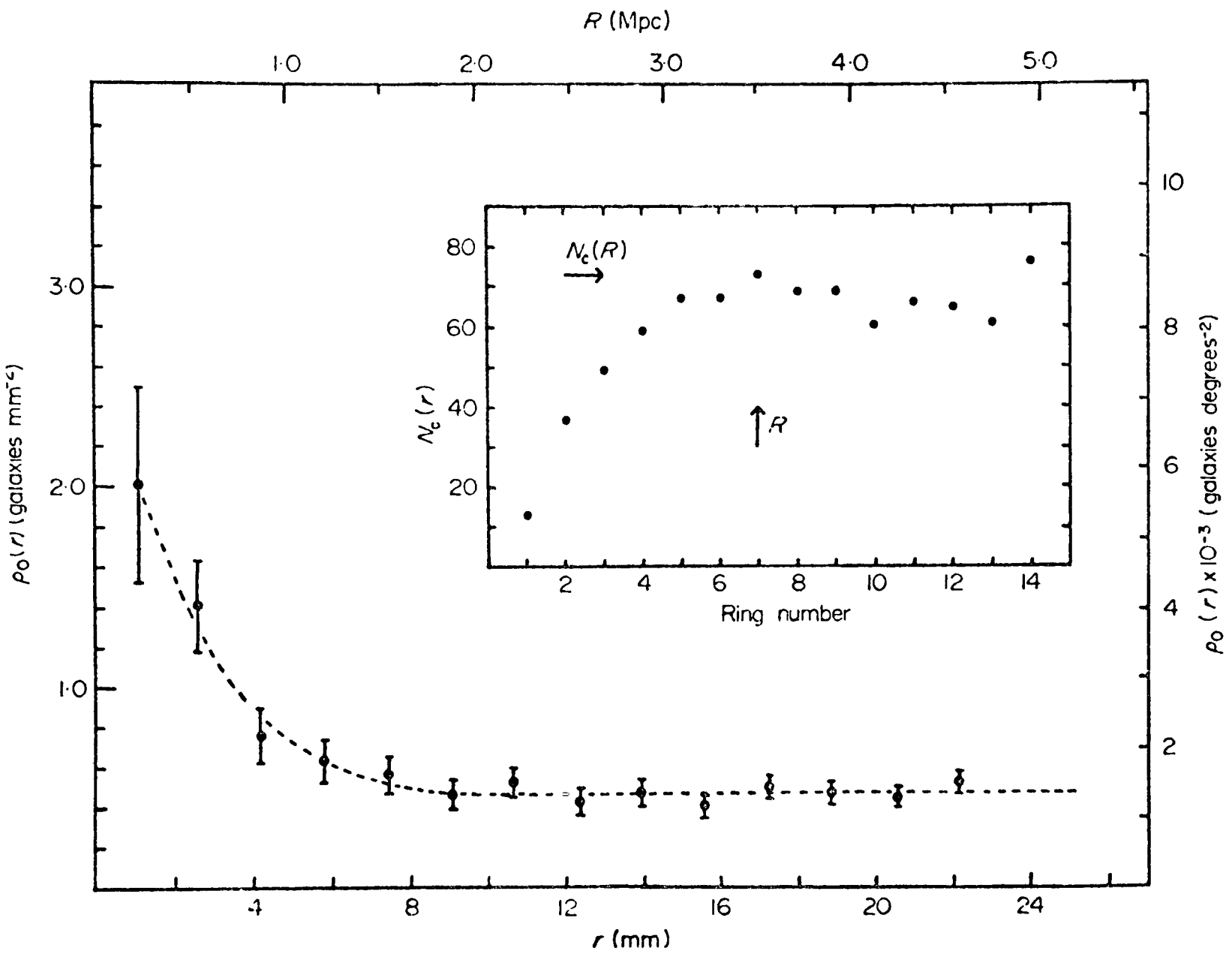

FIG. 1 The surface density distribution for the cluster A1930 in galaxies per square millimetre on the plate and in galaxies per square degree on the sky as a function of distance from the assumed cluster centre in millimetres on the plate and in Mpc in the cluster assuming the distance given by the redshift with $q_o = +1$ and $H_o = 50$ km s^{-1} Mpc^{-1}. Error bars give the statistical error of the count in each ring. The insert gives the cumulative ring count $N_c(r)$ for the same cluster as a function of ring number (cf. part 2.4b). The outermost radius R and the cluster population $N_c(R)$ are indicated. The concentration C = 0.65.

TABLE IV

Counts for cluster A1132

Ring No.	Quadrant				Mean density	Mean radius	$N_o(r)$	$N_c(r)$
	NW	SW	SE	NE	(gal mm^{-2})	(mm)		
1	6	7	7	7	3.40	1.07	27	23
2	12	10	7	11	1.65	2.50	67	48
3	12	18	12	8	1.22	4.07	117	74
4	5	14	21	11	0.90	5.66	168	92
5	20	9	16	14	0.83	7.26	227	109
6	8	13	12	9	0.47	8.89	269	98
7	15	17	21	15	0.65	10.46	337	104
8	19	22	19	18	0.64	12.06	415	110
9	14	19	23	17	0.53	13.66	488	102
10	31	22	20	21	0.61	15.27	582	105
11	29	29	27	25	0.65	16.87	692	116
12	20	42	23	27	0.60	18.48	804	118
13	23	40	23	22	0.53	20.08	912	106
14	19	36	38	29	0.56	21.69	1034	99

Mean background count = 0.59 gal mm^{-2}

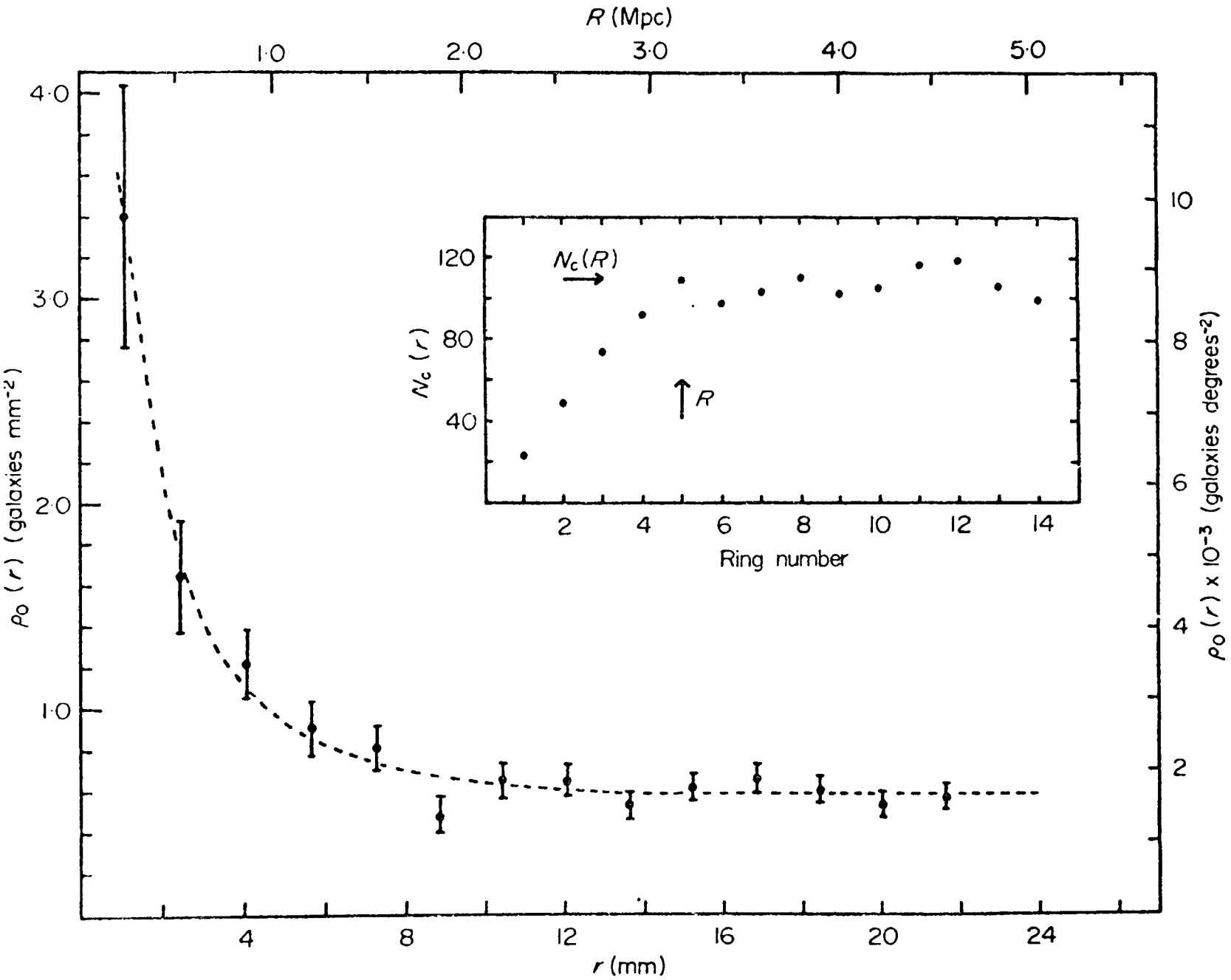

FIG. 2 The cluster A1132. C = 0.44

TABLE V

Counts for cluster A1413

Ring No.	Quadrant				Mean density (gal mm^{-2})	Mean radius (mm)	$N_o(r)$	$N_c(r)$
	NW	SW	SE	NE				
1	4	6	11	2	3.22	0.99	23	19
2	11	5	11	9	1.74	2.32	59	43
3	10	13	18	21	1.75	3.78	121	84
4	14	8	18	9	0.99	5.25	170	105
5	15	9	15	11	0.80	6.73	220	120
6	21	8	17	14	0.78	8.22	280	136
7	20	15	15	13	0.70	9.71	343	147
8	15	15	19	12	0.57	11.20	404	147
9	12	16	12	21	0.51	12.68	465	141
10	18	21	16	24	0.59	14.17	544	144
11	23	25	22	18	0.60	15.66	632	148
12	18	26	18	20	0.52	17.15	714	140
13	24	28	31	14	0.57	18.64	811	140
14	28	15	30	34	0.57	20.13	918	140
15	27	33	32	33	0.62	21.62	1043	150

Mean background count = 0.57 gal mm^{-2}

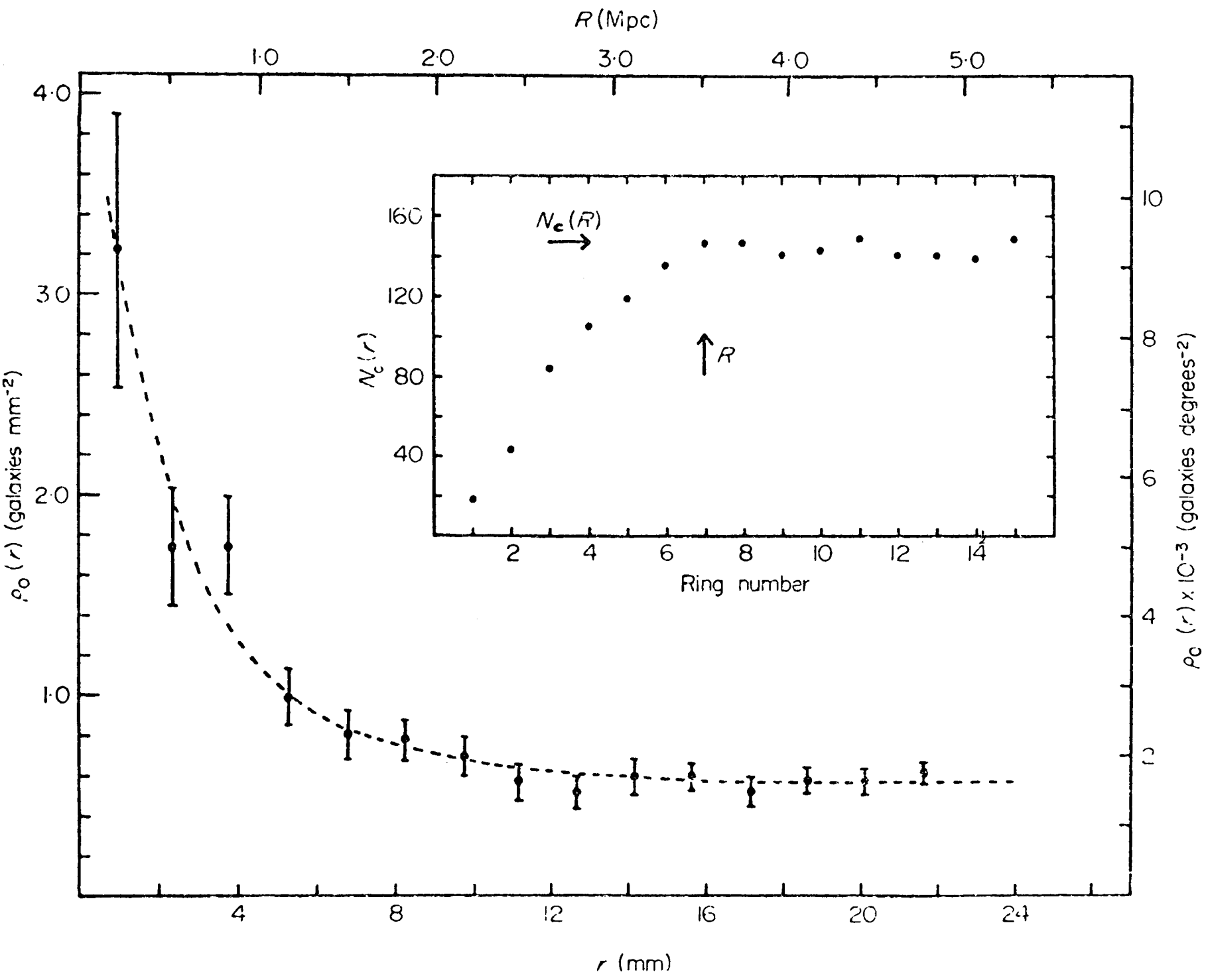

FIG. 3 The cluster A1413. C = 0.50

TABLE VI

Counts for cluster A2100

Ring No.	Quadrant				Mean density	Mean radius	$N_o(r)$	$N_c(r)$
	NW	SW	SE	NE	(gal mm^{-2})	(mm)		
1	3	3	3	6	2.36	0.95	15	10
2	5	9	7	5	1.36	2.22	41	23
3	8	13	9	10	1.24	3.61	81	39
4	5	9	11	8	0.74	5.02	114	40
5	12	12	14	10	0.84	6.43	162	47
6	7	16	21	16	0.86	7.85	222	57
7	21	16	19	18	0.91	9.27	296	72
8	16	20	26	19	0.85	10.69	377	85
9	12	24	13	23	0.67	12.12	449	79
10	17	30	19	26	0.75	13.54	541	84
11	20	38	17	32	0.80	14.96	648	95
12	17	31	26	25	0.68	16.38	747	88
13	25	25	22	31	0.64	17.81	850	77
14	23	41	34	35	0.77	19.23	983	85
15	39	39	24	30	0.72	20.65	1115	85

Mean background count = 0.72 gal mm^{-2}

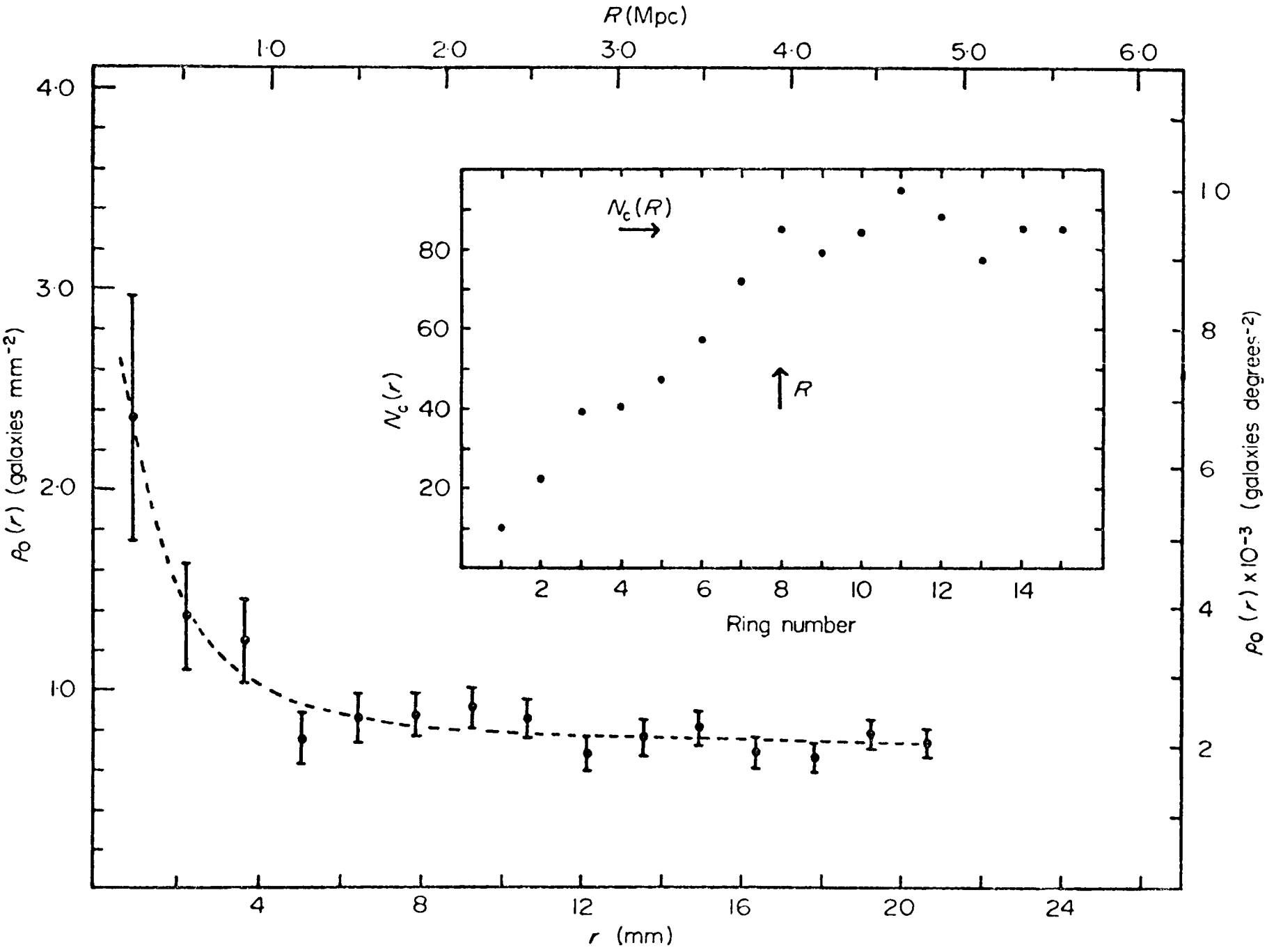

FIG. 4. The cluster A2100. C = 0.26

TABLE VII

Counts for cluster A1553

Ring No.	Quadrant				Mean density	Mean radius	$N_o(r)$	$N_c(r)$
	NW	SW	SE	NE	(gal mm^{-2})	(mm)		
1	10	8	5	3	4.64	0.90	26	24
2	12	6	12	9	2.28	2.10	65	54
3	12	6	15	15	1.68	3.42	113	87
4	11	9	16	12	1.20	4.75	161	114
5	12	9	17	11	0.96	6.09	210	136
6	15	4	18	21	0.92	7.44	268	161
7	15	7	8	9	0.53	8.78	307	161
8	24	9	15	16	0.75	10.13	371	180
9	22	9	11	8	0.52	11.47	421	179
10	22	10	8	17	0.53	12.82	478	180
11	13	12	13	15	0.44	14.17	531	170
12	21	17	17	20	0.57	15.51	606	176
13	29	19	19	28	0.66	16.86	701	195
14	15	17	29	20	0.53	18.21	782	195
15	33	22	25	15	0.57	19.56	877	203
16.5	23	21	22	25	0.40	21.41	991	175
17.8	31	21	29	38	0.48	23.12	1110	163
19.1	34	27	51	51	0.61	24.84	1273	186

Mean background count = 0.52 gal mm^{-2}

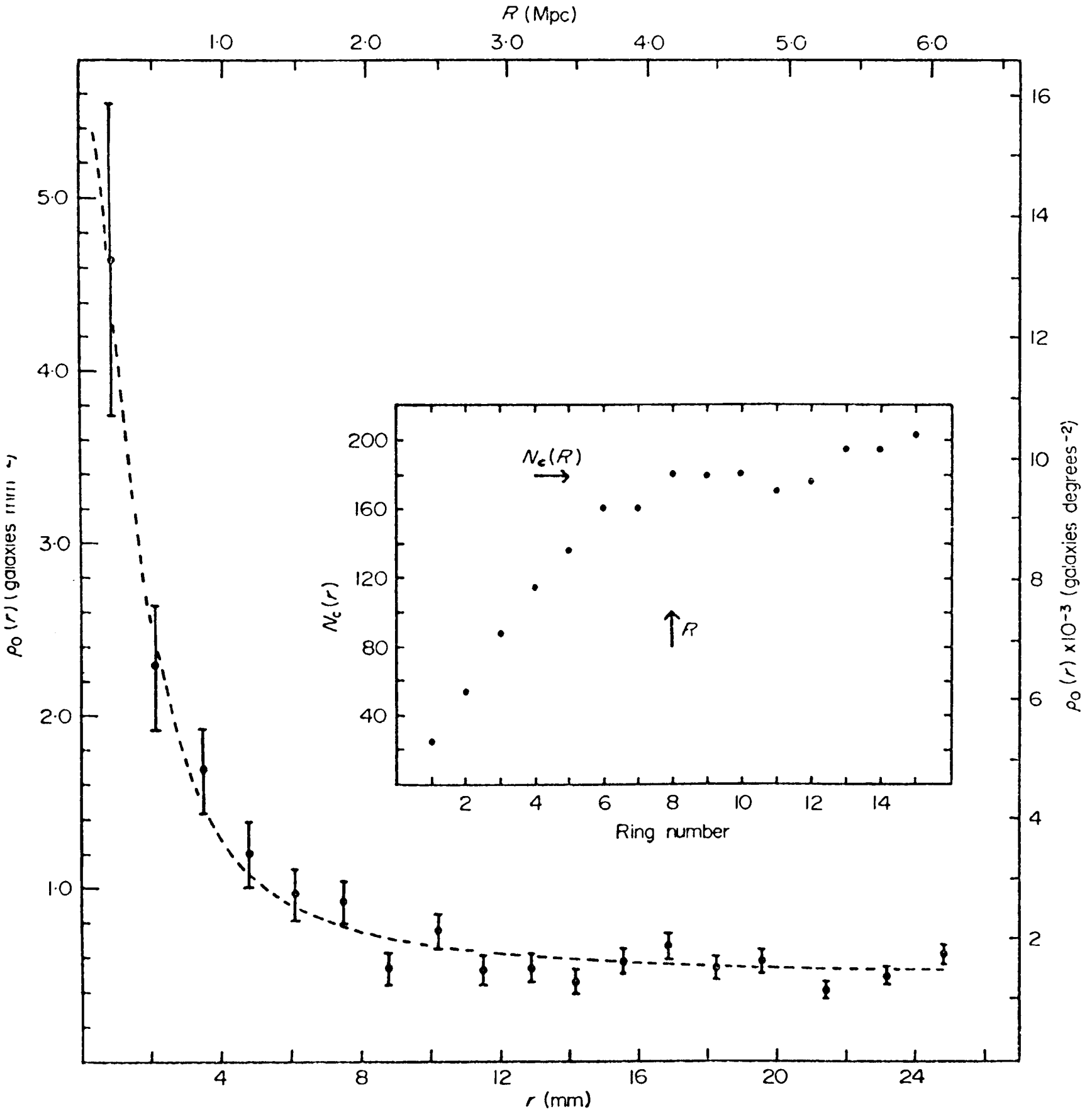

FIG. 5 The cluster A1553. C = 0.35

TABLE VIII

Counts for cluster A1677

Ring No.	Quadrant				Mean density	Mean radius	$N_o(r)$	$N_c(r)$
	NW	SW	SE	NE	(gal mm^{-2})	(mm)		
1	5	4	4	6	3.84	0.84	19	17
2	5	3	9	5	1.52	1.95	41	33
3	11	8	7	7	1.34	3.18	74	56
4	8	5	4	2	0.55	4.42	93	60
5	8	9	9	9	0.79	5.67	128	76
6	9	10	10	6	0.63	6.92	163	87
7	7	3	11	9	0.47	8.17	193	89
8	9	14	7	11	0.55	9.42	234	98
9	13	21	12	10	0.67	10.68	290	119
10	12	12	7	17	0.51	11.93	338	126
11	7	13	14	15	0.47	13.18	387	131
12	17	15	14	14	0.53	14.44	447	143
13	11	11	17	21	0.49	15.69	507	151
14	18	20	12	12	0.46	16.94	569	155
15	11	10	14	18	0.37	18.20	622	147
16.5	14	28	22	19	0.42	19.93	721	145
17.8	24	23	24	27	0.46	21.52	819	151
19.1	21	33	24	22	0.43	23.11	919	152

Mean background counts = 0.43 gal mm^{-2}

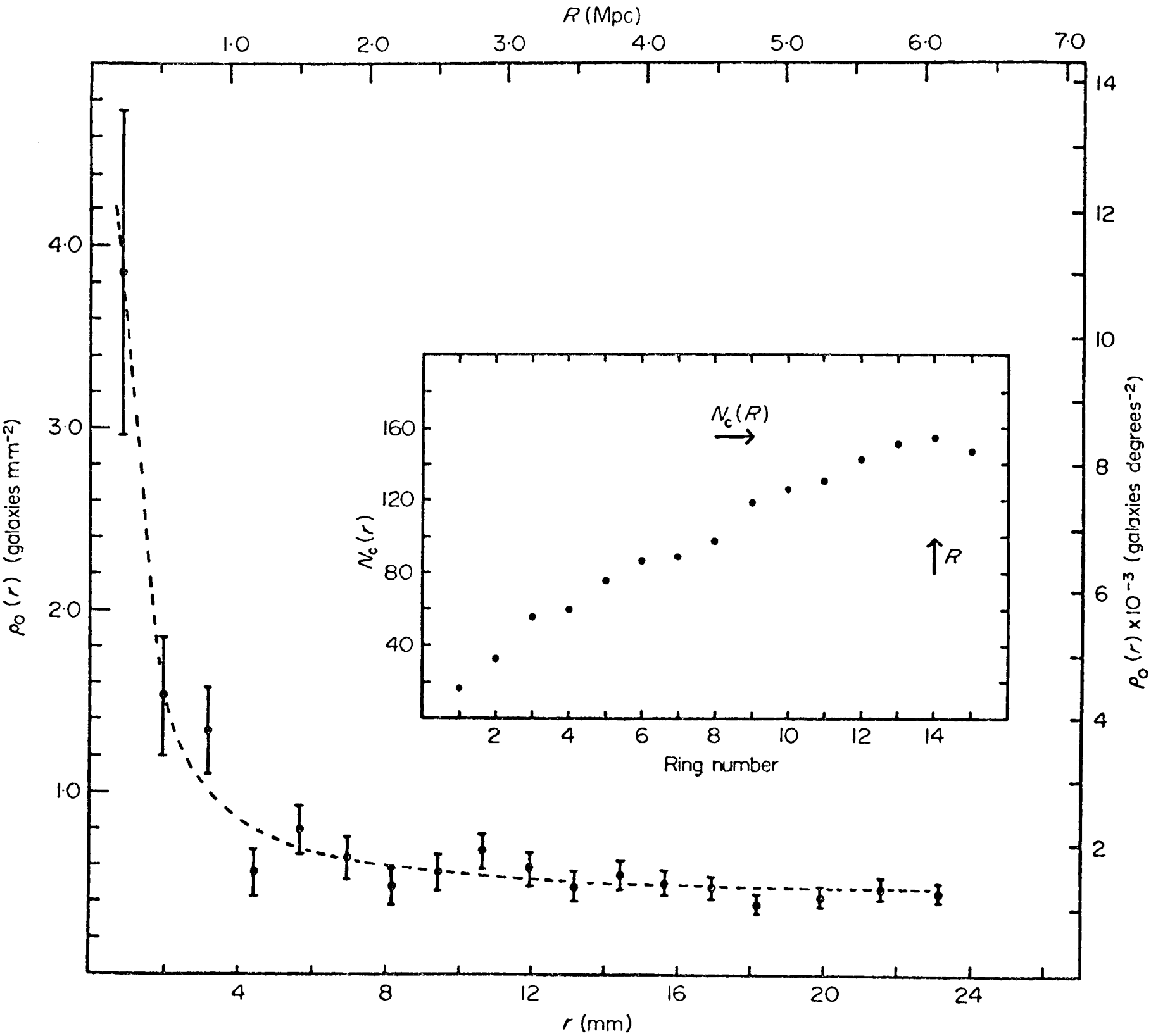

FIG. 6 The cluster A1677. C = 0.12

TABLE IX

Counts for cluster A801

Ring No.	Quadrant				Mean density	Mean radius	$N_o(r)$	$N_c(r)$
	NW	SW	SE	NE	(gal mm^{-2})	(mm)		
1	8	3	3	6	4.20	0.81	20	17
2	9	7	7	13	2.55	1.89	56	45
3	9	9	3	3	1.03	3.08	80	56
4	13	12	12	11	1.48	4.29	128	86
5	10	7	8	8	0.78	5.49	161	95
6	9	9	5	11	0.68	6.71	195	101
7	12	9	6	8	0.58	7.92	230	103
8	16	11	14	6	0.67	9.13	277	111
9	16	8	11	13	0.60	10.35	325	115
10	11	11	17	7	0.52	11.56	371	112
11	24	9	15	8	0.58	12.78	427	114
12	12	20	21	12	0.60	13.99	492	120
13	13	18	18	12	0.52	15.21	553	116
14	19	20	18	11	0.54	16.42	621	114
15	13	22	22	16	0.54	17.64	694	113

Mean background count = 0.55 gal mm^{-2}

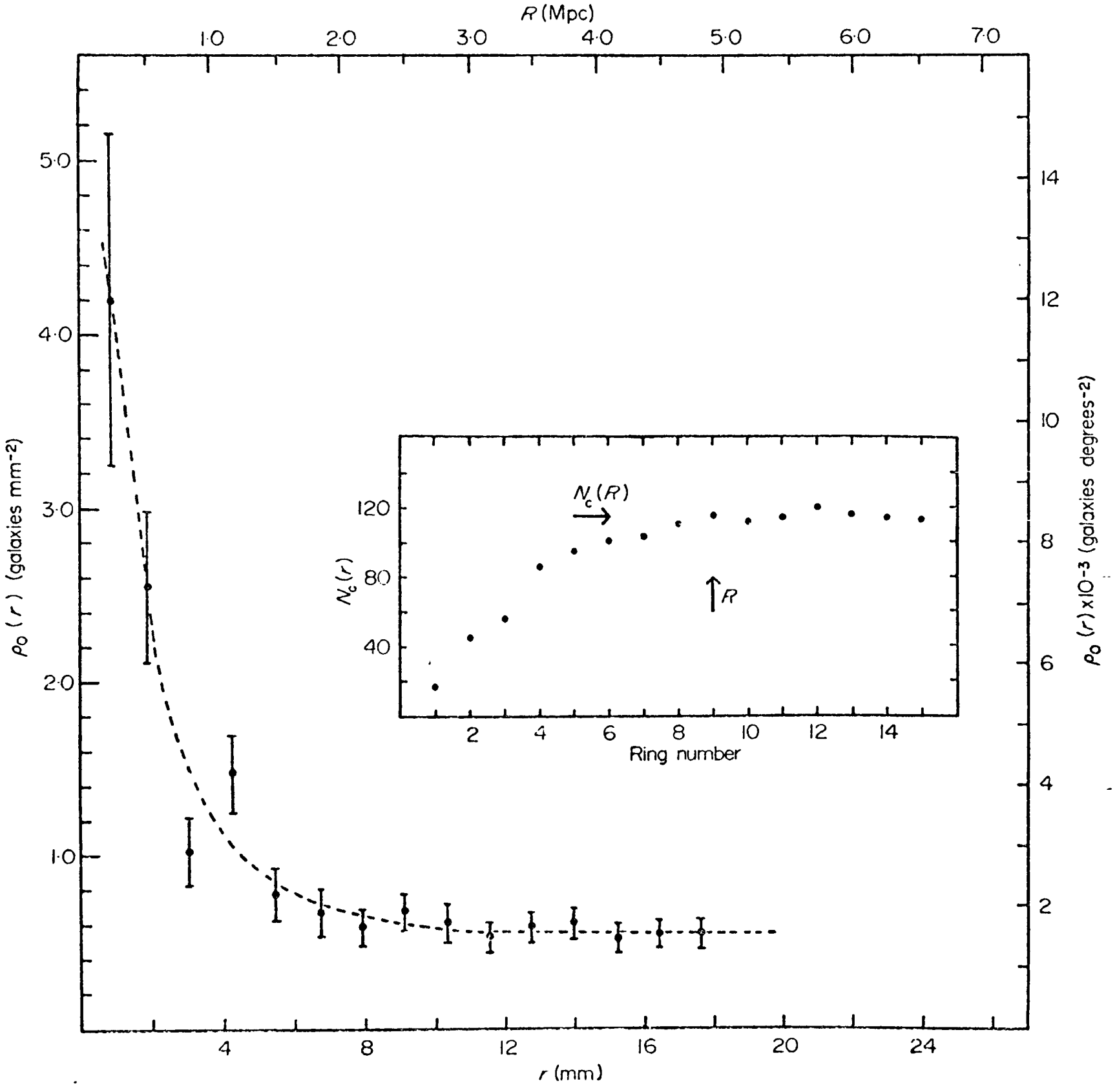

FIG. 7 The cluster A801. C = 0.43

TABLE X

Counts for cluster A1643

Ring No.	Quadrant				Mean Density	Mean radius	$N_o(r)$	$N_c(r)$
	NW	SW	SE	NE	(gal mm^{-2})	(mm)		
1	6	2	6	3	3.86	0.79	17	15
2	6	7	5	6	1.78	1.84	39	33
3	7	4	5	5	0.93	3.00	60	44
4	2	2	4	4	0.39	4.18	72	43
5	6	7	7	8	0.71	5.35	100	54
6	12	9	1	3	0.52	6.53	125	58
7	9	7	2	10	0.49	7.72	153	61
8	8	10	10	7	0.52	8.90	188	67
9	15	9	9	11	0.59	10.08	232	79
10	13	8	5	5	0.37	11.27	263	74
11	7	10	11	11	0.42	12.45	302	73
12	14	10	16	11	0.50	13.63	353	81
13	12	16	15	13	0.50	14.82	409	89
14	13	22	8	8	0.42	16.00	460	87
15	19	13	18	13	0.50	17.19	523	96
16.5	19	19	21	16	0.43	18.82	607	91
17.8	15	19	14	18	0.34	20.32	673	75
19.1	17	29	17	21	0.41	21.83	757	71

Mean background count = 0.43 gal mm^{-2}

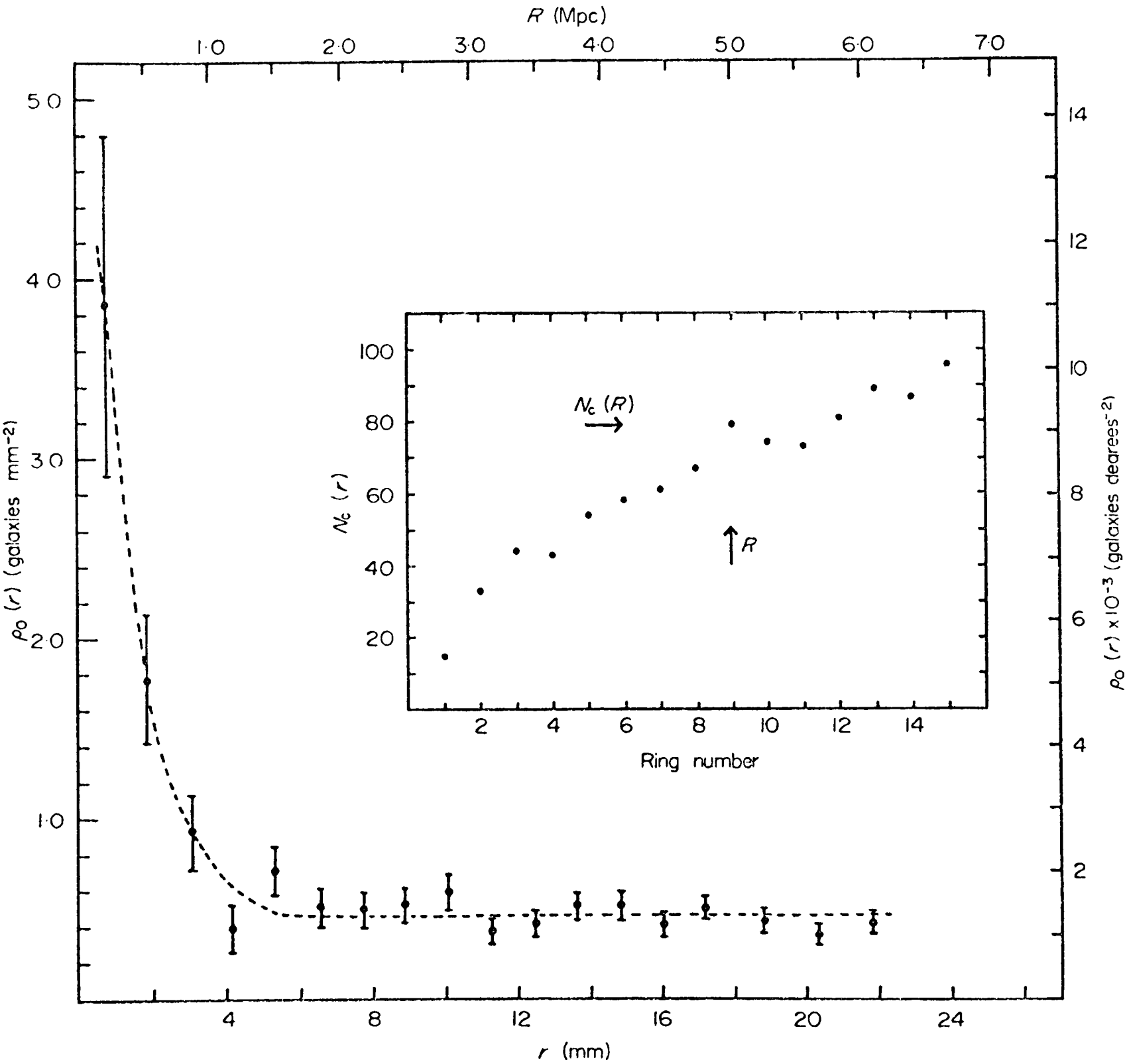

FIG. 8 The cluster A1643. C = 0.28

TABLE XI

Counts for cluster A732

Ring No.	Quadrant				Mean density	Mean radius	$N_o(r)$	$N_c(r)$
	NW	SW	SE	NE	(gal mm^{-2})	(mm)		
1	4	5	4	2	3.36	0.78	15	12
2	6	4	7	2	1.43	1.82	34	24
3	5	6	6	7	1.14	2.97	58	37
4	4	3	7	4	0.60	4.13	76	38
5	12	11	5	7	0.90	5.30	111	52
6	16	5	9	9	0.82	6.47	150	66
7	7	6	7	15	0.59	7.64	185	68
8	12	15	13	12	0.80	8.81	237	85
9	12	10	20	10	0.70	9.98	289	97
10	26	8	16	9	0.70	11.15	348	110
11	14	14	13	11	0.57	12.32	400	112
12	11	20	16	16	0.63	13.49	463	121
13	22	12	16	15	0.61	14.66	528	128
14	16	22	21	9	0.58	15.83	596	133
15	22	16	11	13	0.49	17.01	658	128
16.5	-	-	-	-	0.61	18.62	764	121
17.8	-	-	-	-	0.60	20.11	876	132
19.1	-	-	-	-	0.50	21.60	976	123

Mean background count = 0.56 gal mm^{-2}

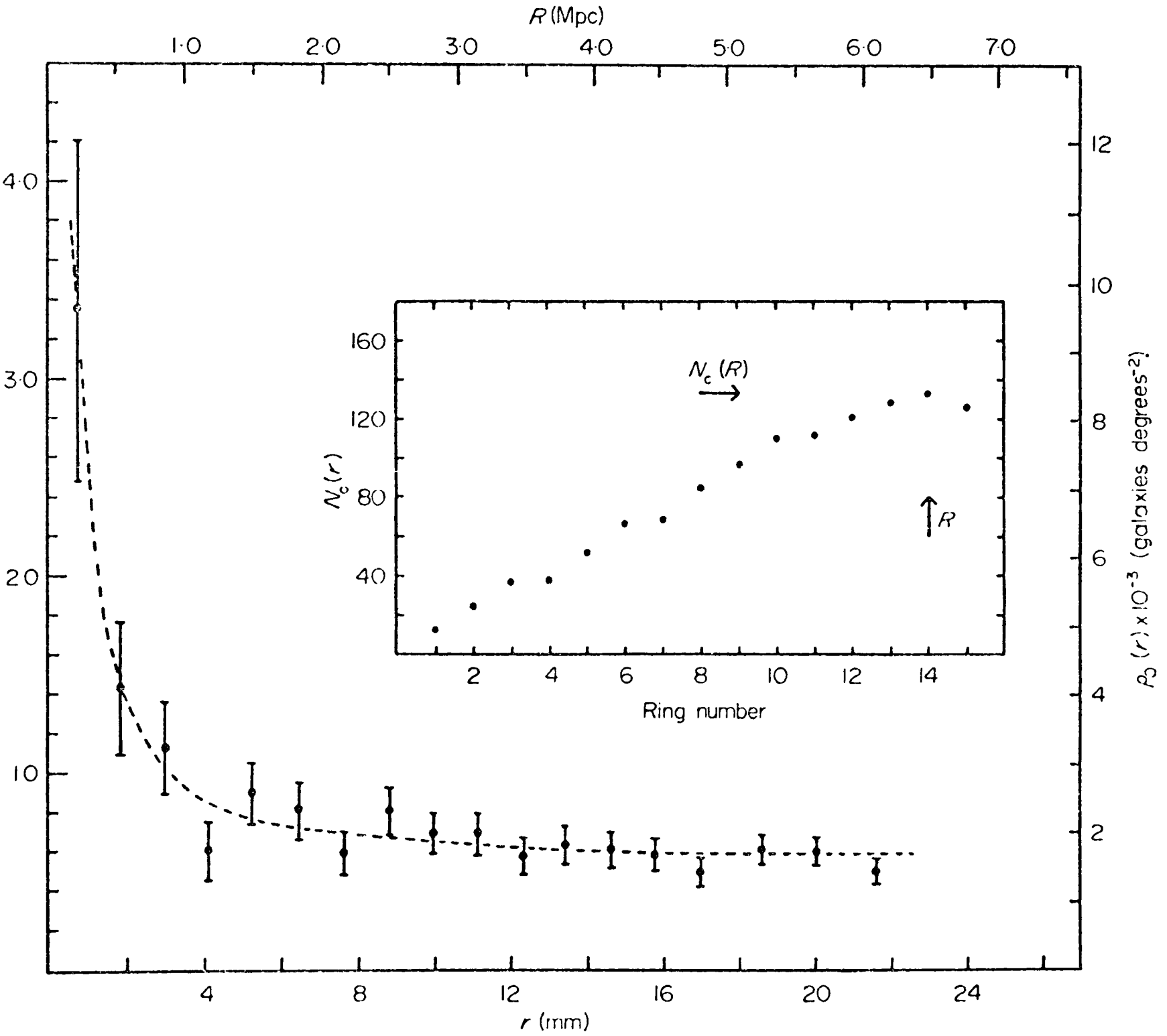

FIG. 9 The cluster A732. C = 0.10

nearby clusters. A1553, which has a deficient SW quadrant, lies in the field of the Virgo cluster, whose centre is about 2.7° to the NW. The counts in the NW quadrant of the cluster are higher than those in the other quadrants. A2100 may lie behind a nearer cluster; the background count near the cluster is some 40% higher than the mean for the other eight clusters, 0.72 gal mm^{-2} as compared to 0.51 gal mm^{-2}; a similar effect is apparent in Zwicky's catalogue (Zwicky and Herzog, 1966). Furthermore, two other rich clusters lie nearby, A2096 and A2093, the former being centred 19 arcmin to the SW and probably overlapping A2100 to within 10 arcmin of its centre. A1413 appears to be elongated NW and SE; this has already been shown in the isopleths of Noonan (1972a) and the elongation seems to lie very roughly along the major axis of the image of the supergiant cD galaxy at the cluster centre (Austin and Peach, 1974b). In Chapter 3 of this thesis it will be shown that the cluster is indeed elongated and that the elongation is a property principally of the fainter galaxies. Sastry (1968) has also studied the brighter member galaxies and has claimed that they show circular symmetry. For A801 the excess in the NW quadrant is confirmed by the isopleths of Zwicky and Herzog (1963). It may be attributable to irregularities in the stellar background; $b^{II} = +43^{o}$ for this cluster and the stellar component of the counts is high.

In the next part of this Chapter these counts are analysed on the assumption of spherical symmetry. This is justified on the basis that most of the sample (A1413 is the only definite exception) have a distribution which is not incompatible with this assumption or whose apparent deviations from symmetry can be plausibly explained as due to contamination of the counts by either

stars or galaxies from other clusters.

2.4 The Determination of a Distance-Independent Characteristic Size

While the counts are unsuited to a study of the detailed structure of rich clusters as so few (~100) member galaxies are above the plate limit, they are adequate for a preliminary study of cluster sizes. Sizes of clusters are difficult to determine because of the indefiniteness of the boundary between a cluster and the field, and sizes based solely on the outermost extent of the cluster are highly sensitive to the adopted background density. The search for the definition of such a size for the Coma cluster has led in the past to a well known controversy, in which Zwicky (1957) claims his counts indicate a radius of 6^{o} and other investigators, Noonan (1961) and Omer, Page and Wilson (1965) find a radius of around 100'. The disagreement stems from a difference in the adopted background density, Zwicky claiming a drop to the background density beyond 6^{o}. On the scale of cluster sizes found here, a radius of Coma of 6^{o} would make it some four times larger than the mean for the sample. Rood et al. (1972) in a recent review of the structure of the Coma cluster, after an analysis of galaxies whose radial velocities put them as clear cluster members, concluded "that it is hard to imagine that the density really reaches zero at a radius of less than 300'". Such an analysis clearly reduces the background interference and it is probable that the other estimates refer to a limit within which the cluster can be readily distinguished from the background. Such differences clearly highlight the need for a cluster size parameter that is not critically sensitive to the field density.

Any definition of a cluster size that will be acceptable as a distance indicator must itself be distance independent. In an investigation of the θ-z relation for clusters using Zwicky's (1957) definition of angular size as the mean diameter of the isopleth at which the surface density of galaxies to a limiting magnitude 3 mag. fainter than the brightest cluster member is twice that of the nearby field, Peach and Beard (1969) showed empirically that there was a strong dependence of size on distance, apart from any conceivable cosmological effects, which was unambiguously attributable to the choice of definition. In this paper they showed that for a sample of 646 Abell clusters identified with clusters in the Zwicky catalogue (Zwicky et al. 1961-1968), whereas the sizes as defined had small (~45%) dispersions, with no discernible dependence on richness class, the sizes were not normally distributed about the means, in the sense that there was an excess of small clusters. The reasons for this and the dependence of size on distance has been discussed by Noonan (1972a, 1973), although Abell (1962) had discussed the problem much earlier.

If the angular field density of galaxies on the sky is given by N_f (i.e. number per solid angle) then the density of cluster galaxies at the defined boundary is also N_f. If D is the angular size distance to the cluster and $\sigma(r)$ is the areal density of cluster members at a projected radius r from the cluster centre (i.e. number per unit area), then it is clear that

$$\sigma(R) = N_f / D^2$$

and this serves to define the linear cluster radius R. However the right hand term depends on the limiting magnitude m as well as on D. For the nearer clusters N_f varies as $10^{0.6m}$ and D varies as $10^{0.2m}$. Thus $\sigma(R)$ is proportional to D for such clusters.

In the outer parts of clusters the projected surface density can be approximated by a variation of $\varsigma(R) \propto R^{-1}$, and so R varies as D^{-1} and the angular diameters are inversely proportional to the square of their distances. These considerations are admittedly somewhat general and may only apply to rich clusters and only over a certain range in distance. If the clusters are too close R may be close to the cluster's edge. For clusters near the faint limit R may be close to the cluster's centre. However it is clear that the observation of Peach and Beard of an excess of small clusters in their sample has a ready explanation in the fact of the distance dependence of the Zwicky size. Three proposed methods of defining an angular size that would not appear to be open to this criticism will now be discussed and their use tested by application to the cluster counts.

2.4a The structural length of the isothermal gas sphere

Zwicky (1941a, 1957) has shown that the observed surface densities of galaxies in the region of a cluster can often be well represented by the projected density of an Emden isothermal gas sphere. It should be iterated that it has not been shown that the distribution of galaxies in rich regular clusters is uniquely represented by the bounded isothermal polytrope and it cannot be concluded with certainty that clusters are in statistical equilibrium. Other investigators have experimented with different mathematical representations of the density distribution in clusters. De Vaucouleurs (1960) has suggested that the surface density of galaxies in the Coma cluster follows closely a law of the form

$$\log \varsigma(r) = ar^{\frac{1}{4}} + b \qquad (2.2)$$

where $\rho(r)$ is the projected density at a distance r from the centre and a and b are constants. This law is similar to that found for the surface brightness distribution of elliptical galaxies (De Vaucouleurs, 1948). Scott (1962) has represented counts of five distant clusters on 200-in. plates taken by Zwicky (1956a) by trivariate normal Maxwellian distributions in which she fits the dispersion parameter σ to the observations. All of these mathematical distributions seem to fit actual clusters about as well as the isothermal one, and each involves the fitting of some sort of scale factor. In following the representation of the isothermal polytrope it is not necessary to be committed to any views on the state of equilibrium of clusters; it is simply used as a convenient parameterisation of the density distribution from which a characteristic size can be derived. With this restriction Bahcall (1972) is followed and $\rho_o(r)$, the observed surface density distribution as a function of radius, is written as

$$\rho_o(r) = \alpha \rho_i(r/\beta) + \gamma \qquad (2.3)$$

or equivalently

$$\alpha^{-1}(\rho_o(r) - \rho_f) = \rho_i(r/\beta) - D \qquad (2.4)$$

where ρ_f is the observed constant background density and $\rho_i(r/\beta)$ is the normalised projected isothermal gas sphere density as a function of the dimensionless radius $\xi = r/\beta$. $\rho_i(\xi)$ has been tabulated by Zwicky (1957). The quantity α is a normalisation factor for the density and γ is related to the background density through the relation $\gamma = \rho_f - \alpha D$ where D is a cut-off parameter in the gas sphere distribution. A non-linear least squares routine was devised to find the best-fitting values of the parameters in the relation (2.4). β, which is called by Zwicky the 'structural length', is given for the sample in

Table I with the estimated standard error of the determination.

In these fits the parameters that are internally well determined are γ which is essentially dependent on the wings of the density distribution, and the product $\alpha\beta$ which is essentially dependent on the core. For the nine clusters in this study the correlation coefficient between α and β has a mean value $r_{\alpha\beta} = -(0.78 \pm 0.23)$, namely a high degree of negative correlation. Since the value of the normalisation factor α has to be determined from the inner ring counts, errors in these counts lead directly to uncertainties in β. The counts in the inner rings are vulnerable to errors other than those due to the intrinsically small number of counts, in particular to the precise centre chosen for the counting and in a lesser degree to the angular resolution of the counting rings. In some clusters trial changes of the cluster centre and the resolution of the ring counts were made, and such changes were found to alter the value of β by one to one and a half times the estimated internal error of the original fit. On average the internal error for β was 24% and external errors are certainly of the same order. For the nine clusters here the fits gave a mean χ^2 probability of 45%, i.e. there is a probability of greater than 45% that a fit less good than the one obtained would be found if the gas sphere distribution were exactly correct. Values ranged from 8% for A1553 to 80% for A1930. The broken lines in Figs 1-9 are the least squares best-fitting lines. It should be remarked here that counting stars as galaxies should not materially affect the value of β as such images would only contribute to a smooth background, but failure to include galaxies could generate a non-statistical noise in the cluster density, since such errors might be proportional to the number counted in each ring and not

to the square root of the number (Yahil, 1974).

2.4.b The characteristic mutual separation of cluster galaxies

A different approach to a definition of angular size has been taken by Noonan (1972b). Let $N_c(r)$ be the number of cluster galaxies within a projected distance r from the cluster centre. Then the mean value of r is

$$\bar{r} = \int_0^R r \frac{dN_c(r)}{dr} dr / N_c(R) \qquad (2.5)$$

which integrates by parts to give

$$\bar{r} = R - \int_0^R \frac{N_c(r)}{N_c(R)} dr \qquad (2.6)$$

Here R is the outermost radius of the cluster. The integrand is derived from the counts after subtraction of the background N_f, writing for $N_o(r)$ the observed counts

$$N_o(r) = N_c(r) + \pi N_f r^2 \qquad (2.7)$$

The derivation of $\bar{r}$ proceeds as follows: a plot of $N_o(r)$ against r^2 gives a curve tending to a slope πN_f beyond a point which gives a value for R. The integral in relation (2.6) is replaced by a summation over the discrete rings. The cumulative ring counts $N_c(r)$ are plotted as a function of ring number in the inserts to Figs 1-9 which also show the adopted value of R and the cluster population $N_c(R)$.

A detailed analysis of the errors inherent in this method is given by Noonan. In marked contrast to β, the derived value of $\bar{r}$ is relatively insensitive to the choice of cluster centre. For the cluster A1413, for example a change of centre of about 0.5 arcmin, i.e. a change of 10% of the value of $\bar{r}$, changed $\bar{r}$ itself by only 0.1 arcmin, about 2%. In all nine cases it is estimated that centring errors as percentages of the derived values of $\bar{r}$

are not greater than 25%, leading to external errors from this cause to less than 6%. Further the values of $\bar{r}$ are not greatly dependent on the value of N_f and R.

If the background N_f is uncertain, then $N_c(r)$ should be written as a function of N_f, $N_c(r,N_f)$ and hence relation (2.7) becomes

$$N_o(r) = N_c(r,N_f) + \pi N_f r^2 \qquad (2.8)$$

and relation (2.6) becomes

$$\bar{r}(N_f) = R(N_f) - \int_o^{R(N_f)} F(r, N_f)\, dr \qquad (2.9)$$

Fluctuations of the field density from point to point are of the order of ±10% and the error in the mean N_f derived for each cluster is less than this at ±5%. The error in $\bar{r}$ caused by this uncertainty is of this order and it is estimated that uncertainties in N_f and R lead to an external error in $\bar{r}$ of no greater than 5%.

The most important uncertainty is due to the discrete nature of the ring counts and in the consequent approximation to the integral in (2.6). It is necessary to approximate the integral by

$$\bar{r} = R - \frac{S - \frac{1}{2}N_c(R)}{N_c(R)}\,\Delta r \qquad (2.10)$$

$$= R + \tfrac{1}{2}\Delta r - {}^{S}/_{N_c(R)}\,\Delta r$$

where $S = \sum_{p=1}^{P} N_c(p\Delta r)$ and $R = P\Delta r$.

The probable error in $\bar{r}$ is given by

$$d\bar{r} = \frac{S\Delta r}{N_c(R)} \left[\left(\frac{\delta S}{S} \right)^2 + \left(\frac{\delta N_c(R)}{N_c(R)} \right)^2 \right]^{\frac{1}{2}} \qquad (2.11)$$

$$\approx (R - \bar{r}) / \sqrt{N_c(R)}$$

if $S >> N_c(R)$.

The standard errors from these approximations have, for this sample, a mean of 13% and are larger than the external error. The

values of $\bar{r}$ and their estimated standard errors for the nine clusters are given in Table I and for clusters analysed by others in Table II.

The value of $\bar{r}$ is essentially determined by the outer parts of the density distribution as opposed to β which is fixed by the core. Large changes in the core density produce only small changes in $\bar{r}$ due to the relatively slow fall off in density outside the core which gives greater weight in the determination to the outer rings.

2.4.c Secondary maxima in the radial density distribution

The possible existence of secondary maxima in the surface density distributions of the Coma, Hydra and Cancer clusters was remarked on by Sharov (1959) in his discussion of counts by Zwicky (1957). Subsequently similar features have been noticed by Omer, Page and Wilson (1965) in Coma, Clark (1968) in A2199 and Bahcall (1971) in A1132. Bahcall noted that the peak seemed to occur at a radial distance of 2.2 ± 0.6 Mpc from the cluster centre and suggested its use as a distance indicator. Recently, Oemler (1974a) has suggested the presence of such a feature in the luminosity distribution of some 15 clusters studied by photographic photometry, and concludes that the feature must be due to the initial distribution of mass in the cluster's vicinity. Saslaw (1972) has interpreted these possible features as signs of the fluctuation correlations produced in the formation of clusters from gravitational instabilities.

Inspection of the counts in Figs 1-9 does indeed show possible secondary maxima in the surface density distributions at a radius of between 1.5 Mpc and 3.0 Mpc in some of the clusters. In some cases this feature appears in three out of the four quadrants,

TABLE II

Clusters for which counts are published and for which values of either β or $\bar{r}$ have been derived

Cluster	Redshift	Bautz–Morgan type	Richness	N_{SH}	Reference for counts	β (arcmin)	$R_{3\beta}$ (Mpc)	$\bar{r}$ (arcmin)	$R_{\bar{r}}$ (Mpc)	C	$\bar{r}_c$ (arcmin)
A1060	0·0115	III	1	51	**5, 10, 11**	4·0 (**13**)	0·243	48·4 ± 8·7 (**7**)	0·979	0·248	48·14
Hydra I											
Pegasus	0·0127	II	0	59	**13**	—	—	32·0 ± 9·3 (**7**)	0·713	—	—
Cancer	0·0159	III	0	17	**13**	1·77 (**13**)	0·147	68·2 ± 5·0 (**7**)	1·891	0·078	45·11
A426	0·0181	II–III	2	63	**13**	3·33 (**13**)	0·314	—	—	—	—
Perseus											
A1367	0·0204	II–III	2	76	**9**	—	—	21·9 ± 3·5 (**7**)	0·772	—	—
A1656	0·0222	II	2	115	**8, 13**	2·0 (**13**)	0·220	43·9 ± 4·8 (**7**)	1·679	0·131	33·50
Coma						2·0 (**3**)					
						1·75 ± 0·24 (**15**)					
A2199	0·0303	I	2	89	**4**	1·76 (**3**)	0·285	20·4 ± 1·1	1·048	0·272	20·63
						1·9 ± 0·12 (**15**)					
A2065	0·0722	III	2	89	**12**	0·9 ± 0·10 (**15**)	0·305	14·9 ± 2·6 (**7**)	1·684	0·181	15·91
Corona Borealis											
A1132	0·1345	II–III	1	35	**1**	0·37 (**3**)	0·209	—	—	—	—
Ursa Major II						0·36 ± 0·08 (**15**)					
A1413	0·1426	I	3	155	**6**	—	—	4·8 ± 1·5 (**7**)	0·944	—	—
A31	0·1595	III	2	64	**2**	0·78 (**2**)	0·391	4·2 ± 0·8	0·901	0·434	6·12
						0·44 (**2**)					
0024 + 1654	0·38	III	2	113	**14**	0·21 (**3**)	0·226	—	—	—	—
						0·24 ± 0·04 (**15**)					

References:

(1) Bahcall (1971)
(2) Bahcall (1972)
(3) Bahcall (1973a)
(4) Clark (1968)
(5) Kwast (1966)
(6) Noonan (1972a)
(7) Noonan (1972b)
(8) Omer, Page & Wilson (1965)
(9) Rudnicki & Baranowska (1966)
(10) Zwicky (1941**b**)
(11) Zwicky (1942**c**)
(12) Zwicky (1956**b**)
(13) Zwicky (1957)
(14) Zwicky (1959)
(15) Calculations by the present authors

e.g. A732, and in the case of A1132 in four quadrants, in agreement with Bahcall's earlier work. Such peaks are, however, never displaced more than one and a half times the natural error $\sqrt{N}$ of the observations from a smooth curve drawn through the whole radial density distribution. Furthermore, relatively small maxima in the surface density distributions imply quite large and as yet physically unexplained maxima in the volume density distributions. The present evidence is not really strong enough to establish their existence as part of the structure of rich clusters. Fluctuations in the field may give rise to spurious features such as those discussed, although it is difficult to account for their appearance in some clusters in all quadrants. Obviously these features cannot be of use as distance indicators until much more is known.

2.4.d Radial segregation of cluster galaxies

The cluster parameters defined above in parts 2.4a and 2.4b, the structural length β and the mean radial distance $\bar{r}$, are estimates of characteristic sizes of clusters which are distance independent on the following fundamental assumption; that there is no radial segregation by luminosity, colour or type of the galaxies in the inner parts of the clusters. If any such segregation exists the inferred values of β and $\bar{r}$ would be a function of the limiting magnitude of the counts, as the detection of galaxies at the plate limit obviously depends on their luminosity, their colour in the plate passband and on their type as it affects their surface brightness.

The observational evidence for and against segregation in clusters is confusing and no definite decision on its existence has yet been reached. If a cluster has reached a state of

equipartition of energy as a result of energy exchanges from galaxy encounters, then the fainter, presumably less massive, galaxies should be more widely distributed in space than the brighter ones. Zwicky (1942a) long held the view that clusters must be relaxed, from a general consideration of equilibrium in the universe, and presented evidence, Zwicky (1942b), that such segregation exists among the brighter Virgo cluster galaxies; but there is also a segregation according to galaxy type, the spirals showing a larger radial distribution than the ellipticals. Both Holmberg (1962) and de Vaucouleurs (1961b) have shown that the mean radial velocities are different for the spirals and ellipticals in the cluster. De Vaucouleurs has argued that the Virgo cluster is really two clusters seen in projection; one being a compact cluster of ellipticals and SO galaxies and the other a loose open cluster consisting mainly of spirals and irregulars. If this is true, differences in the radial distribution of Virgo cluster galaxies of different types and/or magnitudes cannot be regarded as evidence of segregation. Abell (1972) and Bautz and Abell (1973) have argued independently for this difference in mean radial velocity of galaxy types in the Virgo cluster by the method of matching cluster luminosity functions.

Zwicky (1957) has further claimed the existence of segregation in a number of other clusters, in particular in Coma, but Noonan (1961) has re-analysed his observations for this cluster and finds no significant support for this conclusion, although he does write that "the 18-in. points appear to be shifted approximately 2.5 arcmin closer to the centre than the 48-in. points", referring to a plot of the distribution of the cluster population as a function of radial distance from the

cluster centre based on plates taken with the Palomar 18-in. and 48-in. Schmidt telescopes. Omer, Page and Wilson (1965), from the analysis of their own and Shane's counts for Coma arrived at the same conclusion as Noonan. The different conclusion of Zwicky results from a different interpretation of the surface density of field galaxies, as explained earlier in part 2.4. Rood et al. (1972) recently reviewed all the available observations of Coma and found no definite evidence of segregation. They found a slight tendency for bright galaxies in the central 9 arcmin of the cluster to have a lower velocity dispersion, but the result was very dependent on the subsets of the sample considered because of the small numbers of galaxies in each subset. Zwicky and Humason (1964) have claimed that the fainter members in the cluster Al94 have a slightly higher velocity dispersion indicative of a degree of equipartition of energy, but this result vanishes if the 6 brightest galaxies are left out of the analysis. At present no dependence on magnitude has been found for the velocity dispersion of galaxies in a cluster. Rudnicki (1963) counted galaxies in the cluster A426, the Perseus cluster, and claimed that the faint galaxies showed a wider surface distribution than the bright ones. However one side of the cluster is partially hidden by inter-stellar absorption and this may have led to too low an estimate for the field density, leading to the observed segregation in a similar way as that in Coma is found by Zwicky.

There have been many studies of the distribution of dwarf galaxies in clusters. It is emphasised that the dwarfs studied by some investigators have a restricted definition. Reaves (1966) in his study of the Coma cluster used only a small fraction of the faint galaxies. The properties usually assigned to dwarfs are

(1) low surface brightness, (2) low luminosity gradient and (3) no nucleus. Some investigators impose a size restriction. In van den Bergh's (1959) catalogue of dwarfs the diameters exceed 1 min of arc. Hodge (1959, 1960), in his initial study of Fornax-cluster dwarfs, required that major diameters exceed 0.6 min. of arc; however in his final paper, (Hodge, Pyper and Webb, 1965), dwarfs as small as 12 arcsec diameter are used. Hodge et al. compared the distribution of such faint galaxies in the Fornax cluster with that of the brightest members and found that these galaxies showed less central concentration suggesting the existence of a real segregation. This effect appears real but small sample fluctuations or subclustering may have influenced the result. Furthermore the Fornax cluster is very poor in comparison to the rich Abell clusters. Rood and Turnrose (1968) found that dwarfs of low surface brightness near the centre of the Coma cluster were less centrally concentrated than the bright galaxies. Noonan (1971) has studied the distribution of faint dwarf galaxies in the Coma and Corona Borealis clusters (A1656 and A2065), where the term dwarfs referred to galaxies identifiable as galaxies on 200-in. plates but not on 48-in. Schmidt plates. He confirmed the studies of Reaves for Coma and found that the dwarfs were less concentrated than the bright galaxies for these two clusters. It should be remarked that these dwarfs have absolute V magnitudes of around -14.0, compared to galaxies at the plate limit of the nine clusters studied here, which at the general redshift of the sample would have absolute V magnitudes of around -20.0.

Of great interest in the context of the use of the structural length are the investigations of Bahcall (1973a, 1973b) who has

calculated values of β from counts in Coma to three limiting magnitudes and from counts in A2199 to four limiting magnitudes on plates taken with different telescopes and emulsions. In all cases the results agree to within the accuracy of the determinations. Evidence for or against segregation in clusters based on actual photometry, as opposed to counts, is very scarce. Rood (1969) found that concentration towards the cluster centre tended to increase with increasing luminosity for galaxies in the core of the Coma cluster, from photometry of galaxies by Rood and Baum (1967, 1968). Oemler (1974a) has found segregation in the cD clusters A1904, Coma, A2199 and A2670 with the brighter galaxies more centrally concentrated than the fainter ones. To what extent the results in the cD clusters is affected by subclustering or other cosmogonic effects (Icke, 1973) is not clear. Bahcall (1973a) found an anisotropy of the bright galaxies in Coma (V_{26}<15.0 mag) which could arise from sub-clustering around each of the two supergiant cD galaxies, NGC 4874 and NGC 4889, at the centre. However there may be a wider anisotropy. Noonan (1971) has found a similar tendency and Abell (1963) found the cluster to be slightly elongated in the NE-SW direction (Bahcall's anisotropy is in the sense that galaxies are more densely distributed in the E-W direction as compared to the N-S direction). Bahcall (1974) has confirmed the anisotropy of galaxies in the Perseus cluster, although there is no evidence for rotation in the measured velocities of the galaxies (Chincarini and Rood, 1971).

Evidence for forms of segregation of this type and other types for other clusters is necessarily even more incomplete. Sastry (1968) has found a correlation between the orientation of clusters containing cD galaxies and the orientation of the cD

galaxy itself. Rood and Sastry (1972) have examined this result in more detail for the cD cluster A2199 and confirm it, as well as finding other significant correlations, such as a tendency for galaxies of small ellipticity, major axis perpendicular to that of the cD galaxy, red colour, elliptical and SO type to be more concentrated towards the cluster centre than galaxies with large ellipticity, major axis parallel to that of the cD galaxy, blue colour and spiral type. Rood (1974) has further analysed the radial distributions of spirals and irregulars in the sample and has suggested that all or nearly all are field galaxies. Noonan (1972a) has suggested segregation by either colour and/or limiting magnitude in A1413. Austin and Peach (1974b) interpret Noonan's observations and those of Sastry (1968), using results obtained from photometry of cluster galaxies within 5 arcmin radius (~1 Mpc), as showing that the cluster consists of a spherical subsystem of brighter galaxies extending over most of the cluster volume co-existing with a prolate subsystem of fainter galaxies.

It is clear from the short review above that much further work is necessary to assess the importance of radial segregation in relation to the use of the θ-z cosmological test as well as to the general structure of rich clusters. While forms of segregation <u>may</u> exist in some clusters there is no evidence that there is any energy equipartition leading to a classical radial segregation by mass or luminosity.

In principle the effects of segregation could be corrected for if our knowledge about it were sufficiently detailed.

2.5 The Dependence of Cluster Sizes on their structure and population

The data for the nine observed clusters are collected in Table I. The values of β and $\bar{r}$ are given with their estimated standard errors and also given are the intrinsic radii of the clusters as determined by these two parameters in a cosmological model with $q_o = +1$ and $H_o = 50$ km s^{-1} Mpc^{-1}. The intrinsic radius corresponding to $\bar{r}$ is written $R_{\bar{r}}$; for that corresponding to β convention is followed by using 3β, to give a radius $R_{3\beta}$, which is almost exactly equivalent to the radius at half the central density of the projected gas sphere. Also tabulated are the richness of the clusters as defined by Abell (1958), the Bautz-Morgan type (Bautz and Morgan, 1970) and N_{SH}, the population as determined by Sandage and Hardy (1973). N_{SH} is the number of galaxies within 2.5 mag of the third brightest member and should be a better measure of population than N(R) which is dependent on distance and limiting magnitude. The cluster richness has population classes given by 50-79 for richness class 1, 80-129 for richness class 2 and 130-199 for richness class 3. The agreement between the various populations listed in Table I at first glance does not seem very good but it should be remembered that the Abell and Sandage-Hardy counts were counted within circles of fixed linear size at the cluster and took no account of possible variations in the structure of different clusters. Furthermore Abell's circle were on an Euclidean model with $\Theta \propto z^{-1}$, whereas Sandage and Hardy used a world model with $q_o = +1$ and $H_o = 54$ km s^{-1} Mpc^{-1}. At the distances of the clusters these circles correspond to $R_{Abell} \sim 2.3$ Mpc and $R_{SH} \sim 1.8$ Mpc in a model with $q_o = +1$ and $H_o = 50$ km s^{-1} Mpc^{-1}. At these distances the difference in magnitude, between

M_3+2 and $M_3+2.5$ and the limiting magnitude of the plate is small. Taking these variations into account there is overall agreement between the estimates for 5 clusters, A1930, A1413, A1677, A801 and A732. Some of the partial disagreement in the other clusters, for example A2100 and A1553, can be traced to different adopted values for the field density (see previous discussion on the symmetry of these clusters).

Clusters for which counts have been published by other authors and from which it is possible to derive values of β and $\bar{r}$ are listed in Table II. References are given to the source of the counts and to the reduction of β and $\bar{r}$. There are two clusters in common to Tables I and II, A1132 and A1413. For the cluster A1132 the counts in Table I were used in the following analysis because those of Bahcall were made from the vignetted part of a Sky Survey plate copy. In the case of A1413 which is treated in detail in Chapter 3, there is an unresolved problem of the dependence of $\bar{r}$ on colour or limiting magnitude in the results of Noonan (1972a) and here again the counts of Table I are used. Apart from these two clusters the data of both Tables are treated in conjunction and with equal weight in the subsequent discussion.

It is obvious from an inspection of the values of $R_{\bar{r}}$ and $R_{3\beta}$ that both of these measures of cluster size have considerable intrinsic dispersion; the standard deviation of both quantities from their means are about 35% which is considerably larger than the estimated standard errors of their determination. There is, however, a correlation between them in the sense that the larger the value of $R_{\bar{r}}$ for a particular cluster the smaller is $R_{3\beta}$. Recalling the discussion of part 2.4, $R_{3\beta}$ is a measure of the absolute size of the core of the cluster while $R_{\bar{r}}$ is a measure weighted more strongly in favour of the outer parts of the cluster.

Referring to R_r^- as the cluster radius and $R_{3\beta}$ as the core radius, it would appear that the smaller the cluster radius the larger the core. Trial and error indicate that R_r^- goes roughly as the reciprocal of $R_{3\beta}$ and this simple functional form of their relationship is shown in Fig. 10, in which R_r^- is plotted against $R_{3\beta}^{-1}$. For the observed sample of nine clusters the error bars are the estimated standard errors. For the other six clusters they are the mean percentage errors for the two quantities found in the observed sample, namely 24% for $R_{3\beta}$ and 13% for R_r^-. The correlation coefficient of R_r^- on $^1/R_{3\beta}$ is +0.75, which for a sample of 15 is statistically significant at the 5% level. In the figure the regression lines of R_r^- on $^1/R_{3\beta}$ and of $^1/R_{3\beta}$ on R_r^- are drawn. A close inspection of the scatter of points in Fig. 10 suggested that clusters of high population N_{SH} tended to have a larger R_r^- at a given $^1/R_{3\beta}$ than those of low population. This effect is shown in Fig. 11 where the residuals ΔR_r^- of the points of Fig. 10 from the regression line of R_r^- on $^1/R_{3\beta}$ are plotted against N_{SH}. The correlation coefficient of ΔR_r^- on N_{SH} is +0.51 which is statistically significant at the 10% level.

The existence of these two correlations suggests a joint regression of R_r^- on $^1/R_{3\beta}$ and N_{SH} giving an equation

$$R_r^- = (0.31\pm0.02)\,{}^1/R_{3\beta} + (4.36\pm0.49\times10^{-3})N_{SH} - (0.14\pm0.09) \qquad (2.12)$$

where the standard errors in the coefficients are indicated. The conclusion is that R_r^- is determined primarily by $^1/R_{3\beta}$ and to a lesser extent by population. No further correlations between the cluster parameters of Tables I and II have been found.

The relationship between R_r^- and $R_{3\beta}$ shown by equation (2.12) can be made clearer by introducing a parameter C, the concentration,

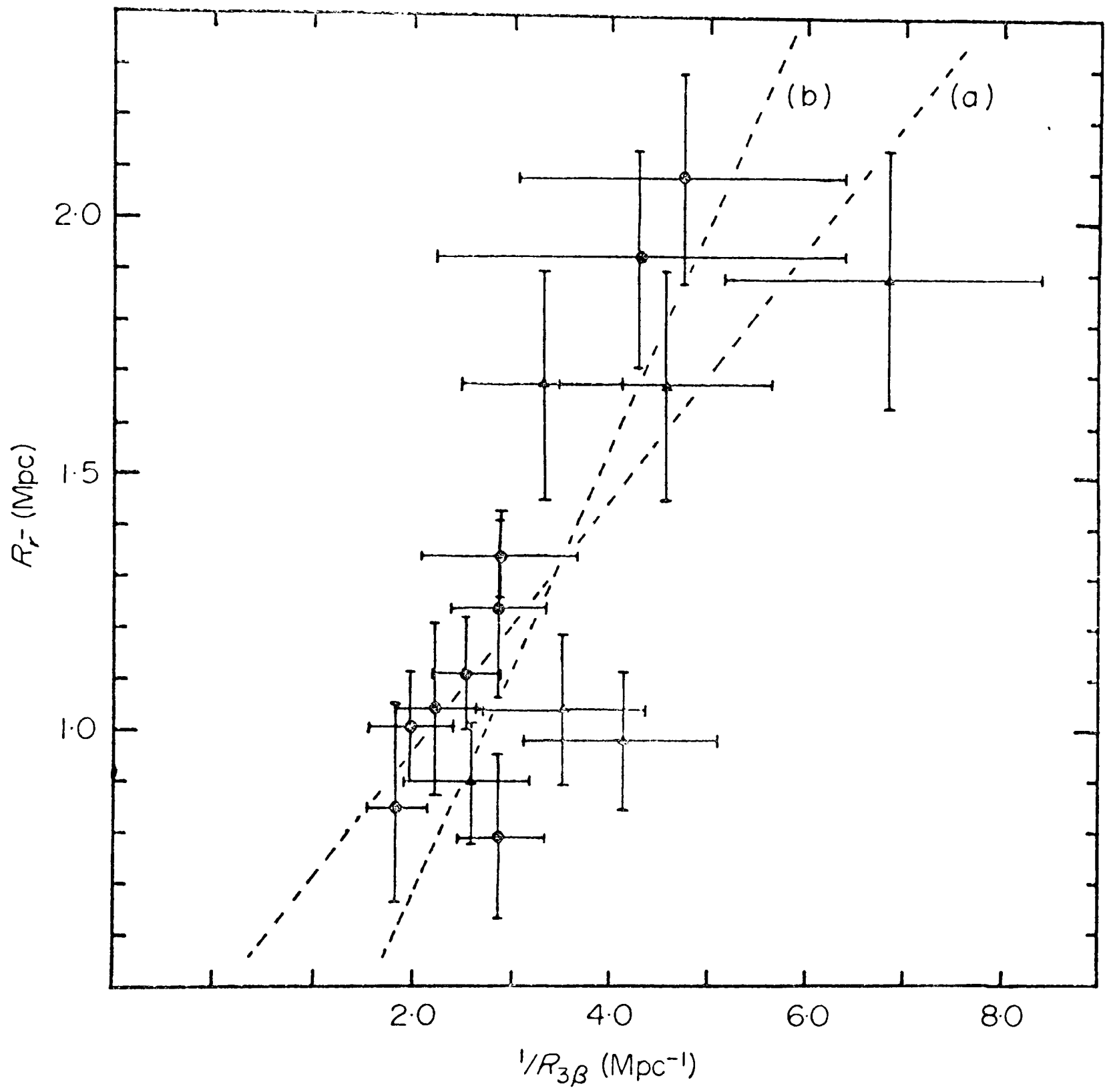

FIG. 10 The cluster radius R_r of 15 clusters as a function of the reciprocal of the core radius $1/R_{3\beta}$. The filled circles are the measurements for the clusters of Table I and the triangles are from Table II. The regression of R_r on $1/R_{3\beta}$ is labelled (a) while that of $1/R_{3\beta}$ on R_r is labelled (b). The correlation coefficient is +0.75. Error bars are the standard errors listed in the Tables.

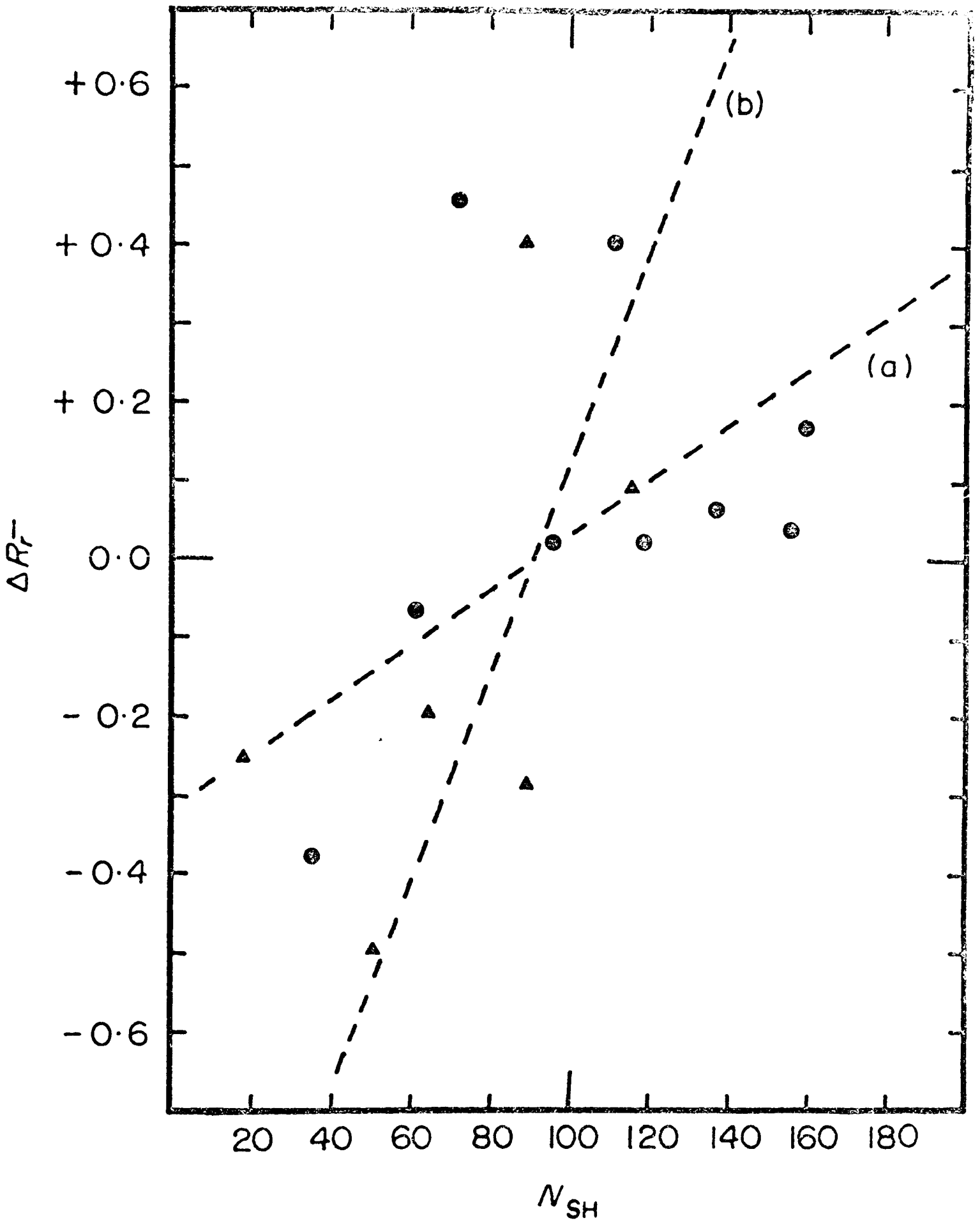

FIG. 11 The residuals ΔR_r^- from the regression line of R_r^- on $1/R_{3\beta}$ in Fig. 10 plotted against population N_{SH}. Filled circles and triangles as in Fig. 10. The regression of ΔR_r^- on N_{SH} is labelled (a) while that of N_{SH} on R_r^- is labelled (b). The correlation coefficient is +0.51.

defined as the ratio of the core radius to the cluster radius, namely $C = R_{3\beta}/R_{\bar{r}} = 3\beta/\bar{r}$. This will be a measure to which the high density core dominates the cluster at the expense of the less dense halo. High values of C correspond to clusters strongly condensed to their centres; an example is A1930 in Fig. 1 where the surface density distribution drops sharply down to the field background. A732 in Fig. 9 is a cluster of low C for which the core merges gradually into an extended halo. In Fig. 12 the cluster radius $R_{\bar{r}}$ is plotted against concentration to illustrate that smaller clusters are more concentrated, a conclusion that was implicit in equation (2.12). This plot also illustrates the dependence of size on population. N_{SH} has been enetered in the diagram beside the observed points and it will be seen that there is a tendency for clusters of low population to fall below the mean curve, thus reflecting the correlation of Fig. 11.

2.6 The Angular Diameter-Redshift Relation

The relationship given in equation (2.12) leads to a procedure for reducing the dispersion in the plot of observed angular radius $\bar{r}$ against redshift shown in the upper part of Fig. 13 by replacing $\bar{r}$ by an operationally defined corrected angular radius $\bar{r}_c$. It is assumed that the dispersion in $\bar{r}$ about the mean line (~35%) is due partly to observational error in $\bar{r}$ and partly to variation in intrinsic cluster radii. But this variation is related by equation (2.12) to two further observable parameters $R_{3\beta}$ (or β and z) and N_{SH}. It is therefore possible to infer from the observed values of β, z and N_{SH} the intrinsic cluster radius $R_{\bar{r}}$ to a precision determined by the uncertainties in the observed quantities and the coefficients of equation (2.12). If a standard cluster is now arbitrarily

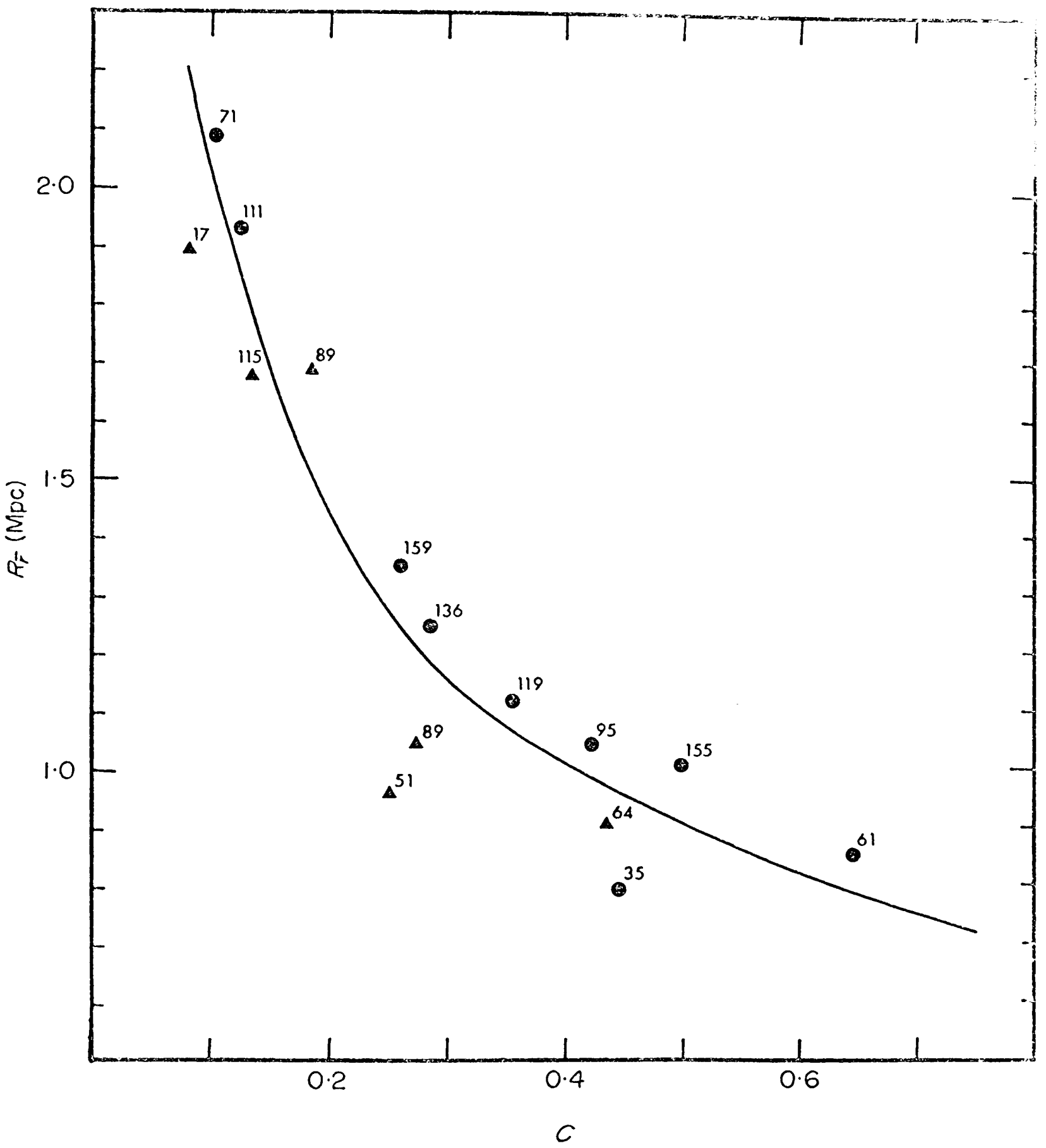

FIG. 12 A plot of the cluster radius $R_{\bar{r}}$ against concentration $C = 3\beta/\bar{r}$. Populations N_{SH} are indicated. The tendency of low population clusters to lie below a mean line drawn through the points should be noted; this illustrates the correlation of Fig. 11.

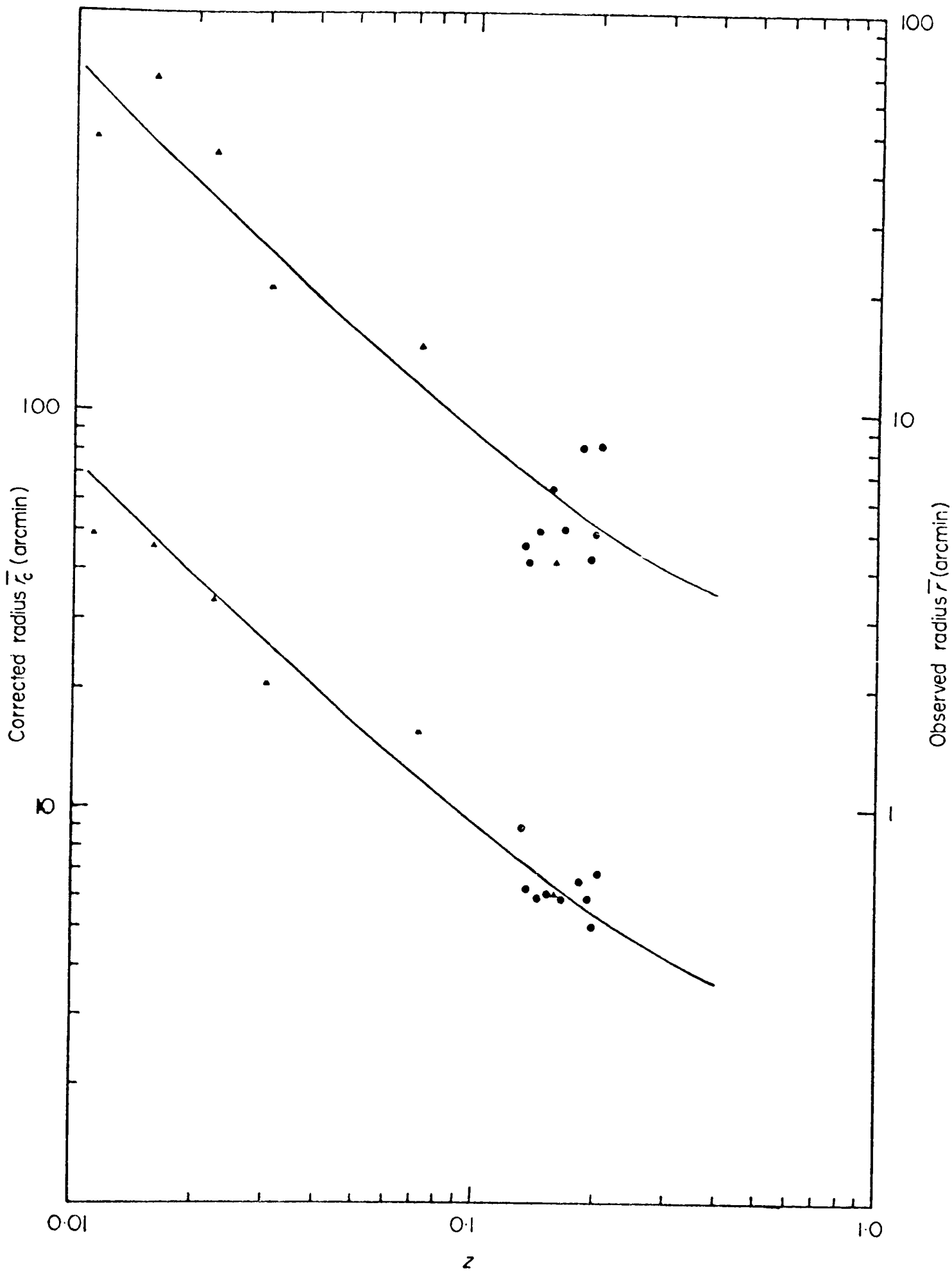

FIG. 13 Plots of angular radius against redshift Z for the uncorrected cluster radius $\bar{r}$ (upper plot and right-hand scale) and for the corrected radius $\bar{r}_c$ (lower plot and left-hand scale). Filled circles and triangles as in Fig. 10. The mean lines drawn through the points are for world models with $q_o = +1$.

defined to be one for which $R_{\bar{r}} = 1.35$ Mpc, the observed value of $\bar{r}$ can be adjusted to that angular radius which would be subtended by the standard cluster at the same redshift by writing

$$\bar{r}_c = \left(1.35/R_{\bar{r}}\right) \bar{r}$$

where $R_{\bar{r}}$ is calculated from equation (2.12).

A plot of $\bar{r}_c$ against z is given in the lower part of Fig. 13. There is a marked reduction in scatter. The dispersion about the mean line compares favourably with the scatter of points in the m-z diagram given for the brightest member of these and other clusters in Fig. 7 of Sandage and Hardy (1973). The standard deviation of Sandage's absolute magnitudes is 28% after application of corrections for aperture effect, K-dimming, galactic absorption, Bautz-Morgan type and richness. The mean value of $R_{\bar{r}}$ before correction is 1.31 ± 0.43 (sd) Mpc, while after correction $R_{\bar{r}_c} = 1.35 \pm 0.25$ (sd) Mpc, that is, the dispersion of corrected angular radii about the mean line of Fig. 13 is only 18%; this should be compared with the estimated error in the determination of $\bar{r}$ of 14%. At face value this implies that this use of the angular diameter-redshift plot is a more powerful method of determining q_o than the m-z plot for cluster galaxies.

There is a degree of circularity in this procedure which is not, however, fatal to this conclusion. The radii $R_{3\beta}$ in equation (2.12) are calculated in a world model with $q_o = +1$ and the coefficients of equation (2.12), being functions of q_o, are therefore only correct for this particular model. The corrected values of the angular diameter $\bar{r}_c$ have consequently been calculated on the assumption of this particular value of q_o and a plot of $\bar{r}_c$ against z such as that in Fig. 13 cannot be used directly to find an independent value. The situation is analogous

to the application of the aperture correction to the apparent magnitudes used in the m-z diagram, and a similar solution to the problem can be applied. It will be necessary to proceed to a final value of q_o by successive approximation, making an initial guess of q_o to find the coefficients of equation (2.12), finding an improved value by fitting to the $\bar{r}_c$-z plot and then using this improved value to recalculate the coefficients. Formally this scheme leads with this data to a value of q_o slightly greater than +1 with an uncertainty of ±1, but little weight should be placed on this conclusion.

CHAPTER 3

THE STRUCTURE AND LUMINOSITY FUNCTION OF THE CLUSTER A1413

3.1 Introduction

The study of the structure and photometric properties of clusters of galaxies is of importance if we are to understand their formation and that of their member galaxies. It has been seen in Chapter 2 that the study of clusters by galaxy counts has so far failed to demonstrate conclusively that they are in statistical equilibrium. Actual luminosity measurements of cluster galaxies should lead to more quantitative results. The determination of the luminosity function of galaxies has led in the past to much confusion and controversy between leading observers, and has led one, Gunn (1971), to write "that there is evidence that the luminosity function in clusters differs from that in the field, and neither is well determined". For these and other reasons the last few years has seen a renewed interest in the determination of the luminosity function of cluster galaxies (Oemler, 1974a; Austin and Peach, 1974b). In parts 3.4 to 3.6 of this Chapter the application of photographic photometry to the study of the structure and luminosity function of the cluster A1413 is described, preceded by a review of the investigations of the galaxian luminosity function to date in part 3.2 and a discussion of methods of galaxy photometry in part 3.3.

3.2 The Luminosity Function of Galaxies

The first study of the galaxian luminosity function was by Hubble (1936b) who determined the distribution of absolute

magnitudes of 134 spiral and irregular galaxies, and represented their luminosity function by a Gaussian error curve having a mean absolute photographic magnitude of -14.2 and a standard deviation of 0.85 magnitudes. (On the distance scale used in this thesis, with H_o = 50 km s^{-1} Mpc^{-1}, the mean would be about 5 mag. brighter). However Hubble's sample was not representative of a standard volume of space, galaxies being overridingly chosen for observation on their apparent brightness. Consequently the observed distribution of absolute magnitude p(M) should be written as

$$p(M) = C\ 10^{-0.6M}\ \phi(M)$$

where $\phi(M)$ is the luminosity function, and $\phi(M)\ dM$ is the number of galaxies in the range of absolute magnitudes between M and M + dM. If p(M) is normally distributed then so is $\phi(M)$. In Hubble's original distribution there was a significant departure from normality, there being an elongation towards fainter magnitudes. Neyman and Scott (1959) found a similar skewness in the distribution of absolute magnitudes of 349 spiral galaxies from the catalogue of Humason, Mayall and Sandage (1956). This asymmetry is such as to render a normal curve for $\phi(M)$ altogether unlikely.

The discovery of faint dwarf galaxies, such as those in Sculptor and Fornax, in the Local Group led Zwicky (1942a) to propose the existence of large numbers of low luminosity galaxies in the universe. From arguments based on the statistical equilibrium between stellar systems of various sizes and their mutual interaction, he predicted that the galaxian luminosity function must increase with decreasing luminosity. While the assumption of equilibrium of systems of galaxies seems now somewhat uncertain, the rise of the luminosity

function with decreasing luminosity is probably correct, at least for cluster galaxies in the observed magnitude ranges. Later, from an analysis of the mean population of clusters as a function of angular diameter, Zwicky (1957) derived the following expression for the integrated luminosity function of cluster galaxies

$$N(\Delta m) = k\ (10^{\Delta m/5} - 1) \qquad (3.1)$$

where $N(\Delta m)$ is the number of galaxies in the range Δm between magnitude m and the magnitude of the brightest cluster galaxy. However the angular diameters as defined by Zwicky are not distance-independent, as assumed in the derivation of equation (3.1) (Abell 1962; Scott, 1962). The reasons for this were discussed in part 2.4 of Chapter 2. Zwicky's formula appears to be qualitatively correct, however, in the fainter magnitude range (Abell, 1974; see Fig. 14).

The published data on galaxy magnitudes has been re-analysed by Kiang (1961) and Van den Bergh (1961). Kiang, from magnitudes of galaxies both in clusters and in the field, concluded that the data was consistent with a cubic law for $\phi(M)$ for the brightest 3 magnitudes and with an exponential Zwicky law for the fainter magnitudes. Van den Bergh has analysed the absolute magnitudes of 240 bright field galaxies, of which 48 are ellipticals. The luminosity functions for both types are in qualitative agreement with Zwicky's formula at faint magnitudes but rise more rapidly at their bright ends. The logarthmic integrated luminosity functions of both types exhibit a discontinuous change of slope after the first 2.5 magnitudes. Shapiro (1971) has analysed the luminosity function of 218 spiral and irregular galaxies and 24 ellipticals from the catalogue of de Vaucouleurs (1964). For the spirals and

irregulars he found the same change in slope in the logarithmic integrated luminosity function, the change occurring at an absolute photographic magnitude of about -19.5, with $H_o = 100 \text{ km s}^{-1} \text{ Mpc}^{-1}$.

Using the specialised technique of extrafocal photometry (Abell and Mihalas, 1966) Abell and his coworkers have determined the luminosity functions of 9 rich clusters consisting predominantly of elliptical galaxies. They have found that the logarithmic luminosity functions log N (Δm) can all be fitted together with horizontal and vertical shifts that depend only on the relative cluster distances and richnesses. Oemler (1974a) in his photometry of 15 Abell clusters finds that the luminosity functions of all the clusters are similar, with a small dispersion in absolute magnitude, even though some clusters are dominated by spirals and some by ellipticals. Such a combined integrated luminosity function is shown for 5 rich clusters, after Abell (1974), in Fig. 14; the clusters are A151, A1656, A2065, A2199 and A2670. The scales are in arbitrary units. The curve labelled Zwicky corresponds to Zwicky's integrated luminosity function as defined in equation (3.1). The function log N (Δm) shows a very definite change of slope after the interval of the brightest 2 to 3 magnitudes. This abrupt change of slope corresponds to a maximum in the differential luminosity function ϕ(M). Abell (1972) has argued that if this feature corresponds to some preferred physical dimension or quantity connected with the formation of galaxies in clusters, it would be expected to occur at the same absolute magnitude in all rich clusters. The apparent magnitude of the feature m* would then be an indicator of relative distance. The method uses measurements of a large number of cluster members and, hence, should be less subject to

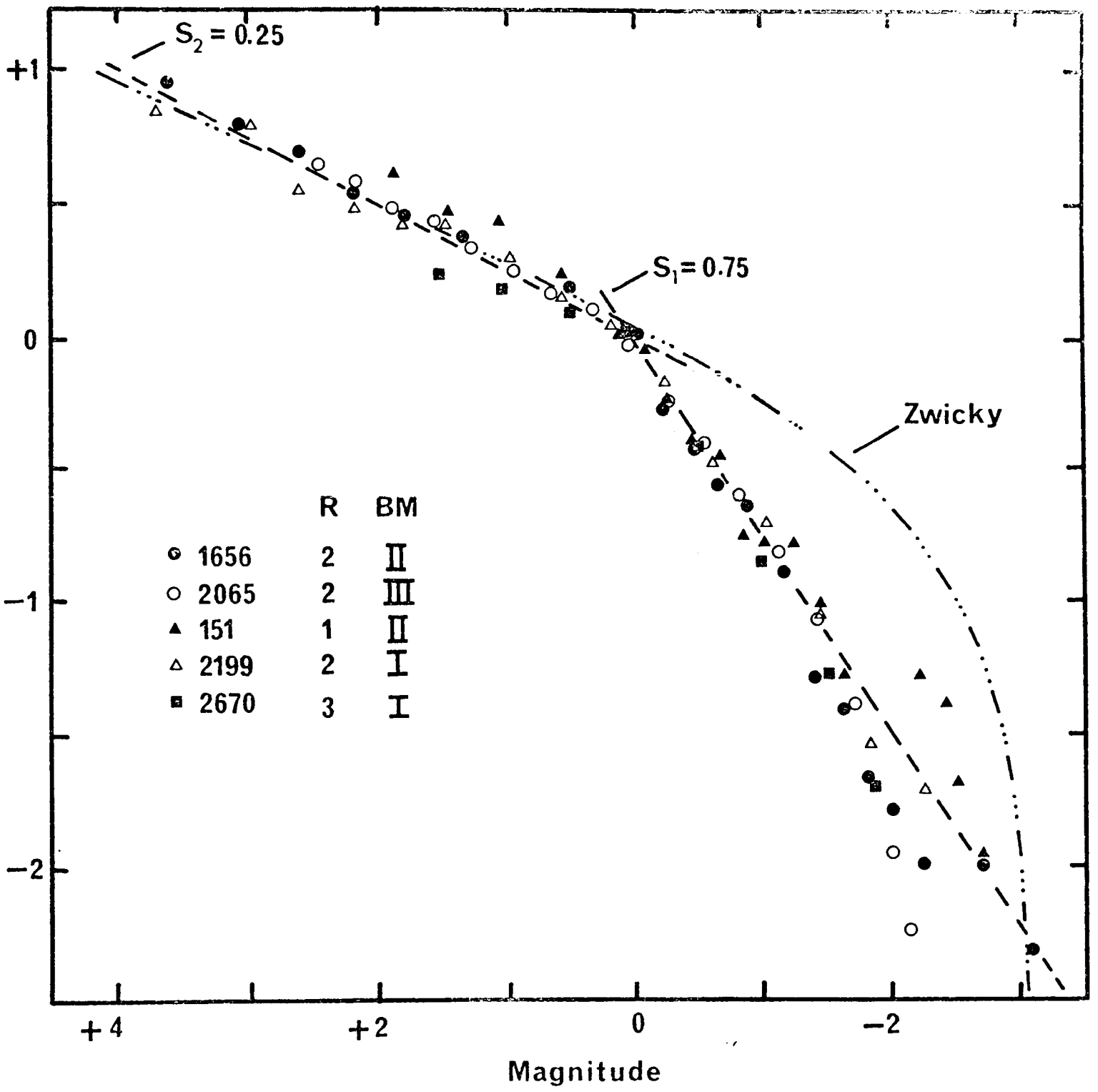

FIG. 14 The logarithmic integrated luminosity functions of five rich clusters of galaxies (after Abell, 1974). The scales are in arbitrary units.

statistical fluctuations than a method that relies on observations of one object. Bautz and Abell (1973), from observations of 9 clusters out to a redshift of 0.078, have shown that the absolute magnitude of the maximum has a dispersion of only 15%.

In comparing different clusters Abell (1965) has approximated the integrated luminosity function log $N(\Delta m)$ by two straight lines

$$\log N(\Delta m) = k_1 + s_1 m \quad \text{for} \quad m \leqslant m^* \qquad (3.2)$$
$$\log N(\Delta m) = k_2 + s_2 m \quad \text{for} \quad m \geqslant m^*$$

For the mean lines in Fig. 14 the values of s_1 and s_2 are 0.75 and 0.25. The departures of log $N(\Delta m)$ for a particular cluster from the mean lines may be functions of cluster richness and Bautz-Morgan type. Bautz and Abell (1973) have found that the difference between m* and the magnitude of the brightest member m(1), called Δ, is a function of both BM type and richness, increasing with richness and decreasing with BM type. Sandage and Hardy (1973) confirmed the correlation of the magnitude of the brightest member with BM type but found no correlation with richness. This discrepancy is at present unresolved. They further found that the luminosities of the second and third brightest members increased with richness and BM type.

The results of Abell and Bautz and Abell are confirmed in this Chapter for the rich cluster Al413, whose differential luminosity function has a maximum at an absolute magnitude which agrees closely with values found previously. The present evidence on the differential luminosity function of galaxies, both in clusters and in the field, is that it displays a maximum characteristic of the formation of galaxies with a preferred mass

and luminosity.

3.3 Methods of Galaxy Photometry

Photometric studies of galaxies that have been made can be divided into two broad classes. The first uses photographic procedures, discussed below, that yield statistically reliable magnitudes, accurate to within ± 0.2 mag., for a large number of objects. The second is concerned with the detailed investigation of the intensity distribution in a few objects, usually bright, producing for them magnitudes accurate to within 0.05 mag. or less.

Class 1 methods

There are essentially three methods in this class: extrafocal, Schraffier, and Fabry photometry. All three methods produce smeared images of approximately uniform surface brightness, and it is very important that the images are large enough to include light from most of the galaxy.

The procedure of extrafocal photometry of Abell and Mihalas (1966) requires the adoption of a common law for the distribution of intensity. Since this is possible only for ellipticals, though it gives good results for SO galaxies, the method is not best suited to the study of spiral and irregular galaxies. This limitation is not severe for studies of rich clusters, since they contain few spirals. The extrafocal image is measured on each of two or more calibrated plates taken different amounts out of focus, and from the sequence of measures and the assumed surface brightness law, its total magnitude can be determined. The calibration is provided by extrafocal exposures of stars of known magnitude (measured photoelectrically).

CLASS 1

Method and Investigation	Programme of Photometry	Calibration Procedure
Extrafocal Photometry		
Abell & Mihalas (1966)	E and SO galaxies in the Coma Cluster	extrafocal stellar images
Abell & Eastmond (1970)	luminosity functions of rich clusters of galaxies	extrafocal stellar images
Gudehus (1971)		
Abell & Mottmann (1972)		
Abell (1974)		
Schraffier Photometry		
Humason, Mayall & Sandage (1956)	NGC galaxies and clusters of galaxies	schraffier images of standard stars
Zwicky et al. (1961-1968)	Single and cluster galaxies on Sky Survey plates	schraffier images of standard stars
Fabry Photometry		
Bigay (1951)	175 bright northern galaxies	comparison with standard stellar sequences

CLASS 2

Method and Investigation	Programme of Photometry	Calibration Procedure
Microphotometric Tracing		
Redman (1936)	NGC elliptical galaxies	Sensitometer and extrafocal stellar imag
Redman & Shirley (1938)		
De Vaucouleurs (1948)	3 NGC elliptical galaxies	sensitometer and night-sky brightness
Holmberg (1950, 158)	300 NGC galaxies, mostly spirals	extrafocal exposures of stars in the NPS
Evans (1951, 1952)	planetary and elliptical nebulae	sensitometer (relative calibration only)
Van Houten (1961)	bright spirals and ellipticals	extrafocal stellar images and photoelectr intensities
Rood & Baum (1968)	all galaxies brigher than V = $17^{m}.5$ in centre of the Coma cluster	sensitometer and photoelectric intensitie
Microphotometry using a scanning isophotometer		
Liller (1960)	ellipticals and spirals in the Virgo Cluster	sensitometer and night-sky brightness
Ables (1972)	bright spirals and irregulars	sensitometer and photoelectric intensitie
Digitised Microphotometry		
Austin and Peach (1974b)	luminosity function of the cluster of galaxies A1413	sensitometer and photoelectric intensitie
Oemler (1974a)	luminosity functions of 15 clusters of galaxies	sensitometer and photoelectric intensitie

In the second method, that of Schraffier photometry, the focal galaxy images are moved in a zig-zag pattern over small squares on the plate during the exposure. To obtain squares of uniform structure the separation of the lines must be smaller than the scattering radius. As in the case of extrafocal photometry, where images taken further out of focus lead to smaller magnitudes, it is necessary for the square to be much larger than the apparent visual diameter. The Schraffier image needs to be at least 2.5 times larger to reduce the systematic error to less than 0.1 mag (Humason, Mayall and Sandage, 1956).

In the third method of Fabry photometry (Bigay, 1951) a small lens placed near the focus of the telescope is used to image the objective on the plate. To limit the background light, a small aperture just large enough to include the telescopic image of the object being measured is placed in the focus of the telescope. The Fabry image is of very nearly uniform surface brightness and in most cases is better than in extrafocal images, where coma and instrumental shadows affect the image. Again the aperture needs to be large to reduce the systematic error (De Vaucouleurs, 1959).

Class 2 methods

Most investigations in this class have involved detailed microphotometry across a large number of sections of the galaxy image, while a recorder traces the density on paper. The densities are then calibrated by techniques discussed below. It is desirable to keep the analysing slit as small as possible, to obtain high resolution, consistent with keeping the granulation noise low. Redman (1936) took tracings at intervals of 0.1 mm, about 6 arcsec on his plate scale. A minimum slit size would be

around 20μ x 20μ, corresponding to 1".3 x 1".3 on a 48-in. Schmidt plate. For the outer regions the slit size should be much higher to improve the signal to noise ratio.

Holmberg (1950, 1958) has published photographic measurements of total magnitudes and colours for over 300 galaxies, mostly spirals. Van Houten (1961) did a detailed investigation and theoretical interpretation of the intensity distribution in many spirals and a few ellipticals. Evans (1951, 1952) obtained 'isophotes' of constant density across several galaxies. Liller (1960) studied galaxies in the Virgo cluster using a scanning isophotometer, from which contours of constant density were traced automatically. Rood and Baum (1968) have recently used the slow tracing method for the investigation of over 300 galaxies in the central region of the Coma cluster of galaxies. Ables (1972) has used the automatic density contouring technique to study the photometric properties of several nearby bright spirals and irregulars. The advent of digitised and fast-scanning microdensitometers has radically changed the possibilities of this class of methods in recent years, and has led to new determinations of the luminosity function of cluster galaxies (Austin and Peach (1974b), Oemler (1974a)).

3.3a) Calibration methods

In all programmes of detailed photometry of galaxies it is most important that great care is taken in the plate calibration, so that unknown systematic errors are minimised. Care is necessary because of the non-linear response of a photographic emulsion.

The calibration is usually done in two steps. Firstly plate transmission or plate density is related to an arbitrary scale of

surface brightness and secondly an absolute scale is established, so that magnitudes can be obtained on the International system. All investigations have so far used various combinations of standard photographic and photoelectric techniques.

Tube sensitometry

In using a tube sensitometer for the relative calibration it is most important that several precautions are taken (King and Hinrichs, 1967). These are:

1) The sensitometer spots must be on part of the plate that is masked off from the celestial exposure.

2) The standard exposure should be of the same duration as the celestial exposure.

3) Both exposures should be made at the same temperature and, if possible, humidity.

4) The sensitometer should use a light source similar in colour to the objects being studied.

5) Development should be as uniform as possible, including adequate agitation to avoid proximity effects in small areas.

Before 1945 it was usual for the calibration spots to be superimposed on the sky fog. Because the reaction of an emulsion to light of high and low intensity is different, this procedure yields indeterminate results (Webb and Evans, 1958). This difference is because light of high intensity is considerably more efficient in building up a stable sublatent photographic image than light of low intensity; the density produced by a series of multiple exposures is dependent on the order of the exposure. The timing precaution is necessary because of the reciprocity

failure of an emulsion. If the timing is not close, the Schwarzschild exponent 1/q of the plate needs to be known (Van Houten, 1961). As to precaution 3, it is well to remember that the galaxy exposure is taken at the telescope focus in the night air and the sensitometer exposure probably in a darkroom. De Vaucouleurs et al. (1956) have found that no significant error results from calibration before or after the sky exposure, as long as the age difference ΔT between the two exposures is negligible compared to the time T between the last exposure and development. In practice they said $\Delta T/T = 0.1$ was sufficient. Nowadays the sensitometer is made an integral part of the telescope, and the two exposures are taken simultaneously, making most of the past worries superfluous.

Standard reference stars

This procedure again requires several important precautions. The extrafocal stellar sequence should be exposed at about the same azimuth and altitude as the galaxy exposure so that there are no large differences in sky fog and atmospheric extinction corrections. Since the exposure of the galaxy and the extrafocal exposure are taken on different halves of the same plate, photometric local errors on the plate may well cause errors in the calibration, especially if a non-linear characteristic curve, relating density to intensity, is used (De Vaucouleurs, 1968). Again, instrumental effects, such as vignetting and coma, can cause differences in sky fog between the sequence region and the galaxy region and can distort the extrafocal images. Holmberg (1950, 1958) used extrafocal images of the North Polar Sequence. Van Houten (1961) and Sandage (Humason et al., 1956) used images of selected area stars that

had been calibrated photoelectrically.

Absolute photoelectric calibrations

In principle such a calibration should be more accurate, since observations using off-set guided photometers and pulse-counting photometers can give any desired level of accuracy (Baum, 1955). Rood and Baum (1968) used photoelectric observations of the inner regions of sixteen galaxies in the Coma cluster to calibrate their observations of over 300 galaxies obtained photographically. They also used unpublished photoelectric V magnitudes made available by Sandage. Liller (1960) obtained a zero point for her relative calibration by a photoelectric measurement of the surface brightness of the night sky. This was compared photoelectrically with star 57 in Selected Area 57, whose magnitude and colour index had been determined by Stebbins, Whitford and Johnson (1950). Oemler (1974a) used observations of several of the brightest galaxies in each of his clusters to calibrate the rest of the magnitudes, and Austin and Peach (1974b) used photoelectric magnitudes of 3 galaxies in their cluster A1413 obtained by Sandage (1972). Unfortunately photoelectric observations of galaxies are few. However, by separating the problems of relative calibration (photographic) and absolute calibration (photoelectric), it is possible to use each method where it performs best.

3.4 Observations and Photometric Techniques

The cluster of galaxies A1413 is of interest for a number of reasons. It is very rich, having a population of 153 in the magnitude interval 2.5 mag. fainter than its third brightest member (Sandage and Hardy, 1973). It is a prime example of a Bautz and Morgan (1970) Type I cluster, being dominated by a

centrally located supergiant cD galaxy which, with an absolute total V magnitude $M_V = -24.89$, is one of the intrinsically brightest galaxies known. It is well positioned for observation, lying in an uncrowded region at high galactic latitude ($b^{II} = +77^{o}$), and with a redshift of 0.1426 is sufficiently distant to minimise the number of field galaxies overlying it while being close enough to enable one to sample it to some 5 magnitudes fainter than its brightest member on 48-in. Schmidt plates. Other observational parameters of the cluster are given in Table I of Chapter 2. In this and subsequent parts of Chapter 3 the measurement of apparent magnitudes of galaxies within 5 arcmin of the cluster centre is described, the luminosity function of the cluster is derived, and a discussion is given of the structure of the cluster as inferred from the photometry and the counts of Chapter 2.

3.4a) The Plate Material and Calibration

The plate PS7756 of the cluster A1413 used in this work is one of a series taken of rich clusters of galaxies in March 1972 with the Palomar 48-in. Schmidt telescope. The plates in the series are 25 min exposures on the plate-filter combination 103aD + Wr12. Observing conditions were above average with a seeing disc of less than 1 arcsec. Plates of all the clusters were also taken in the Blue, 12 min exposures on 103aO + GG13, but such plates produce little useful information for high redshift clusters. They will be of use later in colour studies of the low redshift clusters in the sample. The effective spectral responses of the exposures are shown in Fig. 15, together with the responses of two other V band plate filter combinations commonly in use, 103aD + Wr4 and 103aD + GG14. The response curves include corrections for (a) reflection at one

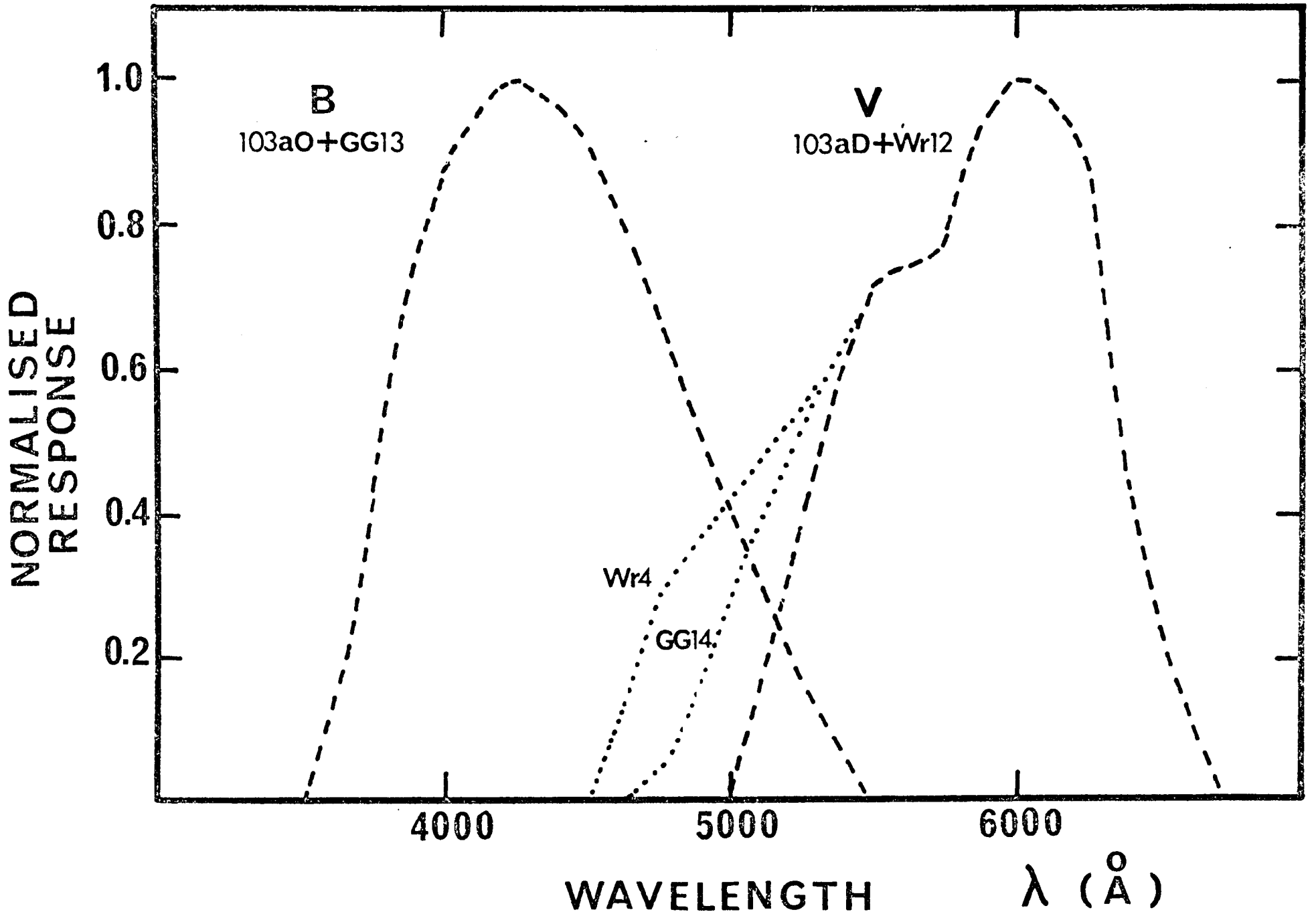

FIG. 15 The normalised photographic responses of some B and V plate-filter combinations as a function of wavelength. The curves are corrected for absorption at the telescope and by the atmosphere, and are plotted for the spectral energy distribution of a gE galaxy at a redshift Z = 0.1426.

aluminised mirror (Allen, 1973), (b) absorption by the Schmidt corrector plate (Arp, 1961) and (c) absorption in the atmosphere of 1 air mass (Melbourne, 1960), and are plotted for the spectral energy distribution of a giant elliptical galaxy at the redshift of the cluster A1413, z = 0.1426 (Schild and Oke, 1971; Whitford, 1971). The high redshift clusters discussed in this thesis were exposed on 5x7 in. plates through the Schmidt field-flattener lens. With an image scale of 67.14 arcsec per mm this corresponds to a field of view of about $2^{o}.4$ x $3^{o}.3$.

Photometry of the plates gives an average V band sky brightness of 21.7 mag arcsec^{-2} and a sky colour of B-V = +0.9. These sky brightness values compare favourably with the faintest found anywhere in California (Walker, 1973), and are almost certainly fainter than those usually obtained at Palomar (Kormendy, 1973). Kormendy showed that conditions in February and April 1972 gave a V band sky brightness of 20.7 mag arcsec^{-2} and a sky colour of B-V = +1.1. The sky brightness in the V band is subject to quite large variability as it is centred on the OI night sky emission line at λ5577 $\mathring{A}$. As a result of these conditions the plates are somewhat underexposed and have not reached the point of optimum exposure (Marchant and Millikan, 1965). The plates were developed in a rocking tray for 5 min. in D-19 at 20^{o}C to an average background density of 0.4. They were then fixed for 5+5 min in a two bath fixer, and before fixing were immersed for 30 seconds in a 1% acetic acid stop-bath. No more than eight 5x7 in. plates were developed in the same solution.

After the sky exposure an intensity calibration was made with a twelve spot tube sensitometer on an unexposed corner of the 5x7 in. plates. Care was taken to make the calibration exposure

of the same length as the sky exposure to avoid errors due to emulsion reciprocity failure. Before reaching the plate the exposing light passed through one diffusing screen, then through one or more neutral density filters, used to control the intensity, through a colour filter to match the sky exposure band and finally through a second diffusing screen. In a later run on the telescope in October 1972 the light was first passed through a Wr79 filter to raise the colour temperature of the sensitometer lamp. The plates were not stored before development as this was impractical in the tight observing schedule. For the V plates this resulted in a difference of about half an hour in the time between exposure and development for the two exposures, with the delay never exceeding about one hour.

Differences in observing conditions and subsequent treatment between the two exposures can cause systematic errors in the relative plate calibration obtained from the sensitometer spots. Such errors from reciprocity effects should be minimal as the two exposures were made equal. Latham (1969) has shown that, for exposures on IIa-O plates developed in D-19 in the wavelength range $\lambda\lambda$3400-6600 $\mathring{A}$, there was a 2% change in the γ of the plates for every 100 $\mathring{A}$ change in the effective wavelength of the exposing light. The errors in this case from a small colour mismatch between the two exposures are unlikely to be larger than this order. Latham also showed that changes in γ from small differences in temperature and humidity during exposure were small. After corrections for reciprocity and wavelength effects in his data Latham still found a 4% scatter in log (Exposure) between the characteristic curves of the plates. He suggested that this was possibly due to differential latent image decay as some of the plates were developed immediately and others after delays as much

as 12 hours. A subsequent discussion suggested further that the major part of such a decay would occur in the first two hours.

In the later run on the telescope in October 1972, a test was made on the size of such a decay for one plate. Four sets of sensitometer spots were put on the corners of a 5x7 in. plate (103aD + Wr12) in sequence, and the plate developed. One set was effectively developed immediately and the others after storage times of half an hour, 1 hour and 2 hours respectively. The differential change in density for each spot as a function of storage time is shown in Fig. 16, where the units of the densitometer readings are such that 410 units correspond to one unit of density. The results of this test are given in Table XIIa for the 10 spots in each set for which a density could be effectively measured. The mean density and densitometer reading for each spot from the 4 sets is given, together with the standard dispersion $\sigma(\bar{N})$ of the reading for each spot (the mean from the 4 sets). A simple linear relation between the densitometer reading and storage time was fitted, although there is a suggestion that the change in the second hour is smaller than that in the first, at least for the lower density spots. The resulting slope $\Delta N/\Delta t$ in half hour units is given in the last column. The half hour decay in density is only greater than the spot dispersion for the two highest density spots, although the total decay in 2 hours is significant for the top four spots. The exact reasons for such a latent image decay are uncertain, although it is probable that oxidation occurs through reactions such as

$$2Ag + \tfrac{1}{2} O_2 + H_2O \rightleftharpoons 2Ag^+ + 2OH^-$$

Latent image decay in nuclear track emulsions is increased as the surrounding temperature and humidity are increased (Mees and James,

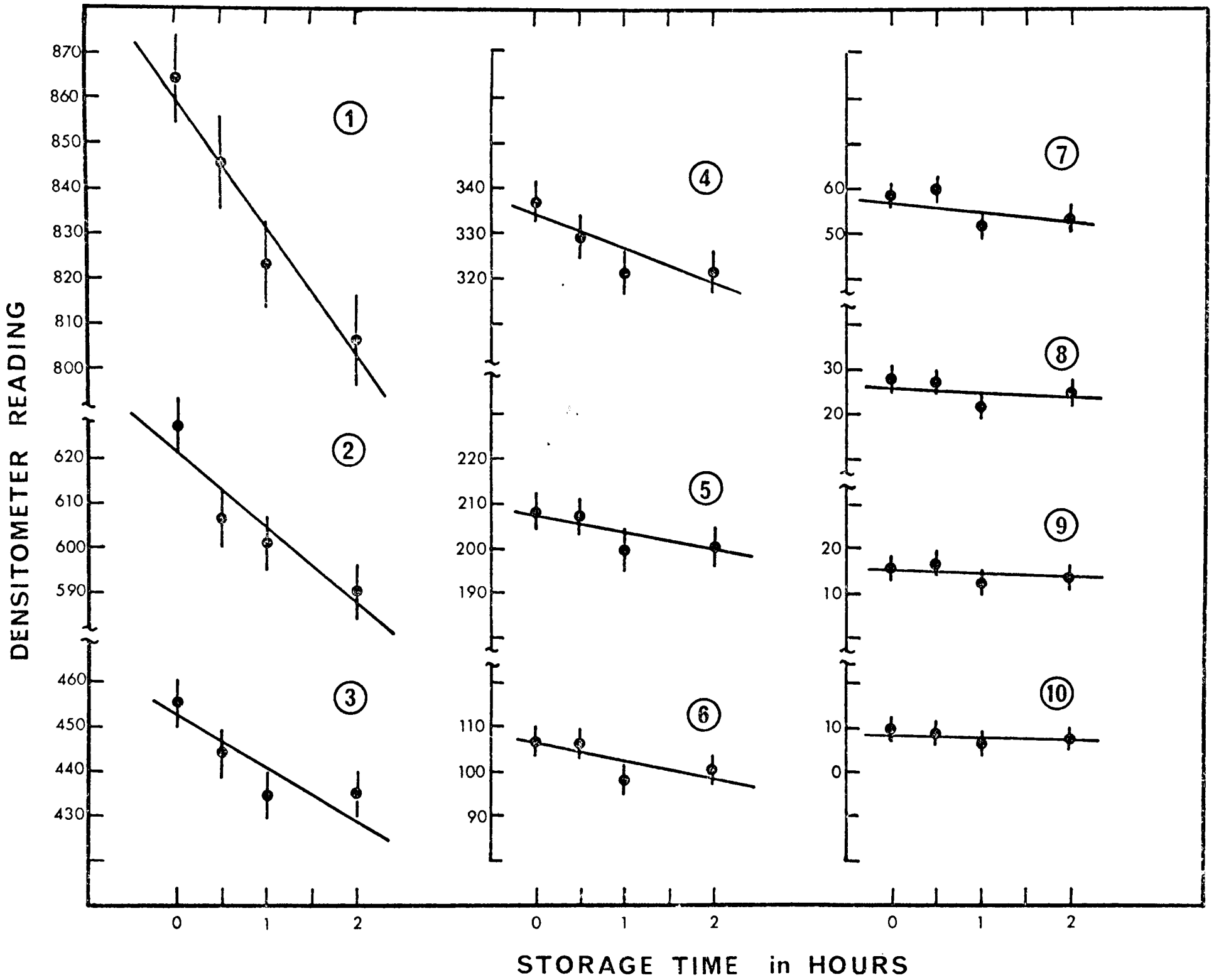

FIG. 16 The changes in the densities of tube sensitometer spots as a function of the storage time between their exposure and development. Plots are given for 10 separate spots. The scale on the vertical axis is such that 410 units correspond to 1 unit of density.

TABLE XIIa

Latent Image Regression Test

Spot No.	$\bar{D}$	$\bar{N}$	$\sigma(\bar{N})$	$\Delta N/\Delta t$
1	2.04	834.5	8.7	14.2 ± 2.4
2	1.48	606.3	6.4	8.5 ± 2.2
3	1.08	442.5	5.3	4.9 ± 2.1
4	0.80	327.4	4.6	3.7 ± 1.5
5	0.50	204.6	4.4	1.8 ± 1.2
6	0.25	102.8	2.8	1.9 ± 1.3
7	0.14	55.7	2.2	1.8 ± 1.1
8	0.06	25.3	2.2	0.8 ± 0.9
9	0.03	14.3	1.8	0.7 ± 0.6
10	0.02	8.0	1.6	0.6 ± 0.4

TABLE XIIb

Surface Brightness	Relative % Error in Intensity		Absolute % Error in Intensity	
	½ hr.	2 hrs.	½ hr.	2 hrs.
19 mag arcsec^{-2}	3%	11%	5%	18%
25 mag arcsec^{-2}	-	-	2%	7%

1969).

In Table XIIb the effects of latent image decay on a galaxy or stellar intensity profile are shown. The results are given for intensities of 19 mag arcsec^{-2} and 25 mag arcsec^{-2} superimposed on a sky brightness of 21.8 mag arcsec^{-2} reaching a plate density of around 0.4. The table gives the relative and absolute percentage errors in intensity that would arise from the use of the wrong calibration curve. The errors are given for half-hour and two hour storage times. The relative errors come from matching the calibration curves at the plate density of 0.4. It is seen that the maximum relative intensity error that would arise from a half-hour time difference in storage time between the two exposures is 3% or a surface brightness change of $0^{m}.03$. This is comparable to the dispersion in fitting a calibration curve. Magnitude errors for galaxies arising from such errors in calibration are therefore of this order. However there is a clear indication that the errors would become significant for larger time differences such as might arise from long IIIaJ exposures on Schmidt telescopes or exposures on large f-number telescopes. It is likely that the effects of latent image decay would be larger for plates that have not been as intensively treated for low intensity reciprocity failure as normal astronomical emulsions.

3.4b) Reduction of galaxy magnitudes

The apparent magnitudes of the images in the core of the cluster A1413 have been determined by scanning the plate with a digitised Joyce-Loebl two-dimensional microdensitometer, and then analysing the density measures using the numerical mapping techniques developed by Jones, Obitts, Gallett and de Vaucouleurs (1967). An area 2 mm x 2 mm in the region to be

measured is sampled in a raster scan with a 25μ (1.68 arcsec) square aperture; the limitation on the size of the scanned area is set by computer capacity. Subsequently a larger area, 5 mm x 5 mm, centred on the same region is scanned with a 200μ (13.4 arcsec) aperture. This latter scan serves, after an iterative procedure correcting for the presence of discrete images, to determine the variation of background density across the inner finely sampled region. A low order polynomial was fitted to any density variation found, although terms beyond the constant seldom gave a significant reduction of the residuals from the fit. The densities in the outer and inner region were converted to intensities using the relative intensity calibration provided by the sensitometer spots. The relative calibration uses a linearised form of the characteristic curve known as the generalised Sampson transform, which is related to the better known Baker-Sampson transform (de Vaucoulers, 1968; for other linearised forms see Baker (1957), Honeycutt and Chaldu (1970) and Mees and James (1969). This relates the intensity E and the density D by

$$E = AS^n$$

where $S = 10^{D/B} - 1$,

and where A, B and n are parameters to be determined. In logarithmic co-ordinates this equation is linear to $\pm$2% over the whole usable density range from 0.02 to 2.2. The results from three plates PS7742, 7745 and 7756 are given in Fig. 17. The linearised form enables any errors in the individual spot calibrations to be more easily recognised than in the normal D - log E plot. It is clear from the figure that the calibration for spot no. 5 (no. 4 in the case for plate PS7745) is in error, and this spot was left out in the fit. The coefficients A, B and

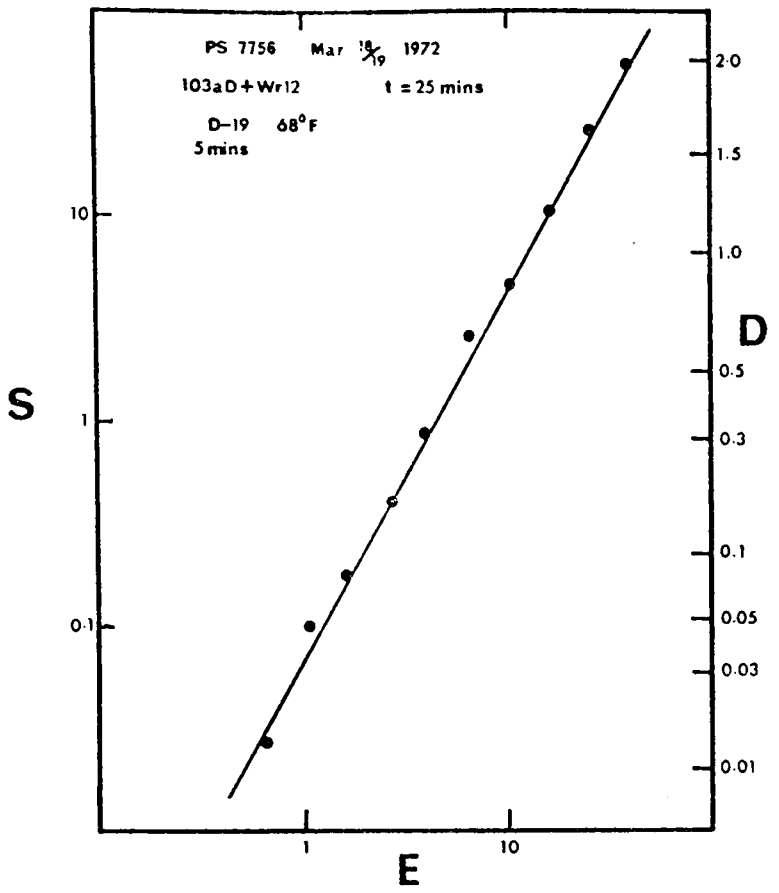

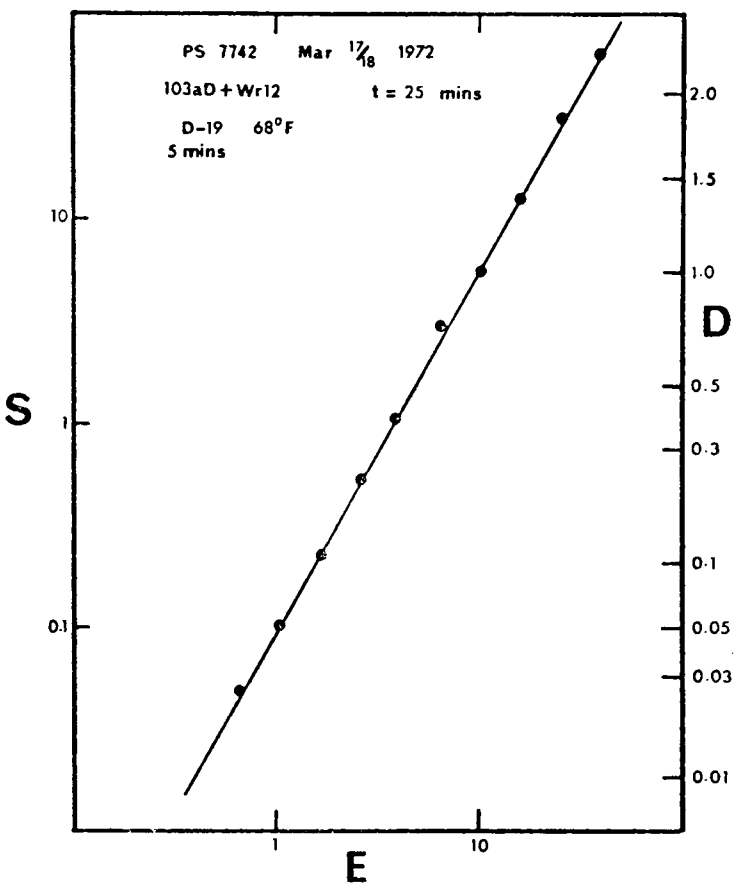

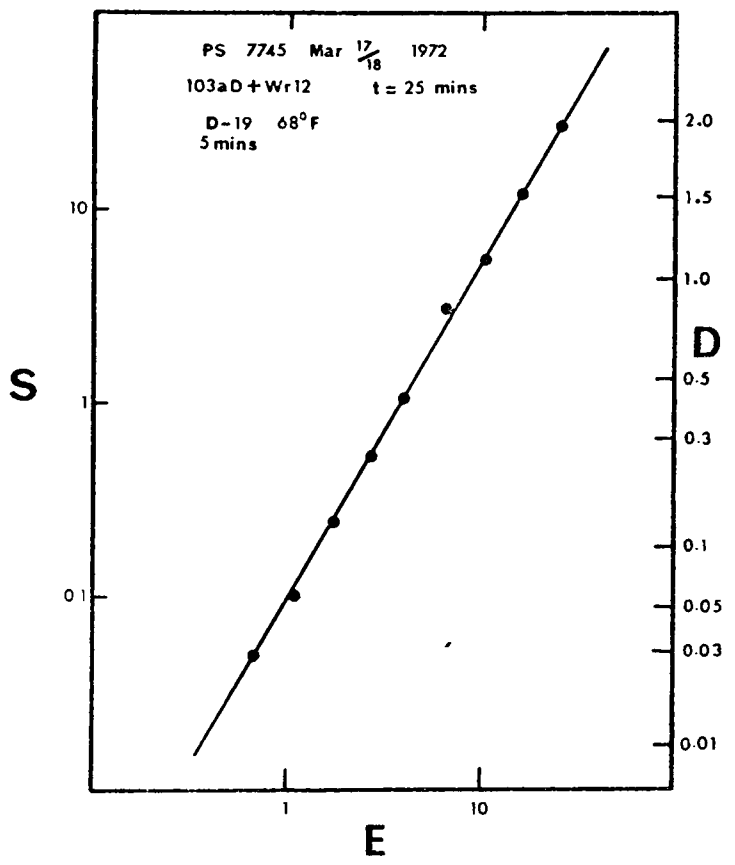

GENERALISED SAMPSON TRANSFORM COEFFICIENTS

	A	B	n
PS7742	3·90 ± 0·20	505 ± 33	0·56 ± 0·02
PS7745	3·86 ± 0·15	550 ± 22	0·57 ± 0·02
PS7756	4·38 ± 0·21	464 ± 27	0·55 ± 0·02

FIG. 17 Linearised characteristic curves for three plates, PS7742, PS7745 and PS7756, calibrated in March 1972. The linearisation was obtained by using the generalised Sampson transform in which $E = AS^n$ where $S = 10^{D/B} - 1$.

n for the three plates are also given in Fig. 17. The plate density variations, apart from discrete images, across the 5 mm x 5 mm regions were always small and generally of the order of $\pm$1%. No systematic variations in background density were measurable across the whole central region of the cluster. Measurement of this region to a radius of 5 arcmin from the centre required 25 separate 2mm x 2mm scans including a small overlap.

After the subtraction of the background intensity from the inner region an intensity contour map is constructed. An example of such a map for the central scan is shown in Fig. 18. Apparent magnitudes can then be derived to a chosen isophote by integration over the areas of the isophotes, and these magnitudes can be placed on an absolute scale using a suitable photoelectric zero point. Magnitudes V_{25} have been measured to include light contained within the 25 mag arcsec^{-2} isophote, which is at about 5% of the sky brightness. The zero-point of the scale is based on Sandage's (1972) photoelectric photometry of the central cD galaxy (see Fig. 18) for which he gives V = 15.93 and 15.53 for circular apertures of 18.8 and 30.6 arcsec diameter respectively. This fixes the sky brightness at 21.82 $\pm$ 0.05 mag arcsec^{-2}. Apparent magnitudes on this scale are listed in Table XIII for 135 objects within 5 arcmin of the cluster centre with $V_{25}<20.0$. A finding chart is given in Fig. 19; the objects are numbered in order of decreasing brightness. Also listed in Table XIII is the mean surface brightness within the 25 mag arcsec^{-2} isophote. The accuracy of the magnitudes is dependent to some extent on the presence of neighbouring objects whose isophotes may overlap. In the central region shown in Fig. 18 the field is crowded and the magnitudes may contain a substantial correction for overlap.

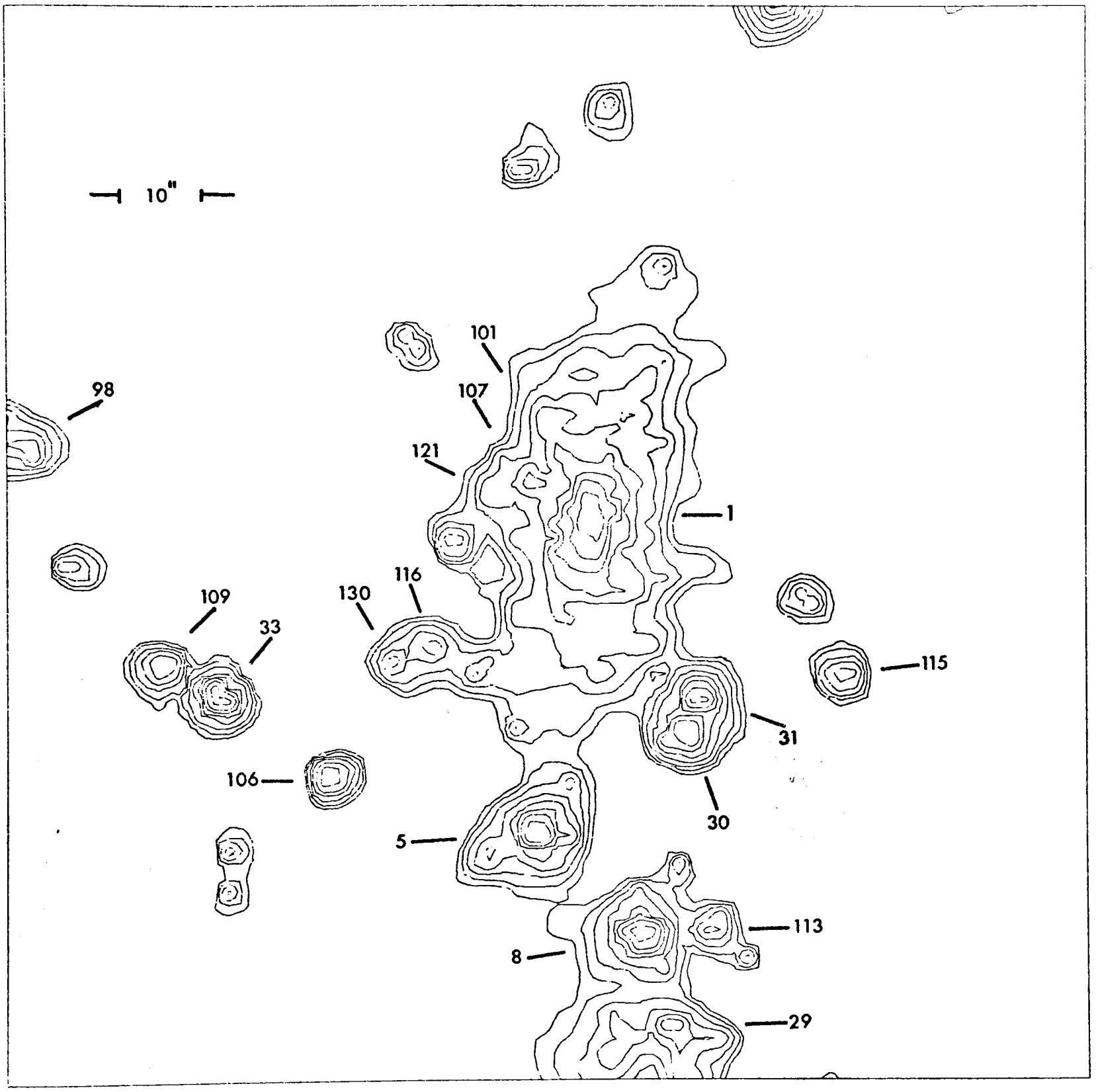

FIG. 18 Isophotes of a 2x2 mm area centred on the brightest cluster member. The outermost contour in each set is 25 V mag arcsec^{-2}, and the contour interval is 0.5 mag. The numbering of galaxies corresponds to that in Fig. 19 and Table XIII. North is to the top and East to the left.

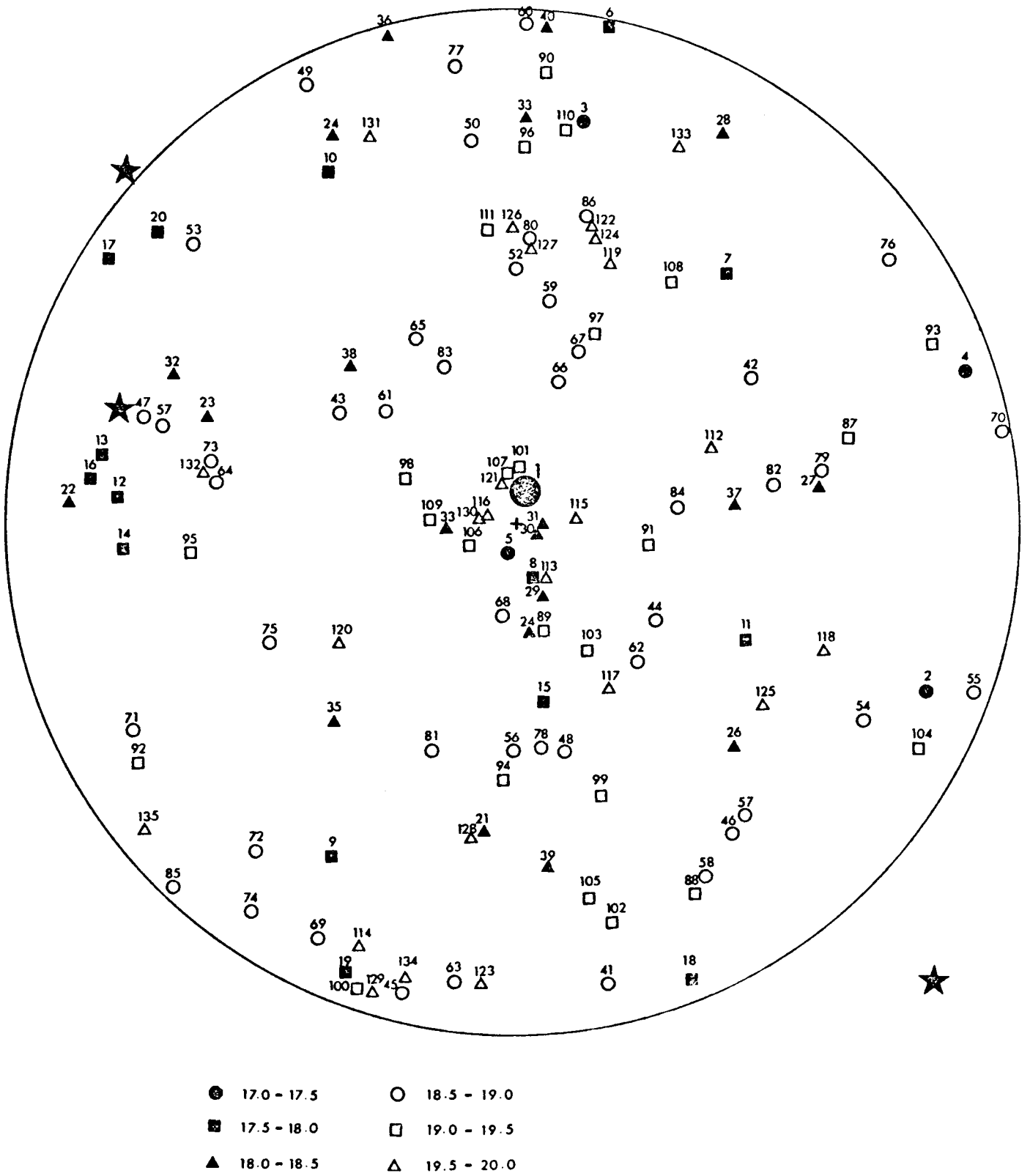

FIG. 19 A finding chart for A1413. The cluster centre at $\alpha_{1950} = 11^h\ 52^m.7$, $\delta_{1950} = +\ 23^o\ 40.6$ is marked by a cross and the circle has a radius of 5 arcmin. Three bright foreground stars are marked. The numbering is in order of decreasing brightness and the symbols indicate the apparent magnitude V_{25} in 0.5-mag. intervals.

TABLE XIII

Magnitudes and mean surface brightnesses for the objects identified in Fig. 19

No.	V_{25}	Mean Surface brightness V mag.arcsec^{-2}	No.	V_{25}	Mean Surface brightness V mag.arcsec^{-2}
1	15.32	22.98	21	18.00	23.13
2	17.28	23.00	22	18.04	23.26
3	17.30	22.85	23	18.06	23.00
4	17.46	23.05	24	18.08	23.12
5	17.47	23.15	25	18.08	23.16
6	17.61	23.01	26	18.09	23.23
7	17.65	22.77	27	18.13	23.22
8	17.65	23.27	28	18.15	22.91
9	17.68	23.02	29	18.17	23.59
10	17.70	22.64	30	18.20	23.05
11	17.73	22.95	31	18.22	23.03
12	17.83	23.10	32	18.24	23.09
13	17.87	23.52	33	18.26	23.23
14	17.87	23.10	34	18.26	23.09
15	17.88	22.85	35	18.28	23.17
16	17.93	22.86	36	18.32	23.54
17	17.94	23.37	37	18.35	22.77
18	17.98	22.94	38	18.37	23.22
19	17.98	23.21	39	18.40	23.33
20	18.00	23.38	40	18.45	23.30

TABLE XIII (cont.)

Magnitudes and mean surface brightnesses for the objects identified in Fig. 19

No.	V_{25}	Mean Surface brightness V mag.arcsec^{-2}	No.	V_{25}	Mean Surface brightness V mag.arcsec^{-2}
41	18.46	23.35	61	18.73	23.21
42	18.48	23.28	62	18.73	23.29
43	18.48	23.26	63	18.73	23.39
44	18.48	23.09	64	18.74	23.34
45	18.49	23.32	65	18.74	23.10
46	18.49	23.01	66	18.76	23.54
47	18.57	23.11	67	18.76	23.50
48	18.58	23.61	68	18.78	23.42
49	18.60	23.54	69	18.78	23.28
50	18.60	23.21	70	18.81	23.36
51	18.60	23.18	71	18.81	23.37
52	18.60	23.20	72	18.81	23.36
53	18.63	23.32	73	18.83	23.62
54	18.65	23.57	74	18.84	23.53
55	18.67	23.03	75	18.85	23.44
56	18.68	23.32	76	18.86	23.52
57	18.68	23.06	77	18.87	23.75
58	18.68	23.31	78	18.88	23.63
59	18.70	23.65	79	18.89	23.39
60	18.73	23.39	80	18.92	23.27

TABLE XIII(cont.)

Magnitudes and mean surface brightnesses for the objects identified in Fig. 19

No.	V_{25}	Mean Surface brightness V mag.arcsec^{-2}	No.	V_{25}	Mean Surface brightness V mag.arcsec^{-2}
81	18.92	23.36	101	19.31	23.38
82	18.95	23.40	102	19.33	23.70
83	18.96	23.74	103	19.34	23.54
84	18.98	23.32	104	19.35	23.58
85	18.99	23.59	105	19.36	23.66
86	19.00	23.60	106	19.37	23.40
87	19.05	23.71	107	19.38	23.33
88	19.06	23.12	108	19.44	23.65
89	19.11	23.63	109	19.44	23.50
90	19.12	23.55	110	19.46	23.49
91	19.13	23.17	111	19.49	23.70
92	19.14	23.84	112	19.52	23.52
93	19.14	23.62	113	19.55	23.61
94	19.14	23.50	114	19.62	23.75
95	19.18	23.78	115	19.66	23.67
96	19.18	23.48	116	19.67	23.53
97	19.23	23.55	117	19.67	23.78
98	19.26	23.68	118	19.67	23.44
99	19.26	23.49	119	19.68	23.66
100	19.30	23.59	120	19.69	23.74

TABLE XIII (cont.)

No.	V_{25}	Mean Surface brightness V mag.arcsec^{-2}
121	19.71	23.41
122	19.72	23.63
123	19.73	23.79
124	19.75	23.77
125	19.75	23.88
126	19.76	23.69
127	19.77	23.61
128	19.77	23.35
129	19.79	23.59
130	19.80	23.51
131	19.84	23.93
132	19.89	23.86
133	19.93	23.82
134	19.94	23.71
135	19.94	23.71

In such situations it is estimated, from repeat scans, that errors may be as high as 0.25 mag in complicated cases. For isolated objects the internal accuracy as estimated from repeated scans is much less at about 0.06 mag. This is comparable, for faint objects, to the error expected from a 1% variation in the background fit. The mean magnitude dispersion for all galaxies for which there is more than one measurement is 0.15 mag and this is an appropriate average value for the results of Table XIII. Sandage has also published photometry for two of the fainter galaxies in the cluster but there is a problem over the identification of one of them. One is number 7 but it is not clear whether the second is number 5 or number 8. Comparison of the photometry in the sense of Here - Sandage for the most probable combinations gives a mean and dispersion of -0.10 ± 0.12 mag.

3.5 The cluster luminosity function

The luminosity function of the cluster volume sampled can be constructed from the data of Table XIIIonly after the application of three corrections - for contamination of the data by field galaxies, for the possible inclusion of faint stars in the sample and for incompleteness of the sample towards fainter magnitudes. The first two effects are best dealt with together.

It is impossible to make an absolute correction for field galaxies and stars, so the correction has been based on their average surface density as determined by the counts in the region of the cluster as described in Chapter 2. It is estimated that to the magnitude limit of $V_{25} = 20.0$ the total field density of objects which are not unambiguously stars is 1624 deg^{-2}. This will include a number of faint stars, some of which may have been measured for Table XIIIin error. Using Sternberg's (1972) analysis

of star counts by Becker (1965) and Fenkart (1967), it is estimated that there are about 600 stars deg^{-2} in the V_{25} magnitude interval between 18.0 and 20.0, where 18.0 is the faintest magnitude at which stars can be confidently distinguished from galaxies. A field correction is then constructed, based on

(i) a density of field stars between V_{25} = 18.0 and 20.0 of 600 stars deg^{-2} distributed in magnitude according to

$$\log N(m \leqslant V_{25}) = -0.79 + 0.19\ V_{25}$$

and

(ii) a total density of field galaxies of 1024 deg^{-2} distributed in magnitude according to

$$\log N(m \leqslant V_{25}) = -8.99 + 0.6\ V_{25}$$

where their spatial density has been assumed to be constant. $N(m \leqslant V_{25})$ is the number of galaxies with magnitudes less than or equal to V_{25}. This expression gives a density to V_{25} = 17.8 of 49 deg^{-2} in good agreement with the figure used by Rood and Abell (1972) in the field of the Coma cluster. The constant -8.99 is very close to the mean -9.00 ± 0.19 from 23 other estimates of the density of field galaxies that have been made in the literature over the years.

This correction is applied in Fig. 20 where the differential luminosity function is presented as a histogram. The continuous lines show the uncorrected, and the dashed the corrected values of $N(V_{25})$, where $N(V_{25})$ is the number of galaxies in the magnitude interval V_{25} - 0.1 to V_{25} + 0.1. The correction does not amount to more than the natural error in the numbers in each 0.2 magnitude interval until V_{25} = 19.0. The histogram of Fig. 20 shows a clear maximum at V_{25} = 18.8 similar to those appearing

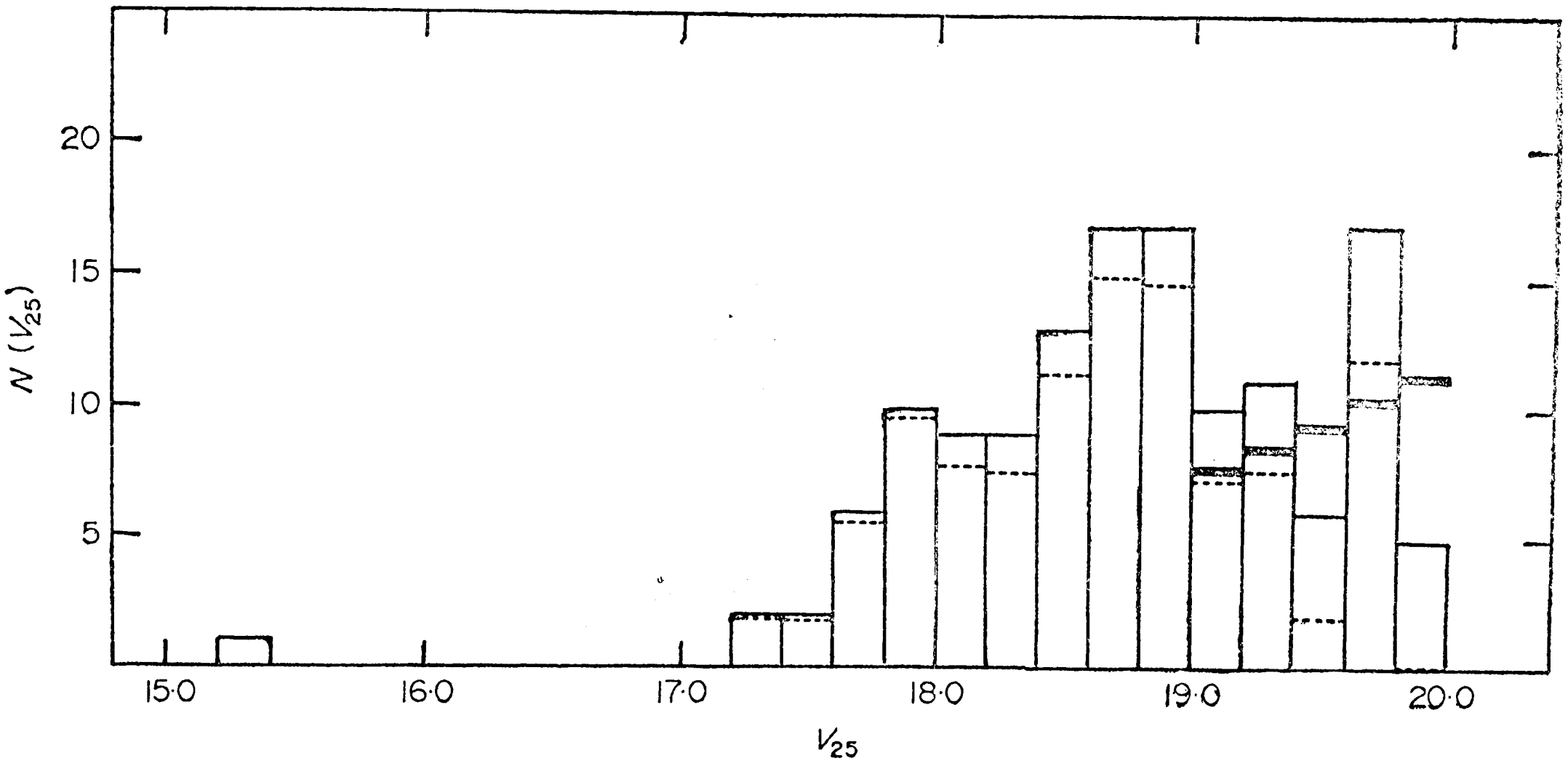

FIG. 20 The differential luminosity function from the data of Table XIII. is shown as a histogram formed by continuous lines. The broken lines show the effect of correcting for the field as described in part 3.5. The heavy lines for $V_{25}>19.0$ show the effect of this correction when combined with a correction for incompleteness.

in the data for other clusters at about 2 or 3 magnitudes fainter than the brightest member (Bautz and Abell, 1973). In previously studied clusters the photometry has been essentially complete to some few magnitudes beyond the maximum so that its occurrence could be unambiguously ascribed to a real property of the cluster. A1413 is more distant than those previously studied, and we must investigate the possibility that the maximum is due to an incompleteness effect setting in suddenly beyond V_{25} = 19.0. There is some suggestion in the data of Table XIII that there is a minimum surface brightness of about 23.8 mag arcsec^{-2} in the sample representing the limit of detection, and the general trend of decreasing surface brightness with increasing magnitude begins to flatten off slowly beyond 19.0. A plot of the mean surface brightness SB_{25} in V mag arcsec^{-2} against magnitude V_{25} is given in Fig. 21. Galaxies are marked as filled circles and the brightest galaxy is marked as a filled square. Identified stars, not in Table XIII, are marked as open triangles and the mean linear regression between SB_{25} and V_{25} for the thirteen stars is plotted as a dotted line. The residuals of the points from this line have dispersions of $\sigma(SB_{25})$ = 0.05 mag arcsec^{-2} and $\sigma(V_{25})$ = 0.08 mag. It is not possible, however, to use this flattening to estimate the degree of incompleteness quantitatively as the true distribution of surface brightnesses per unit magnitude interval is not known. It does suggest, however, that incompleteness is unlikely to be of great importance at magnitudes brighter than the maximum at V_{25} = 18.8 and further that the maximum is unlikely to be due to a high degree of incompleteness setting in sharply beyond 19.0. There is an indirect quantitative confirmation of this conjecture which will now be discussed.

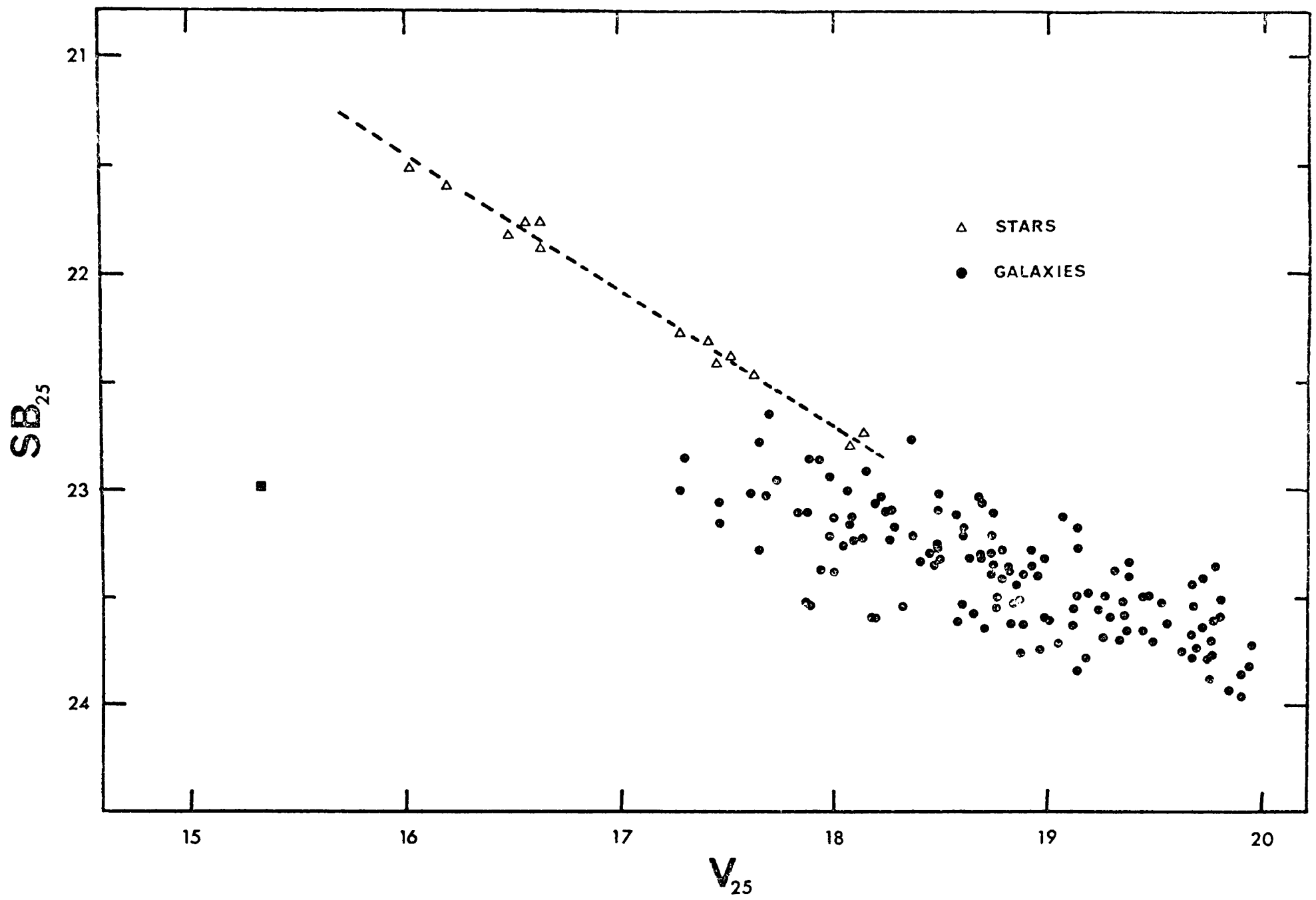

FIG. 21 The mean surface brightnesses SB_{25} in V mag arcsec^{-2} of the galaxy and star images in the central region of the cluster A1413 as a function of their magnitude V_{25}. The galaxy data are listed in Table XIII. The brightest galaxy is marked as a filled square. The mean regression line for the 13 stars is shown dotted.

The logarithmic integrated luminosity function log $N(m<V_{25})$ is plotted in Fig. 22 with the field correction which was illustrated in Fig. 20. This is constructed from the data of Fig. 20 with the addition of two points at the faintest magnitudes which have been calculated from the galaxy counts of Noonan (1972a). These counts, which were made to fainter limits than V_{25} = 20.0 on a IIIaJ Schmidt plate and a 200-in. 103aO plate, can be used to give the number of galaxies within 5 arcmin of the cluster centre for two magnitude limits. These limits have been estimated from a comparison of the field count used here of 1624 deg^{-2} with his values of 4870 and 1.09 x 10^4 deg^{-2}; extrapolating the field corrections his limits are estimated to be 20.9 and 21.6 respectively. It is assumed that his criteria for marking galaxies on his plates produce in practice results similar to those found here. Following Abell (1965) it is now assumed that the data fainter than the maximum at V_{25} = 18.8 in Fig. 20, which is reflected in the discontinuity in the logarithmic integrated luminosity function, can be represented by the straight line drawn in Fig. 22. If this is assumed to lie through the Noonan points and through the discontinuity, it implies that the data points found here, which fall systematically further below this line as one moves to fainter magnitudes, are incomplete by a factor which can be inferred from the shortfall in each magnitude interval. Following this through suggests the data is 30% incomplete between 19.0 and 19.5 and 60% incomplete between 19.5 and 20.0. The effect this would have on the differential luminosity function is shown in Fig. 20; the data corrected both for such an effect and for the field are shown as heavy lines. This strongly suggests that the peak at V_{25} = 18.8 is real and indicates that a much higher

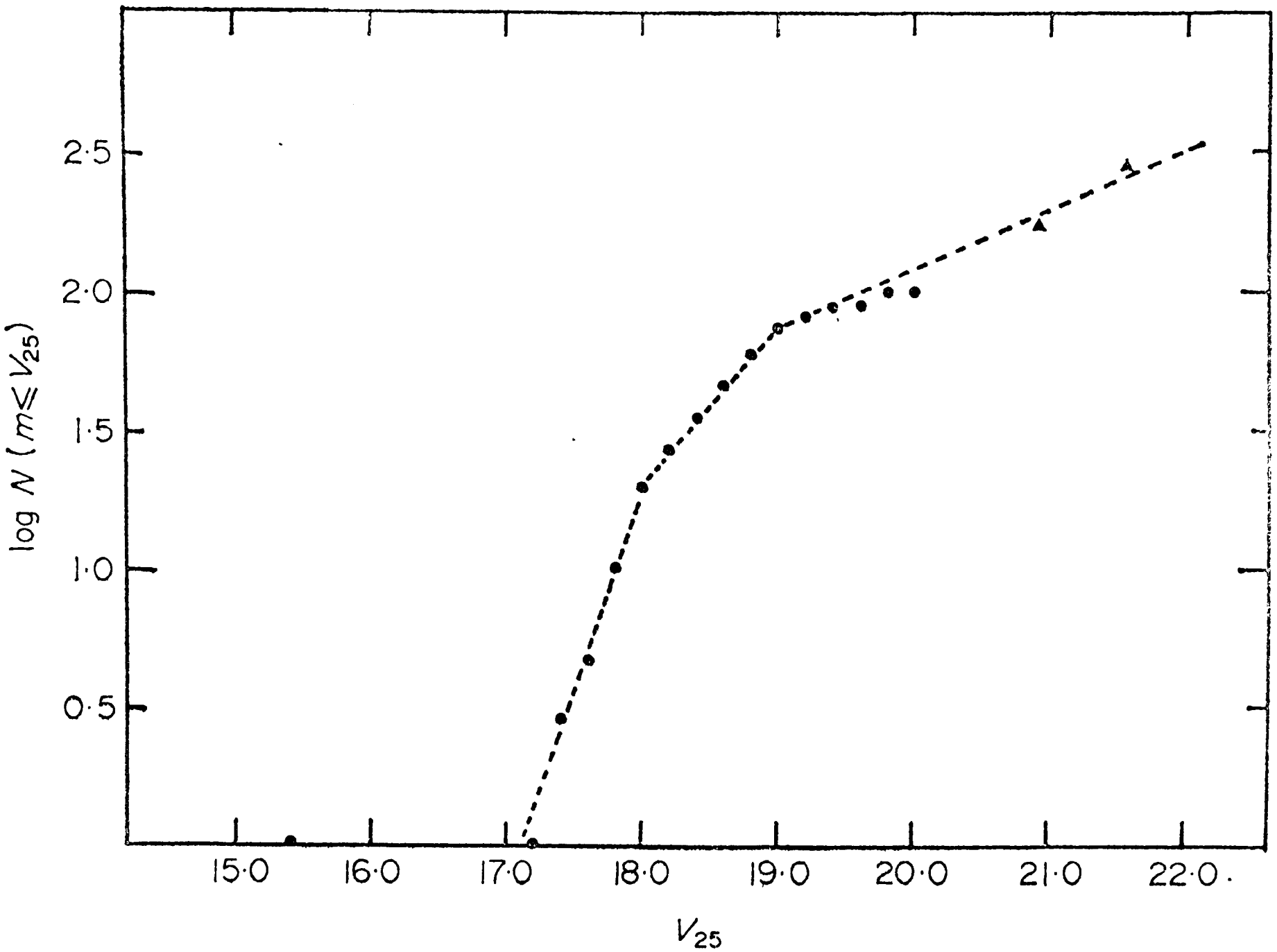

FIG. 22 The logarithmic integrated luminosity function after correction for the field. The two triangles at V_{25} = 20.9 and 21.6 are based on Noonan's (1972) counts as described in part 3.5. The straight lines have slopes 1.43, 0.61, and 0.21.

level of incompleteness than seems probable would be needed to account for the dip in the function for V_{25}>19.0.

Published luminosity functions for other rich clusters seem well represented by two lines of slope 0.75 and 0.25 (Abell, 1965; see also Fig. 14). The results here seem in fair agreement at the fainter end - the inferred slope fainter than 18.8 in Fig. 22 is 0.21 - but would not be fitted by a single line for brighter magnitudes. There is a further discontinuity in slope at 18.0 due to the small peak in the differential luminosity function, which may be due to a statistical fluctuation as the numbers in each magnitude interval are low, and which makes any single straight line a poorer approximation than seems the case in other clusters. Two lines of slopes 1.43 and 0.61 have been drawn in Fig. 22 but no great weight should be placed on this representation; the effect might not be preserved over a larger cluster volume.

Abell (1965) has argued that the major change in slope in the logarithmic integrated luminosity function occurs at the same absolute magnitude in all rich clusters, and as it effectively averages over the properties of a large number of cluster members should be less liable to statistical variation than the absolute magnitude of the brightest member. He designates the apparent magnitude of the feature as m* and has shown (Bautz and Abell, 1973) that a plot of m* against z shows very small scatter (σ(m*) $\simeq$ 0.15 mag). The discontinuity occurs in A1413 at V_{25} = 18.8. A correction of -0.2 mag is applied to convert this to a total magnitude on his scale using the Abell-Mihalas (1966) model for the light distribution of a typical elliptical galaxy. This model gives a light distribution in an elliptical galaxy of

$$I = I_o/(r/a + 1)^2 \qquad r/a \leqslant 21.4$$

$$I = 22.4\ I_o/(r/a + 1)^3 \qquad r/a \geqslant 21.4$$

where I_o is the central intensity, r the radius along either axis and a a scale parameter along either axis to be determined separately for each galaxy. A value of a, in linear measure, of 300 kpc is taken for a galaxy at this absolute magnitude from the plots of Gudehus (1973) obtained from photometry on four low redshift clusters A754, A1367, A1656 and A2065. Then with a modulus of 39.66 (H_o = 50 kms^{-1} Mpc^{-1}; q_o = + 1), a K-correction of K_v = 0.24 mag (Whitford, 1971) and galactic absorption A_v = 0.0 mag (Sandage, 1972), we find M_v^* = -21.30 as compared with -21.16 ± 0.15 for Abell's sample of 9 clusters (Bautz and Abell, 1973). Similarly the absolute total V magnitude for the brightest cluster member using an Abell-Mihalas law is $M_v(1)$ = -24.89 and $M_v^* - M_v(1)$ = + 3.59 in fair agreement with the value + 3.3 found by Bautz and Abell for A2670 which has the same richness and Bautz-Morgan type. In Fig. 23 a plot of total corrected apparent magnitude of the maximum $V^* - K_v - A_v$ against redshift z is given, where the data for the 9 Bautz-Abell clusters are plotted as filled circles, and the two triangles represent firstly the observation here for A1413 at z = 0.1426 and secondly the observation for another cluster A1930 of the sample in Chapter 2 at z = 0.1312 (Austin, Godwin and Peach, 1974). The line represents a world model with q_o = +1. The dispersion of the observations from the mean line is $\sigma(V^* - K_v - A_v)$ = 0.14 mag. This suggests that the use of the (V^* - z) plot as a classical apparent magnitude - redshift cosmological test is better than firstly the (m-z) test as applied to brightest cluster galaxies by Sandage and Hardy (1973) (dispersion ~28%) and secondly the apparent diameter - redshift (θ-z) test as applied to clusters by

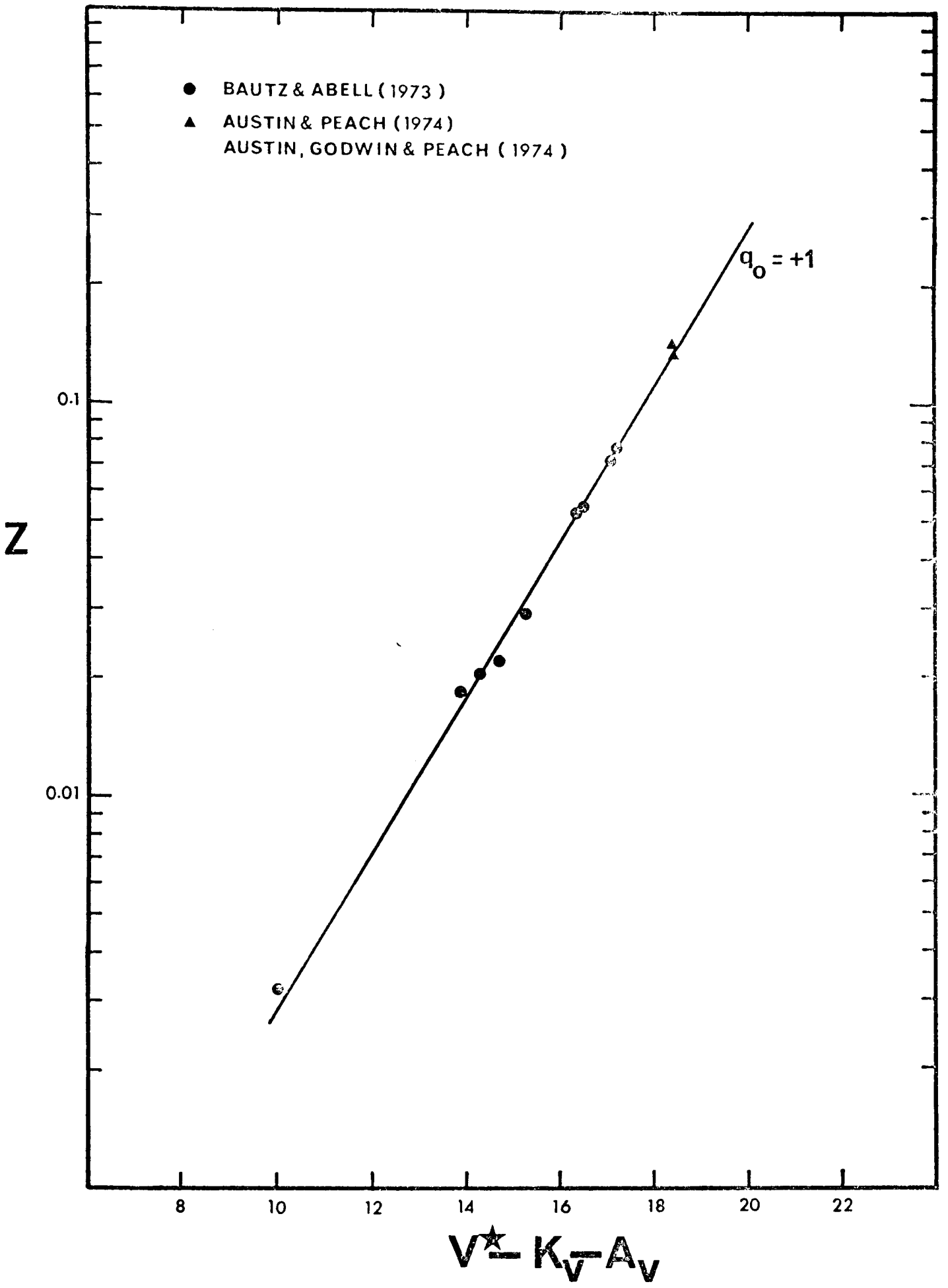

FIG. 23 The total corrected V magnitudes of the maxima in the differential luminosity functions of 11 rich clusters of galaxies as a function of redshift Z. The mean line is for a world model with $q_o = +1$.

Austin and Peach (1974a) (dispersion ~18%).

3.5a The Brightest Cluster member

The brightest galaxy in the cluster A1413 is the central cD galaxy and it is a member of the "supergiant cD" group discussed by Morgan and Lesh (1965). Sandage (1972) refers to the galaxy as having a conspicuous halo and an abnormal integrated magnitude growth curve. Humason, Mayall and Sandage (1956) refer to a 'knot' designated 1A which according to Noonan (1972a) is only visible on 200-in. plates. An inspection of a print from a plate taken in the red on the new 4 metre telescope at the Lick Observatory (Oemler, 1974b) suggests that the 'knot' is in fact a galaxy with a magnitude similar to that of the other faint galaxies surrounding the brightest member (see Figs 18 and 19).

In Fig. 24 the intensity profiles of the galaxy along its major and minor axes are plotted as a function of radius. Beyond a radius of about 9 arcsec the ellipticity is effectively constant at 0.43. The curve through the minor axis is a fit of an Abell-Mihalas law with a scale parameter $\underline{b}_{minor}$ of 1.98 kpc. The curve through the major axis is a fit of an Abell-Mihalas law with a scale parameter $\underline{a}_{major}$ of 3.47 kpc, taking the minor axis value of 1.98 and assuming the ellipticity of 0.43. It is clear that inside 8 to 9 arcsec the drop in surface brightness is much flatter than that expected from an Abell-Mihalas law.

To see to what extent this could be caused by the scattering function of the plate, the mean scattering function was derived from the 13 stars shown in Fig. 21. This is shown in Fig. 25. The surface brightness scale of each star has been normalised to that of the star at V_{25} = 16.01 by a straightforward vertical shift. The left hand plot shows the data for these 13 stars. The

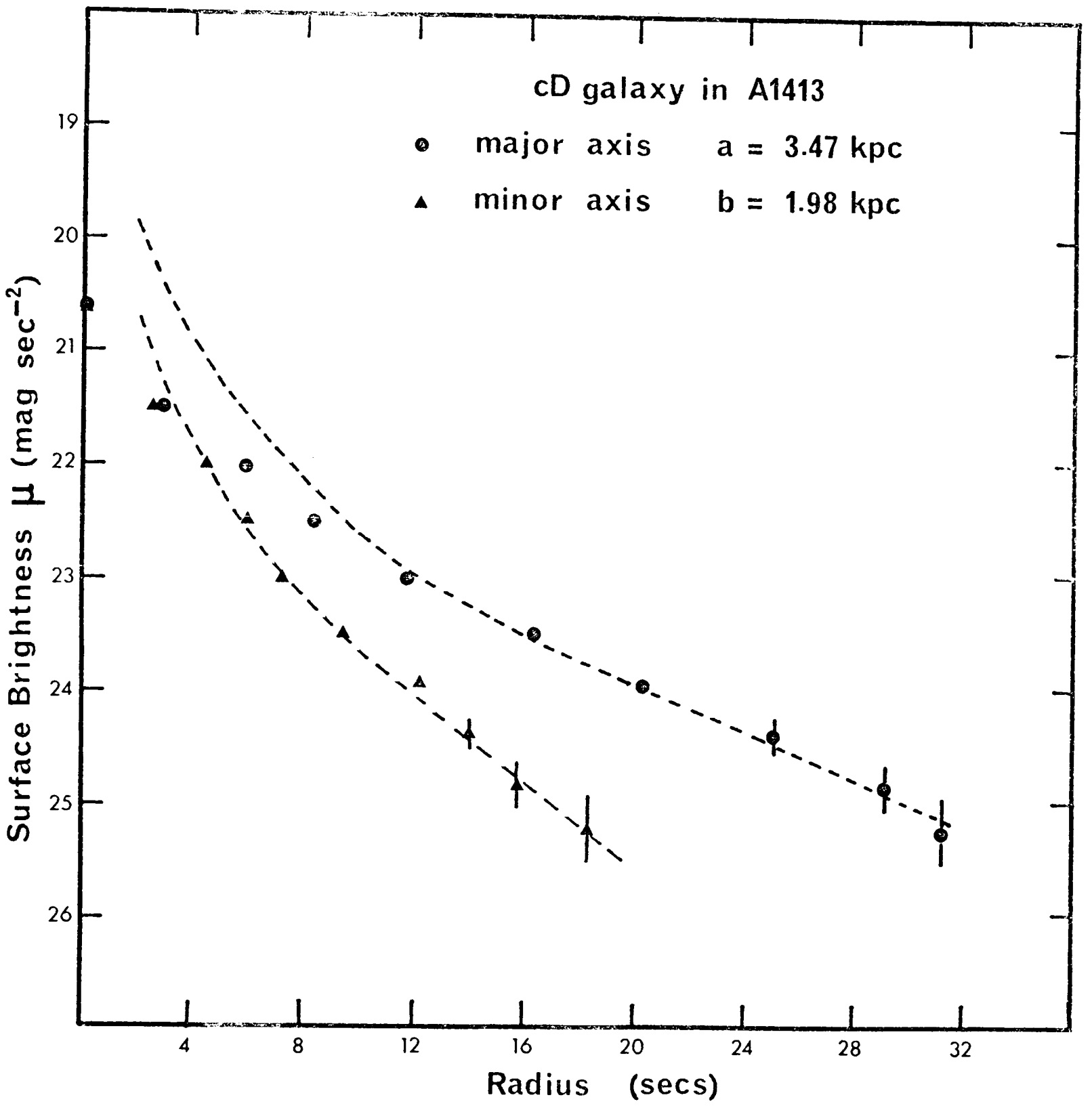

FIG. 24 The surface brightness profiles of the brightest cluster galaxy in A1413 along its major and minor axes. The dotted curves are fits to the data of the Abell-Mihalas (1966) formula for the light distribution in a normal elliptical galaxy. The scale parameters a and b are given in a world model with $q_o = +1$ and $H_o = 50$ km s^{-1} Mpc^{-1}.

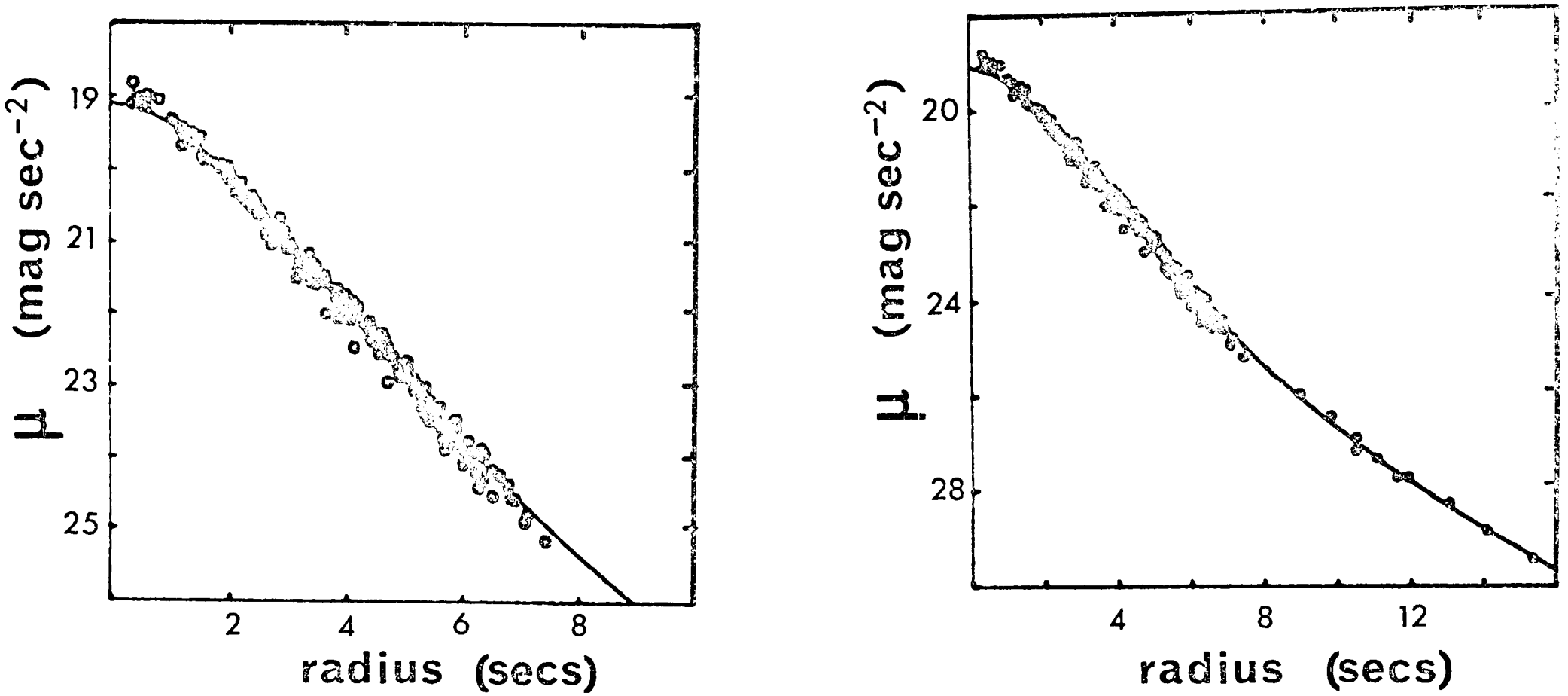

FIG. 25 The scattering function for the plate PS7756. The left-hand plot shows the function as determined from the light distributions of the 13 stars plotted in Fig. 21. The curve is the best fit to the data of the empirical Moffatt (1969) formula for the light distribution in an infocus stellar image (cf. part 3.5a). The right-hand plot shows the same inner region with the addition of points determined from the outer parts of the light distributions of 3 saturated stars not plotted in Fig. 21.

plot on the right shows the same inner region with the addition of the outer points of 3 saturated stars not shown in Fig. 21. The curve is a fit to the empirical Moffatt (1969) law for the distribution of surface brightness in an infocus stellar image given by

$$I = I_o/(1 + (r/R)^2)^{\beta}$$

where I_o is the central intensity and R and β are parameters to be determined. For this plate the values of R and β are

$$R = 52\mu = 3.5 \text{ arcsec} \qquad \beta = 3.15$$

The dispersion in the fit is $\sigma(\mu) = 0.16$ mag arcsec^{-2}.

Such a scattering function would drop the surface brightness within 1 arcsec^2 by about 3 mag., but this is still not sufficient to explain the flatness of the curve. It is clear that this part of the curve is heavily influenced on our plate by the unresolved knot. From the 4 metre print it is seen that the knot would affect the profile markedly between 4 and 8 arcsecs. The extrapolation to the total magnitude discussed in the previous part 3.5 was made using an effective scale length $a^* = \sqrt{a_{major} \times b_{minor}}$ of 2.62 kpc. This is of the same order as that found for the brightest galaxy NGC 4889 in the Coma cluster as shown by Gudehus (1973) from the plots of Brookes and Rood (1971). The total apparent magnitude has the value 15.01.

Wolf and Bahcall (1972) have studied the masses of several giant ellipticals that appear to be members of double-galaxy systems, including this cD galaxy and its 'knot'. From radial velocity measurements of Jenner (1970), which agree closely with those of Humason et al. (1956), they derived best-guess and upper estimates of the total mass of the system. These values are

$$M_{bg} = 3 \times 10^{11} M_{\odot}$$

$$M_{ue} = 1.4 \times 10^{13} M_{\odot}$$

These estimates are considered to be 50% and 80% upper limits - that is for the upper estimate one would expect that in 80% of cases the real value would lie below this limit. With a total absolute magnitude of $M_V(1) = -24.89$, these estimates give V mass to light ratios of

$$(M/L)_{bg} = 0.8\ h\ (M/L)_{\odot}$$

$$(M/L)_{ue} = 36\ h\ (M/L)_{\odot}$$

with $H_o = 50\ h$ km s^{-1} Mpc^{-1}. It is clear that the upper estimate gives values comparable to those normally found for elliptical galaxies (Burbidge and Burbidge, 1974). It should be noted that the brightest galaxy, although 21 times brighter than the mean of all the other galaxies in the sample, has a mean surface brightness of only 1.5 times the mean for the sample (see Fig. 21).

3.6 The structure of the cluster

The galaxy counts in the field of the cluster have been used in Chapter 2 to derive the core radius 3β and the cluster radius $\bar{r}$. It was remarked then that of the sample of nine clusters only A1413 was unambiguously non-spherically symmetric in structure. The same counts have been used to construct the contours of equal galaxy density (isopleths) shown in Fig. 26. These make it clear that the cluster is elongated in a NS direction as previously shown by Noonan (1972a). The last closed contour is 22 arcmins (4.3 Mpc) from the centre in the NS direction, and 10 arcmins (2.1 Mpc) in the EW. The ellipticity of the isopleths increases with radius and there is a suggestion of a bending of the major axis in the outer regions. The major

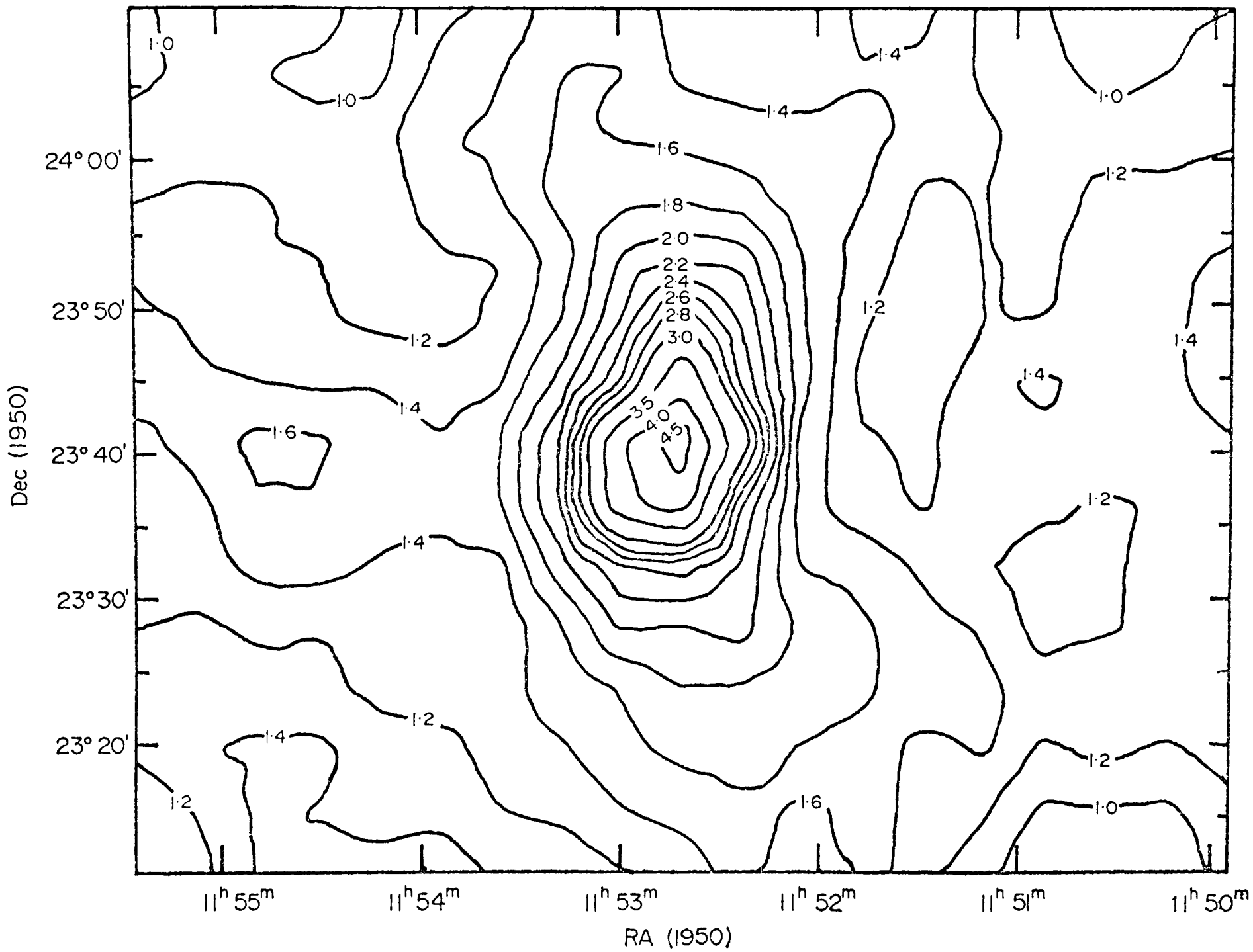

FIG. 26 Isopleths of galaxies in the field of A1413. The units are 1000 galaxies deg^{-2}. With Z = 0.1426, 1 arcmin is 0.19 Mpc.

axis of the central cD galaxy also lies in the NS direction (see Fig. 18).

The galaxies in the central region shown in Fig. 19 reflect the ellipticity of the outer regions but only for the fainter members. Dividing the galaxies of Fig. 19 into those falling into NS quadrants bounded by angles 315^{o} - 45^{o} and 135^{o} - 225^{o} and those in EW quadrants bounded by 45^{o}-135^{o} and 225^{o}-315^{o}, we find 79 galaxies in the NS quadrants and 56 in the EW quadrants. However, for galaxies brighter than V_{25} = 18.5 the numbers are 25 to 21 while for fainter galaxies they are 54 to 35 respectively. Application of a field correction to the latter group would tend to increase the asymmetry as a similar correction would be applied to each quadrant; the correction of part 3.5 results in a number ratio of 39 to 20, while the brighter group is not significantly affected. These results are consistent with Sastry's (1968) conclusion that the 21 brightest galaxies within 8 arcmin of the cluster centre showed circular symmetry. A picture emerges of a spherical subsystem of brighter galaxies extending over most of the cluster volume coexisting with a prolate subsystem of fainter galaxies. The isopleths of Fig. 26 reflect the symmetry of the latter system as there is a higher proportion of galaxies with $V_{25}>18.5$ in the counts than brighter objects.

The problem of the radial dependence of the galaxy number density is now examined. In Fig. 27 the number density of galaxies grouped in three magnitude intervals, 17.0 to 18.0, 18.0 to 19.0 and 19.0 to 20.0, are plotted as a function of radius; each group is normalised to a total population of 20 and the field correction has been applied. The error bars show the natural error $\sqrt{N}$ of the original number. There is no significant difference

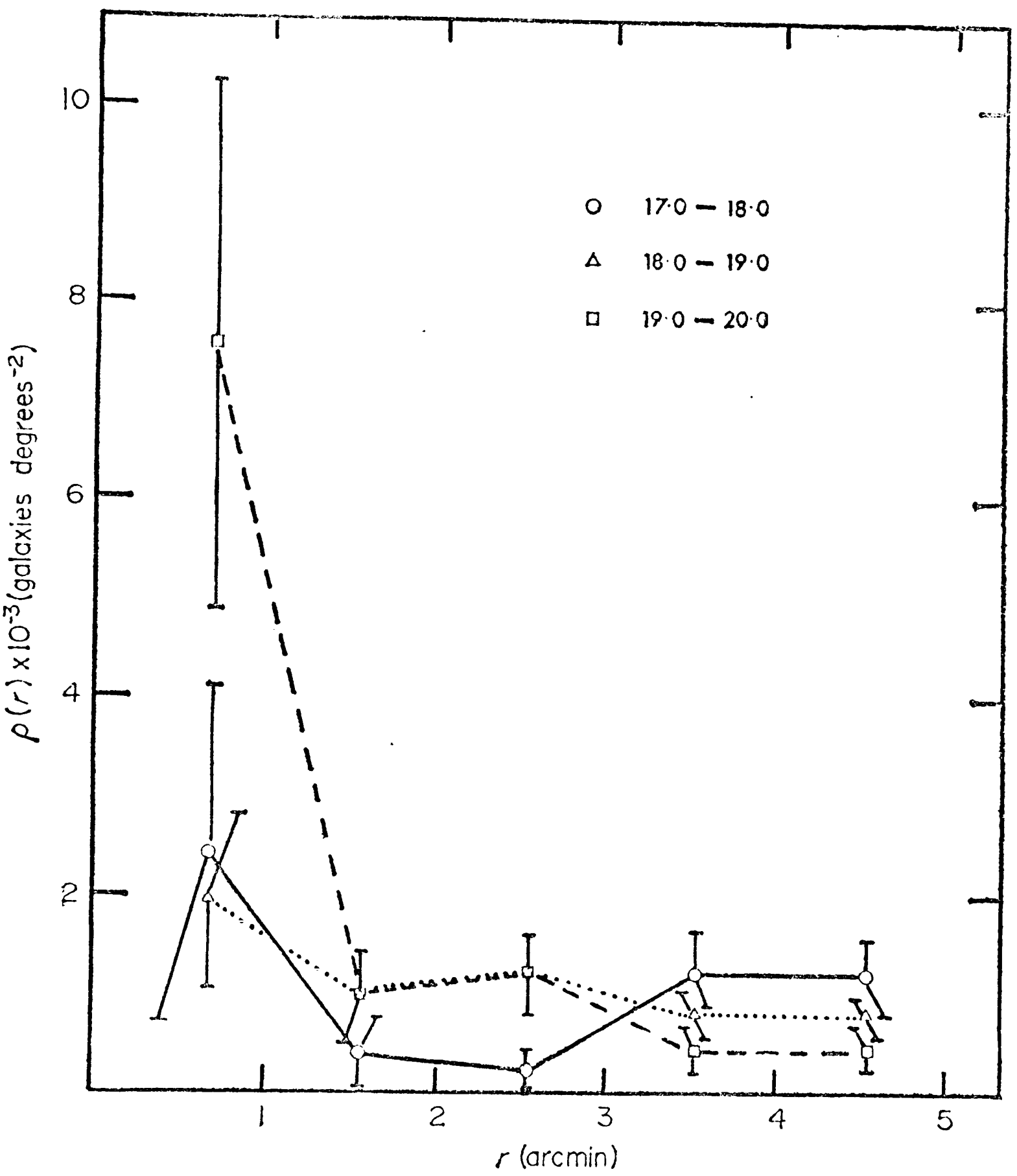

FIG. 27 The surface density of galaxies as a function of radial distance for three magnitude intervals. The continuous line is for $17<V_{25}<18$, the dotted line for $18<V_{25}<19$ and the dashed line for $19<V_{25}<20$. The error bars show the square root of the number forming each point.

between the distributions except for the data of the innermost 1 arcmin where there appears to be an excess of faint galaxies. References to Figs 18 and 19 will show that this is attributable to a clustering of faint galaxies around the central cD galaxy. Five of these, Nos 101, 107, 121, 130 and 116 actually fall within the outermost isophote of the central galaxy, and the first three are perhaps better described as condensations within it than independent objects. It is concluded that there is no significant difference in the density distributions within 5 arcmin of the centre. Noonan (1972), however, has suggested the existence of either colour or luminosity segregation between radii of 4 and 10 arcmin on the basis of counts in two colours. These were analysed on the assumption of spherical symmetry and showed a broader central peak in counts made in the red to a limiting magnitude of about 19 than in blue counts a limit of about 22. It is suggested here that this result finds a ready explanation in terms of the conclusion that bright and faint galaxies are distributed with different symmetry. The deeper counts will show the prolate distribution of the fainter members; summing these counts in <u>circular</u> rings will lead to a spuriously broader central peak than that shown by the counts of the brighter galaxies which have spherical symmetry.

CHAPTER 4

SUMMARY AND DISCUSSION

4.1 Results

The results of Chapters 2 and 3 raise at least three general problems for which there is at present no solution. Firstly, there is a need for a physical explanation of the correlation between $R_{\bar{r}}$, C and N_{SH}, and secondly, but not independently, we must answer a number of questions relevant to the use of the correlation in the θ-z diagram. Thirdly we need an explanation of the observations of a peak in the differential luminosity function of rich clusters, and the observation in A1413 of a magnitude dependent radial density distribution, the fainter galaxies being distributed with a different symmetry than that of the brighter galaxies.

The N-body calculations on clusters of galaxies offer only faint clues as to an explanation of the correlation of $R_{\bar{r}}$ and C. The theoretical clusters tend to relax to a core-halo structure that becomes more marked as time advances and forms more rapidly for more massive systems (Aarseth, 1971). Velocity dispersions are available for only three of the clusters, Coma, A2199 and Corona Borealis, and for these the calculated crossing times (Rood, Rothman and Turnrose, 1970) are shorter for larger C. If this slender evidence is taken as implying that a high C cluster is more relaxed then it could be assumed that its core dominates the counts because the halo is now too extended to appear above the field galaxy background. It would be of interest on this hypothesis to compare the luminosity functions of clusters with extreme values of C to see if high C clusters are dominated by more massive galaxies. On the other hand the absence of the extended

halo in high C objects may be real and the low C cluster may be more relaxed. With the present information one cannot make a reasoned choice between these (and other) possibilities.

This ignorance is to some degree irrelevant to the cosmological use of the θ-z plot; similar ignorance exists as to the reason for the small dispersion of the absolute magnitudes of brightest members of clusters, although these objects are accepted as good distance indicators. But the relation between size, concentration and population presumably contains implications for the evolution of the systems and about possible segregation effects. There is indirect evidence that evolution in size over the light travel time to z = 0.2, viz. 5×10^9 years, has been small, in that the plot of Fig. 13 in Chapter 2 implies that the data is well represented by $q_o = +1$ which is the same value as that given independently by the m-z plot; this conclusion applies equally to the evolution in luminosity of the cluster galaxies, unless the two effects cancel one another fortuitously. Mass segregation effects for rich clusters must by a similar argument be small, but a thorough treatment of this problem must await more extensive photometric data on cluster galaxies.

4.2 Galaxy Formation

Theories of galaxy formation are at present in too primitive and uncertain a state to make it realistic to attempt a very detailed comparison of their predictions with observation. There are two current hypotheses on the origin of structure in an expanding universe. The first is the fragmentation hypothesis, according to which large rudimentary structures first form and then by fragmentation give birth to a second generation of component structures, which in turn may fragment successively into smaller and less massive components. The second is the

clustering hypothesis, according to which small scale entities first form and then interact to create larger and larger systems. A recent model of this type is that due to Press and Schechter (1974), in which 'seed' masses of 10^7 to 10^9 $M_\odot$, existing after recombination, condense into aggregates of higher mass, this process proceeding in time to aggregates of several larger scales and higher masses.

4.2a) Icke's model

Here, however, it is worth mentioning two points of contact between the results for A1413 in Chapter 3 and Icke's (1973) model for the formation of cluster galaxies, which is presented in such a way as to invite observational comparison. This model can be summarised as follows. After recombination of the cosmic plasma in an Einstein-De Sitter Universe, $q_o = +\frac{1}{2}$, some spheroidal regions of space expand somewhat slower than others. These slow-expansion regions, which have a mass between 5×10^{15} $M_\odot$ and 5×10^{17} $M_\odot$, eventually stop expanding and subsequently collapse to high density. If such a region is not exactly spherical its deviation from sphericity will increase throughout the evolution. The turbulence inside this proto-cluster leads to the formation of galaxies by velocity perturbations of the collapsing prolate spheroid. The proto-clusters collapse within about 10^{17} secs predominantly into highly elongated clusters. The time needed for a galaxy to cross such a cluster is 4×10^{17} secs, so that many of these clusters have not yet reached virial equilibrium at the present time.

The condensations which form during the collapse owe some peculiar properties to the fact that they form inside a cluster. Firstly, they can develop more easily (i.e. from a smaller initial

perturbation) than if they were to be formed isolated in the universe. Secondly, their space velocities are directed along the major axis of the parent cluster. Thirdly, they have masses ranging from those of dwarf galaxies ($\sim 10^{8} M_{\odot}$) up to those of giants ($\sim 10^{13} M_{\odot}$). The dwarfs separate out before the giants. Fourthly, the galaxies show some preference to align with the axis of the cluster. Fifthly, the most massive members have rather uniform properties. Sixthly, the model predicts peaks in the mass spectrum of the protogalaxies. This is because certain wavenumbers of the perturbations are more strongly amplified within the cluster than others. The first protogalaxies to collapse reheat the surrounding gas, effectively increasing the Jeans mass and shifting the mass spectrum of subsequently formed galaxies to larger masses.

Thus this model makes at least two testable predictions. It gives a rough form for the mass spectrum and hence the luminosity function, and predicts that, as the cluster tends to become more prolate with time the distribution of the less massive and older galaxies will be less prolate than that of the more massive and younger galaxies.

Icke's luminosity function for a wide range of initial conditions bears some resemblance to that in Fig. 20 in Chapter 3, showing a small peak about half a magnitude brighter than a major peak. His prediction as to the relative spatial distributions of bright and faint galaxies is, however, the opposite of the result in part 3.6 of Chapter 3. For A1413 at least there must be a fundamental misconception in the model.

4.3 Future Work

It is proposed to look for similar effects in other elongated clusters, prime candidates being cD clusters, such as A2199 where Rood and Sastry (1972) have qualitatively suggested segregation of this type. Other observations that need to be made are studies of the colour and types of galaxies around the peak in the luminosity function and the colours and types of galaxies near the proposed peak in the radial density distribution. Abell (1974) has pointed out that the magnitude at which Virgo cluster ellipticals begin to show a colour dependence on luminosity (de Vaucouleurs 1961a; Baum, 1959) is near his magnitude m*. Oemler (1974a) has claimed that, in low redshift cD clusters with radial density peaks the ellipticals seem to participate the most, and the spirals the least, in the feature. A qualitative look at the data of Rood and Sastry (1972) for A2199 suggests that there is a colour and/or type change on passing through the feature. This feature might be a result of shock waves produced by the infall of matter into clusters (Gunn and Gott, 1972).

By obtaining more detailed observations along these lines, and by further study of the angular diameter correlations of Chapter 2, it is to be hoped that a little more understanding will be gained of the formation and evolution of clusters of galaxies and their overall place in theories and models of the universe.

ACKNOWLEDGEMENTS

I should like to thank my supervisor Dr. John Peach for all his help, encouragement and enthusiasm throughout the course of this investigation. My thanks are also due to Professor D.E. Blackwell for allowing me the use of the facilities of the Department of Astrophysics, and to all members of the Department for their encouragement.

I should like also to thank the Director of the Hale Observatories for grants of time on the Palomer 48-in. Schmidt telescope to Dr. John Peach and myself in March and October 1972, and for the hospitality afforded us on the two visits.

I gratefully acknowledge a three year maintenance grant from the Science Research Council and their provision of travel funds for the two visits to the Hale Observatories.

REFERENCES

AARSETH, S.J. (1971), Astrophys. & Space Science, 14, 20.

ABELL, G.O. (1958), Astrophys. J. Suppl. Ser., 3, 211.

(1962), "Problems of Extragalactic Research", I.A.U. Symposium No. 15, G.C. McVittie, ed., (New York: MacMillan).

(1963), Astron. J., 68, 271.

(1965), Ann. Rev. Astron. & Astrophys., 3, 1.

(1972), "External Galaxies and Quasi-Stellar Objects", I.A.U. Symposium, No. 44, D.S. Evans, ed., (Holland: D. Reidel).

(1974), "Galaxies and The Universe", Vol. IX, Stars and Stellar Systems, A.R. Sandage, ed., (Chicago: Chicago Univ. Press).

ABELL, G.O. and EASTMOND, S., (1970), Bull. A.A.S., 2, 179.

ABELL, G.O. and MIHALAS, D.M. (1966), Astron. J., 71, 635.

ABELL, G.O. and MOTTMANN, J. (1974), in preparation.

ABLES, H.D. (1971), Publ. U.S. Naval Obs., Vol. XX, Part IV (Washington).

ALLEN, C.W. (1973), "Astrophysical Quantities", (3rd ed., Univ. of London, Athlone Press).

ARP, H. (1961), Astrophys. J., 133, 869.

(1966), "Atlas of Peculiar Galaxies", (Pasadena; Cal. Inst. of Tech.).

AUSTIN, T.B. and PEACH, J.V. (1974a), M.N.R.A.S., 167, 437.

(1974b), M.N.R.A.S., 168, in press.

AUSTIN, T.B., GODWIN, J. and PEACH, J.V. (1974), in preparation.

BAKER, E.A. (1957), Journ. Phot. Sci., 5, 94.

BAHCALL, N.A. (1971), Astron. J., 76, 995.

(1972), Astron. J., 77, 550.

(1973a), Astrophys. J., 183, 783.

(1973b), Astrophys. J., 186, 1179.

(1974), Astrophys. J., 187, 439.

BAUM, W.A. (1955), Sky and Telescope, 14, 264.

(1959), Publ. Astr. Soc. Pacific, 71, 106.

BAUTZ, L.P. and ABELL, G.O. (1973), Astrophys. J., 184, 709.

BAUTZ, L.P. and MORGAN, W.W. (1970), Astrophys. J. Letters, 162, L149.

BECKER, W. (1965), Z. Astrophys., 62, 54.

BERGH, S. van den, (1959), David Dunlap Obs. Pub., 2, 147.

(1961), Z. Astrophys., 53, 219.

BIGAY, J.H. (1951), C.R., 232, 312 (Publ. Obs. Haute Provence, 2, 15).

BOGART, R.S. and WAGONER, R.V. (1973), Astrophys. J., 181, 609.

BROOKES, R.A. and ROOD, H.J. (1971), Astrophys. Letters, 8, 61.

BURBIDGE, G.R. (1970), Ann. Rev. Astron. & Astrophys., 8, 369.

BURBIDGE, E.M. and BURBIDGE, G.R. (1974), "Galaxies and The Universe", Vol. IX, Stars and Stellar Systems, A.R. Sandage, ed., (Chicago: Chicago Univ. Press).

CLARK, E.E. (1968), Astron. J., 73, 1011.

EVANS, D.S. (1951), M.N.R.A.S., 111, 526.

(1952), M.N.R.A.S., 112, 606.

FENKART, R.P. (1967), Z. Astrophys., 66, 390.

FRIEDMANN, A. (1922), Z. Astrophys., 10, 377.

GUDEHUS, D. (1971), Ph.D. Thesis, Univ. of California, Los Angeles.

(1973), Astron. J., 78, 583.

GUNN, J.E. (1971), Astrophys. J., 164, L113.

GUNN, J.E. and GOTT, J.R. (1972), Astrophys. J., 176, 1.

HAUSER, M.G. and PEEBLES, P.J.E. (1973), Astrophys. J., 185, 757.

HODGE, P.W. (1959), Publ. Astr. Soc. Pacific, 71, 28.

(1960), Publ. Astr. Soc. Pacific, 72, 188.

HODGE, P.W., PYPER, D.M. and WEBB, C.J. (1965), Astron. J., 70, 559.

HOLMBERG, E. (1950), Lund. Medd. Ser. II, No. 128.

(1958), Lund. Medd. Ser. II, No. 136.

(1962), "Problems of Extragalactic Research", I.A.U. Symposium No. 15, G.C. McVittie, ed., (New York: MacMillan).

HONEYCUTT, R.K. and CHALDU, R.S. (1970), A.A.S. Photobulletin, No. 2, 14.

HOUTEN, C.J. van, (1961), Bull. Astr. Inst. Netherlands, 16, 1.

HUBBLE, E.P. (1925), Observatory, 48, 139.

(1934), Astrophys. J., 79, 8.

(1936a), Astrophys. J., 84, 517.

(1936b), "The Realm of the Nebulae", (London: Oxford Univ. Press).

HUMASON, M.L., MAYALL, N.U. and SANDAGE, A.R. (1956), Astron. J., 61, 97.

ICKE, V. (1973), Astron. & Astrophys., 27, 1.

JENNER, D.C. (1970), Ph.D. Thesis, unpublished, (Univ. of Washington).

JONES, W.B., GALLETT, R.M., OBITTS, D.L., VAUCOULEURS, G. de., (1967), Publ. Dept. Astron., Univ. of Texas, Ser II, No. 8.

KIANG, T. (1961), M.N.R.A.S., 122, 263.

KIANG, T. and SASLAW, W.C. (1969), M.N.R.A.S., 143, 129.

KING, I.R. and HINRICHS, E.L. (1967), Publ. Astr. Soc. Pacific, 79, 226.

KORMENDY, J. (1973), Astron. J., 78, 255.

KWAST, T. (1966), Acta. Astron., 16, 45.

LATHAM, D.W. (1969), Bull. A.A.S., 1, 147.

LAYZER, D. (1956), Astron. J., 61, 383.

LILLER, M.H. (1960), Astrophys. J., 132, 306.

LIMBER, D.N. (1953), Astrophys. J., 117, 134.

(1954), Astrophys. J., 119, 655.

LONGAIR, M.S. and REES, M.J. (1973) "Observational Cosmology", (Cargese Lectures in Physics, Vol. 6, E. Schatzmann, ed., (New York: Gordon & Breach).

MARCHANT, J.C. and MILLIKAN, A.G. (1965), J. Opt. Soc. Am., 55, 907.

MATTIG, W. (1958), Astron. Nach., 284, 109.

McVITTIE, G.C. (1956), "General Relativity and Cosmology", (London: Chapman & Hall).

MEES, C.E.K. and JAMES, T.H. (1969), "The Theory of the Photographic Process", (3rd ed.; New York, MacMillan).

MELBOURNE, W.G. (1960), Astrophys. J. 132, 101.

MOFFATT, A.F.J. (1969), Astron. and Astrophys., 3, 457.

MORGAN, W.W. (1961), Proc. Nat. Acad. Sci. U.S., 47, 905.

MORGAN, W.W. and LESH, J.R. (1965), Astrophys. J., 142, 1364.

NEYMAN, J. and SCOTT, E.L. (1952), Astrophys. J., 116, 144.

(1959), "Handbuch der Physik", 53, 416. (Berlin; Springer-Verlag).

NEYMAN, J., SCOTT, E.L. and SHANE, C.D. (1953), Astrophys. J., 117, 92.

(1954), Astrophys. J., Suppl. Ser., 1, 269.

NOONAN, T.W. (1961), Publ. Astr. Soc. Pacific, 73, 212.

(1971), Astron. J., 76, 182.

(1972a), Astron. J., 77, 9.

(1972b), Astron. J., 77, 134.

(1973), Astron. J., 78, 227.

OEMLER, A. (1974a), preprint.

(1974b), private communication.

OMER, G.C., PAGE, T.L. and WILSON, A.G. (1965), Astron. J., 70, 440.

PEACH, J.V. (1969), Nature, 223, 1140.

(1970), Astrophys. J. 159, 753.

(1972), "External Galaxies and Quasi-Stellar Objects", I.A.U. Symposium No. 44, D.S. Evans, ed., (Holland: D. Reidel).

PEACH, J.V. and BEARD, J.M.C. (1969), Astrophys. Letters, 4, 205.

PEEBLES, P.J.E. (1974), Astron. & Astrophys., 32, 197.

PRESS, W.H. and SCHECHTER, P. (1974), Astrophys. J., 187, 425.

REAVES, G. (1966), Publ. Astr. Soc. Pacific, 78, 407.

REES, M.J. (1971), "General Relativity and Cosmology", (New York: Academic Press Inc.).

REES, M.J. and SCIAMA, D.W. (1968), Nature, 217, 511.

REDMAN, R.O. (1936), M.N.R.A.S., 96, 588.

REDMAN, R.O. and SHIRLEY, W.G. (1938), M.N.R.A.S., 98, 613.

ROBERTSON, H.P. (1935), Astrophys. J., 82, 284.

ROBERTSON, H.P. (1936), Astrophys. J., 83, 187.

(1955), Publ. Astr. Soc. Pacific, 67, 82.

ROOD, H.J. (1969), Astrophys. J. 158, 657.

(1974), Publ. Astr. Soc. Pacific, 86, 99.

ROOD, H.J. and ABELL, G.O. (1973), Astrophys. Letters, 13, 69.

ROOD, H.J. and BAUM, W.A. (1967), Astron. J., 72, 348.

(1968), Astron. J., 73, 442.

ROOD, H.J., PAGE, T.L., KINTNER, E.C. and KING, I.R. (1972), Astrophys. J., 175, 627.

ROOD, H.J., ROTHMAN, V.C.A. and TURNROSE, B.E. (1970), Astrophys. J., 162, 411.

ROOD, H.J. and TURNROSE, B.E. (1968), Astrophys. J., 152, 1057.

ROOD, H.J. and SASTRY, G.N. (1972), Astron. J., 77, 451.

RUDNICKI, K. (1963), Acta Astron., 13, 230.

RUDNICKI, K. and BARANOWSKA, M. (1966), Acta. Astron., 16, 55.

RYLE, M. (1958), Proc. Roy. Soc., A, 248, 289.

SACHS, R.K. and WOLFE, A.M. (1967), Astrophys. J., 142, 73.

SANDAGE, A.R. (1961a), Astrophys. J., 133, 355.

(1961b), "Hubble Atlas of Galaxies", (Carnegie Inst. of Washington, Pub. 618).

(1972), Astrophys. J., 178, 1.

SANDAGE, A.R. and HARDY, E. (1973), Astrophys. J., 183, 743.

SASLAW, W.C. (1972), Astrophys. J., 177, 17.

SASTRY, G.N. (1968), Publ. Astr. Soc. Pacific, 80, 252.

SCHEUER, P.A.G. (1974) "Galaxies and the Universe", Vol. IX, Stars and Stellar Systems, A.R. Sandage, ed., (Chicago: Chicago Univ. Press).

SCHILD, R. and OKE, J.B. (1971), Astrophys. J., 169, 209.

SCHMIDT, M. (1968), Astrophys. J., 151, 393.

SCOTT, E.L. (1957), Astron. J., 62, 248.

(1962), "Problems of Extragalactic Research", I.A.U. Symposium No. 15, G.C. McVittie, ed., (New York: MacMillan).

SCOTT, E.L., SHANE, C.D. and SWANSON, M.D. (1954), Astrophys. J., 119, 91.

SHANE, C.D. and WIRTANEN, C.A. (1954), Astron. J., 59, 285.

(1967), "The Distribution of Galaxies", (Lick Obs. Publ., 22, Pt. 1).

SHAPLEY, H. (1933), Proc. Acad. Sci. U.S., 19, 591.

(1957), "The Inner Metagalaxy", (New Haven: Yale Univ. Press).

SHAPLEY, H. and AMES, A. (1932), "A Survey of the External Galaxies brighter than the thirteenth magnitude", (Harvard Obs. Annals, 88, No. 2).

SHAPIRO, S.L. (1971), Astron. J., 76, 291.

SHAROV, A.S. (1959), Astr. Zh., 36, 807.

STEBBINS, J., WHITFORD, A.E. and JOHNSON, H.L. (1956), Astrophys. J., 112, 469.

STERNBERG, J. (1972), D.Phil Thesis, Univ. of Oxford.

VAUCOULEURS, G. de, (1948), Ann. d'Astrophys., 11, 247.

(1959), Ann. de La Houga Obs., Vol. 2, Pt. 1.

(1960), Astrophys. J., 131, 585.

(1961a), Astrophys. J. Suppl. Ser., 5, 233.

(1961b), Astrophys. J. Suppl. Ser., 6, 213.

(1964), "Reference Catalogue of Bright Galaxies", (Austin, Texas: Univ. of Texas Press).

(1968), Applied Optics, 7, 1513.

(1970), Science, 167, 1203.

(1971), Publ. Astr. Soc. Pacific, 83, 113.

VAUCOULEURS, G. de, DIAGESCO, J., and SELME, P. (1956), "Manuel de Photographie Scientifique", (Revue d'Optique, Paris).

WALKER, A.G. (1936),Proc. London Math. Soc., 42, 90.

WALKER, M.F. (1973), Publ. Astr. Soc. Pacific, 85, 508.

WEBB, J.H. and EVANS, C.H. (1938), J. Opt. Soc. Am., 28, 249.

WHITFORD, A.E. (1971), Astrophys. J., 169, 215.

WOLF, R.A. and BAHCALL, J.N. (1972), Astrophys. J., 176, 559.

YAHIL, A. (1974), Astrophys. J., in press.

YU, J.T. and PEEBLES, P.J.E. (1969), Astrophys. J., 158, 103.

ZWICKY, F. (1941a), "Applied Mechanics", Theodore von Karman Anniversary Volume, (Cal. Inst. of Tech)..

(1941b), Proc. Nat. Acad. Sci., 27, 264.

(1942a), Phys. Rev., 61, 489.

(1942b), Astrophys. J., 95, 555.

(1942c), Proc. Nat. Acad. Sci., 28, 150.

(1956a), Publ. Astr. Soc. Pacific, 68, 331.

(1956b), Proc. Third Berkeley Symp. on Math. Stat. and Prob., III, J. Neyman, ed., (Berkeley; Univ. of Cal. Press).

(1957), "Morphological Astronomy", (Berlin: Springer-Verlag).

(1959), "Handbuch der Physik", 53, 390 (Berlin: Springer-Verlag).

(1962), "Problems of Extragalactic Research", I.A.U. Symposium No. 15, G.C. McVittie, ed., (New York: MacMillan).

ZWICKY, F. and HERZOG, E. (1963), "Catalogue of Galaxies and Clusters of Galaxies", Vol. II, (Pasadena; Cal. Inst. of Tech.).

(1966), "Catalogue of Galaxies and Clusters of Galaxies", Vol. III, (Pasadena; Cal. Inst. of Tech.).

ZWICKY, F., HERZOG, E., WILD, P., KARPOWICZ, M. and KOWAL, T.C., (1961-1968), "Catalogue of Galaxies and Clusters of Galaxies", 6 vols, (Pasadena; Cal. Inst. of Tech.).

ZWICKY, F. and HUMASON, M.L. (1964), Astrophys. J., 139, 269.